AD 672735

GOODYEAR AEROSPACE

CORPORATION

AKRON 15, OHIO

Mathematical Model and Computer Program for the Ascent and Descent of High-Altitude Tethered Balloons

TASK REPORT NO. 4

Schedule Sub-Line Item IAD

GER 13714 1 February 1968

By

George R. Doyle, Jr.
Jerome J. Vorachek

Contract F19628-67-C-0145

Sponsored by

ADVANCED RESEARCH PROJECTS AGENCY
DEPARTMENT OF DEFENSE

AFCRL Project Monitors: Mr. Lewis Grass
Edward Young, Captain, USAF

Monitored by

Air Force Cambridge Research Laboratories
United States Air Force
Bedford, Massachusetts

CLEARINGHOUSE

CODE IDENT NO. 25500

GOODYEAR AEROSPACE

CORPORATION

AKRON 15, OHIO

AD 672735

Mathematical Model and Computer Program for the Ascent and Descent of High-Altitude Tethered Balloons

TASK REPORT NO. 4

Schedule Sub-Line Item IAD

GER 13711 1 February 1968

By

George R. Doyle, Jr.
Jerome J. Vorachek

Contract F19628-67-C-0145

Sponsored by

ADVANCED RESEARCH PROJECTS AGENCY
DEPARTMENT OF DEFENSE

AFCRL Project Monitors: Mr. Lewis Grass
Edward Young, Captain, USAF

Monitored by

Air Force Cambridge Research Laboratories
United States Air Force
Bedford, Massachusetts

This document has been approved for public release and sale; its distribution is unlimited

D. D. C.
RECEIVED
AUG 1 1968
B

REF: ENGINEERING PROCEDURE S-017

S-ID-26(7-64)206-52

FOREWARD

The main body of this report is being presented by Mr. Jerome J. Vorachek (Project Engineer) and Mr. George R. Doyle, Jr. The equations of motion were derived by Mr. Doyle who would like to thank Mr. Bernard Burzlaff and Mr. Nicholas Odrey for offering suggestions and reviewing the mathematical approach and derivation of the equations. This derivation is presented in Appendix A. Appendix B contains an explanation of the computer program used to obtain the results. This program was written by Mr. Doyle.

REF: ENGINEERING PROCEDURE 5.017

TABLE OF CONTENTS

Section	Title	Page
FOREWARD		ii
LIST OF FIGURES		iv
I	INTRODUCTION	1
II	RESULTS OF ASCENT AND DESCENT FEASIBILITY STUDY	3
III	CONCLUSIONS	8
IV	RECOMMENDATIONS	9
V	REFERENCES	45
APPENDICES		
A	Equations of Motion	A-1
	1. General	A-1
	2. Cable Representation	A-2
	3. Balloon and Harness Representation	A-6
	4. Inertia Terms	A-8
	5. Generalized Forces	A-23
B	Computer Program	B-1
	1. Wind Profile	B-1
	2. Tether Profile	B-1
	3. Winching Rate	B-3
	4. Translational Dynamics of Balloon and Tether	B-4
	5. Tension	B-6
	6. Physical Aspects of the Balloon	B-10
	7. Numerical Integration Techniques	B-12
	8. Determination of Number of Links	B-13
	9. Inputs	B-16
	10. Outputs	B-19
	11. Fortran IV Program	B-20
	12. Recommendations	B-22
C	Program Listing	C-1

REF: ENGINEERING PROCEDURE 5.017

LIST OF FIGURES

Figure No.	Title	Page
1	Summer I Wind Profile.	10
2	Winter I Wind Profile.	11
3	Comparison of Zero-Drag Tether to Tether With Drag	12
4	30 x 10^6 Ft^3 Balloon, Summer I - 75% Wind, Variable Ascent Rates, Altitude vs Range.	13
5	30 x 10^6 Ft^3 Balloon, Summer I - 75% Wind, Variable Ascent Rates, Winch Tension vs Cable Length. . .	14
6	30 x 10^6 Ft^3 Balloon, Summer I - 75% Wind, Variable Ascent Rates, Altitude vs Balloon Tension. . . .	15
7	30 x 10^6 Ft^3 Balloon, Summer I - 75% Wind, Variable Ascent Rates, Altitude vs Dynamic Pressure.....	16
8	30 x 10^6 Ft^3 Balloon, Winch Rate = 3000 ft/min, Variable Summer I Winds, Altitude vs Range . . .	17
9	30 x 10^6 Ft^3 Balloon, Winch Rate = 3000 ft/min, Variable Summer I Winds, Winch Tension vs Cable Length	18
10	30 x 10^6 Ft^3 Balloon, Winch Rate = 3000 ft/min, Variable Summer I Winds, Altitude vs Balloon Tension.	19
11	30 x 10^6 Ft^3 Balloon, Winch Rate = 3000 ft/min, Variable Summer I Winds, Altitude vs Dynamic Pressure	20
12	Summer I - 90% Wind, Winch Rate = 3000 ft/min, Variable Lift, Altitude vs Range	21
13	Summer I - 90% Wind, Winch Rate = 3000 ft/min, Variable Lift, Winch Tension vs Cable Length . .	22
14	Summer I - 90% Wind, Winch Rate = 3000 ft/min, Variable Lift, Altitude vs Balloon Tension . . .	23

REF: ENGINEERING PROCEDURE 5.017

LIST OF FIGURES (Continued)

Figure No.	Title	Page
15	Summer I - 90% Wind, Winch Rate = 3000 ft/min, Variable Lift, Altitude vs Dynamic Pressure. . .	24
16	24 x 10^6 Ft^3 Balloon, Summer I - 90% Wind, Variable Descent Rate, Altitude vs Range.	25
17	24 x 10^6 Ft^3 Balloon, Summer I - 90% Wind, Variable Descent Rate, Winch Tension vs Cable Length. . .	26
18	24 x 10^6 Ft^3 Balloon, Summer I - 90% Wind, Variable Descent Rate, Altitude vs Balloon Tension. . . .	27
19	24 x 10^6 Ft^3 Balloon, Summer I - 90% Wind, Variable Descent Rate, Altitude vs Dynamic Pressure . . .	28
20	Summer I - 90% Wind, Winch Rate = -1500 ft/min, Variable Lift, Altitude vs Range	29
21	Summer I - 90% Wind, Winch Rate = -1500 ft/min, Variable Lift, Winch Tension vs Cable Length . .	30
22	Summer I - 90% Wind, Winch Rate = -1500 ft/min, Variable Lift, Altitude vs Balloon Tension . . .	31
23	Summer I - 90% Wind, Winch Rate = -1500 ft/min, Variable Lift, Altitude vs Dynamic Pressure. . .	32
24	24 x 10^6 Ft^3 Balloon, Winch Rate = -200 ft/min, Variable Summer I Winds, Altitude vs Range . . .	33
25	24 x 10^6 Ft^3 Balloon, Winch Rate = -200 ft/min, Variable Summer I Winds, Winch Tension vs Cable Length	34
26	24 x 10^6 Ft^3 Balloon, Winch Rate = -200 ft/min, Variable Summer I Winds, Altitude vs Balloon Tension.	35
27	24 x 10^6 Ft^3 Balloon, Winch Rate = -200 ft/min, Variable Summer I Winds, Altitude vs Dynamic Pressure	36

REF: ENGINEERING PROCEDURE S.017

LIST OF FIGURES (Continued)

Figure No.	Title	Page
28	79 x 10^6 Ft^3 Balloon, Winter I - 25% Wind, Winch Rate = 2000 ft/min, Altitude vs Range.	37
29	79 x 10^6 Ft^3 Balloon, Winter I - 25% Wind, Winch Rate = 2000 ft/min, Winch Tension vs Cable Length	38
30	79 x 10^6 Ft^3 Balloon, Winter I - 25% Wind, Winch Rate = 2000 ft/min, Altitude vs Balloon Tension	39
31	79 x 10^6 Ft^3 Balloon, Winter I - 25% Wind, Winch Rate = 2000 ft/min, Altitude vs Dynamic Pressure	40
32	79 x 10^6 Ft^3 Balloon with 19% He Valved, Winter I- 25% Wind, Winch Rate = -200 ft/min, Altitude vs Range	41
33	79 x 10^6 Ft^3 Balloon with 19% He Valved, Winter I- 25% Wind, Winch Rate = -200 ft/min, Winch Tension vs Cable Length.	42
34	79 x 10^6 Ft^3 Balloon with 19% He Valved, Winter I- 25% Wind, Winch Rate = -200 ft/min, Altitude vs Balloon Tension	43
35	79 x 10^6 Ft^3 Balloon with 19% He Valved, Winter I- 25% Wind, Winch Rate = -200 ft/min, Altitude vs Dynamic Pressure.	44
A-1	Tether Model	A-2
A-2	A Typical Link	A-3
A-3	Balloon and Harness.	A-6
A-4	Forces Acting on Balloon	A-24

REF: ENGINEERING PROCEDURE 5.017

LIST OF FIGURES (Concluded)

Figure No.	Title	Page
B-1	Tether Profiles.	B-2
B-2	Winching Rate.	B-3
B-3	Horizontal and Vertical Forces Acting on Balloon .	B-8
B-4	Horizontal and Vertical Forces Acting on "N"th Link	B-9
B-5	Comparison of Three Links Versus Five Links on Altitude - Range Graph	B-14
B-6	Tether Profile for Three and Five Links.	B-15

REF: ENGINEERING PROCEDURE S.017

SECTION I - INTRODUCTION

The desire to place a payload at altitudes of 100,000 ft and to be able to retrieve it prompted a study of the ascent and descent dynamics of a balloon-tether system. The basic incentive of this study is to establish the feasibility of deploying and retrieving high altitude tethered balloons through high wind velocity regions at intermediate altitudes. It was necessary to establish the technical ability to analyze such a system, and to develop a computer program which would define the dynamics of the tether and balloon by integrating the equations of motion. Lagrange's equation was used to derive the equations of motion; Runge-Kutta numerical integration was used to solve the equations of motion; and the computer program was written in Fortran IV for the IBM 360.

The system is assumed to be comprised of rigid bodies connected by frictionless hinges. The tether is simulated by "N" straight links. All of the links are the same length and grow at the same rate, but do not have the same weight or aerodynamic reference area. For this preliminary study, the balloon is considered to be a thin spherical shell which expands as it rises in proportion to density ratio change with altitude.

The results of a limited number of computer runs is being presented not as an extensive study of balloon-tether systems, but rather as a demonstration

REF. ENGINEERING PROCEDURE 5.017

that such systems are feasible under certain conditions. Also presented is an understanding of the abilities and limitations of the computer program to simulate the system. The major emphasis is placed on ascent and descent through a Summer I wind profile. A more limited effort is also presented on ascent and descent of a balloon in a Winter I wind profile.

Figures 1 and 2 show the Summer I and Winter I wind profiles as the computer interprets them. Summer I 75 percent and Winter I 75 percent wind profiles may be found in Reference 3. Summer I 90 percent, 95 percent and Winter I 25 percent come from Reference 4.

REF: ENGINEERING PROCEDURE S.017

SECTION II - RESULTS OF ASCENT AND DESCENT FEASIBILITY STUDY

The feasibility study was conducted using two balloon-tether system - one suitable for Summer I wind conditions and one for Winter I wind conditions.

A description of the balloon-tether systems is given in Appendix B-2 and B-6. The design of the systems is further discussed in Reference 5. The basic criteria of each system is that the balloon support a cable (factor of safety equal 2) at 100,000 ft in a 75 percent wind profile. This defines static conditions. It is the purpose of this study to determine whether or not the same system can satisfy dynamic conditions of ascent and descent. In general, it has been found that some conditions can be satisfied and some can not, but this study does not attempt to define limiting conditions. Effects of wind profile, winching rate and balloon size are established.

In order to show that a zero drag tether does not adequately simulate the balloon trajectory, Figure 3 is presented. An obvious divergence can be seen above 20,000 ft. At 40,000 ft, the divergence becomes more pronounced. This can be attributed to the fact that the region of high dynamic pressure is between 35,000 and 40,000 ft. In one trajectory, the system still experiences the high dynamic pressure through the tether even though the balloon is approaching a lower dynamic pressure region. In the other, the system experiences only the dynamic pressure at the altitude of the balloon causing it to start to drift back to the vertical.

REF: ENGINEERING PROCEDURE S.017

Figures 4, 5, 6, and 7 demonstrate the effects of pay-out rate. It is realized that a rate of 3000 ft/min is pushing the "state-of-the-art" of winches. However, a more reasonable rate of 1000 ft/min pushes the strength of the tether. Figure 4 shows that a pay-out rate of 2000 ft/min is fast enough to allow the balloon to transverse the high dynamic pressure region before it is blown down range. A pay-out rate of 1000 ft/min is too slow. Figure 5 further justifies a pay-out rate of 2000 ft/min. A 1000 ft/min pay-out rate is dangerously close to the ultimate cable strength, while a 2000 ft/min pay-out rate seems to maintain a factor of safety of 1.6. Figure 6 shows that the tether is in no danger of breaking at the balloon for any pay-out rate. Figure 7 considers the dynamic pressures acting on the balloon as it ascends. Such results would be important when designing the balloon structurally. A graph of dynamic pressure versus altitude is presented for each run in the results. Their importance is obvious at this point and will not be discussed further.

The second set of Figures (8, 9, 10, 11) compares the effects of three different Summer I wind profiles. It is clear (from Figure 8) that the 30 million cubic foot balloon lacks the buoyant lift to pull it through the high dynamic pressure region in a 95 percent or 90 percent wind. However, this same balloon will ascend in a 75 percent wind. The increasing range at the high altitudes for the 75 percent wind can be attributed to the increasing tether weight.

REF: ENGINEERING PROCEDURE 5.017

The net vertical force of the system has decreased to such an extent that it is comparable to the horizontal drag acting on the system. Consequently, the horizontal drag force effects the balloon's motion as much as the vertical forces. Figure 9 also demonstrates that a balloon of this size will break its tether if launch is attempted in a 90 percent wind. But an ascent in a 75 percent wind does not seriously stress the tether. Figure 10 indicates that the tether strength at the balloon is more than adequate for a launch in a 75 percent wind.

At this point, it was reasoned that an excess of helium at launch would give the balloon more net lift, thereby allowing it to pass through the high dynamic region before it was blown down range. The results of a Summer I - 90 percent wind profile are presented in Figures 12, 13, 14, 15. As was expected, the ascent was accomplished as can be seen in Figure 12. However, Figure 13 clearly shows that the tether undergoes greater stresses and actually reaches its ultimate cable strength quicker than the normal balloon does. Figure 14 also shows a large increase in tension at the balloon.

The next endeavor was to study descent trajectories in Summer I wind profiles. First consideration was given to variable descent rates in a 90 percent wind (Figures 16, 17, 18, 19). It should be noted that the balloon used in this run is the 30 million ft^3 balloon with 20 percent of the helium valved. This would result in a buoyant lift which would support the tether payed-out when the

REF: ENGINEERING PROCEDURE 5.017

balloon is at 50,000 ft in Figure 8. Figure 16 simply shows that a slower winch rate allows the balloon to be blown down range a greater distance than a fast winching rate. This is to be expected. Figure 17 leaves no doubt that an attempted descent at any rate would stress the tether beyond its strength.

Figures 20, 21, 22, 23 compare the descent of the normal balloon with the one discussed above (20 percent helium valved). A computer run with 33.3 percent of the helium valved was also ran and plotted. Tension values are not availabe for this run.

In order to demonstrate a successful descent trajectory, a 75 percent wind was used. Figures 24, 25, 26, 27 show that it is possible to retrieve in this wind if a slow winching rate is employed. Even at 200 ft/min the factor of safety approaches about 1.3 at one point along the trajectory.

A second, larger balloon was simulated for winter wind conditions. Observing that a Winter I-25 percent wind profile is similar to a Summer I-75 percent wind profile, it is reasonable to expect similar results. Comparing Figure 28 with Figure 4, both trajectories of 2000 ft/min are very close. Also, Figures 29 and 5 predict about the same factor of safety at the winch throughout the trajectory.

REF: ENGINEERING PROCEDURE 5.017

After valving out 19 percent of the helium, a descent trajectory was attempted from 50,000 ft. Figures 32, 33, 34, 35 show the results. As in the previous ascent, this trajectory compares favorably to a descent in a Summer I-75 percent at 200 ft/min, except that the dynamic pressure is 50 percent higher.

REF: ENGINEERING PROCEDURE 5.017

SECTION III - CONCLUSIONS

The results of this preliminary study indicate that it is feasible to launch and retrieve high-altitude balloons under certain conditions. It has been shown that a 30 million ft^3 balloon can be launched in a Summer I-75 percent wind profile at 2000 ft/min, and retrieved in the same wind at -200 ft/min with 20 percent of the helium valved off. Although launch and retrieval are possible in the Winter I wind profile, it is more restricted. The 79 million ft^3 balloon in the Winter I 25 percent wind show results similar to the 30 million ft^3 balloon in the Summer I 75 percent wind.

The results of this feasibility study can be used as preliminary design criteria for components of the tethered balloon-systems-balloon, tether and winch.

REF: ENGINEERING PROCEDURE S-017

SECTION IV - RECOMMENDATIONS

Since this report presents the results of a feasibility study, the only immediate conclusion reached is that such a system can achieve the desired objective of deploying tethered balloons through high wind velocity regions and retrieving them. Since the physical description of the balloon and tether are somewhat idealized (Appendix B-2 and B-6), no attempt was made to study the system in detail. It is recommended that a balloon-tether system be designed and its aerodynamic properties determined. With such a system, a detailed parametric study could be achieved.

Further recommendations (relative to the computer simulation) are made at the end of Appendix B.

REF. ENGINEERING PROCEDURE 5.017

GOODYEAR AEROSPACE
CORPORATION
AKRON 15, OHIO

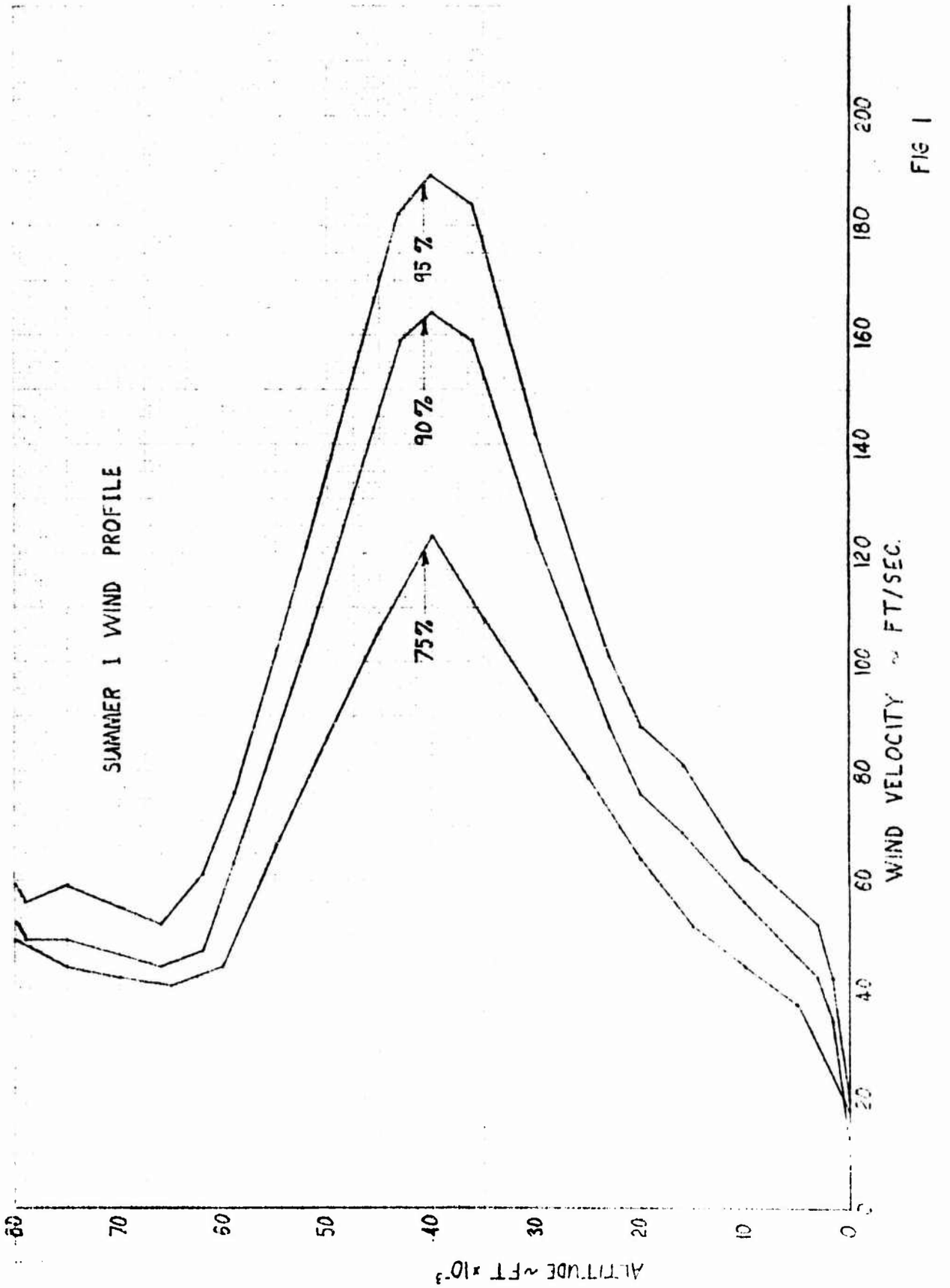

FIG 1

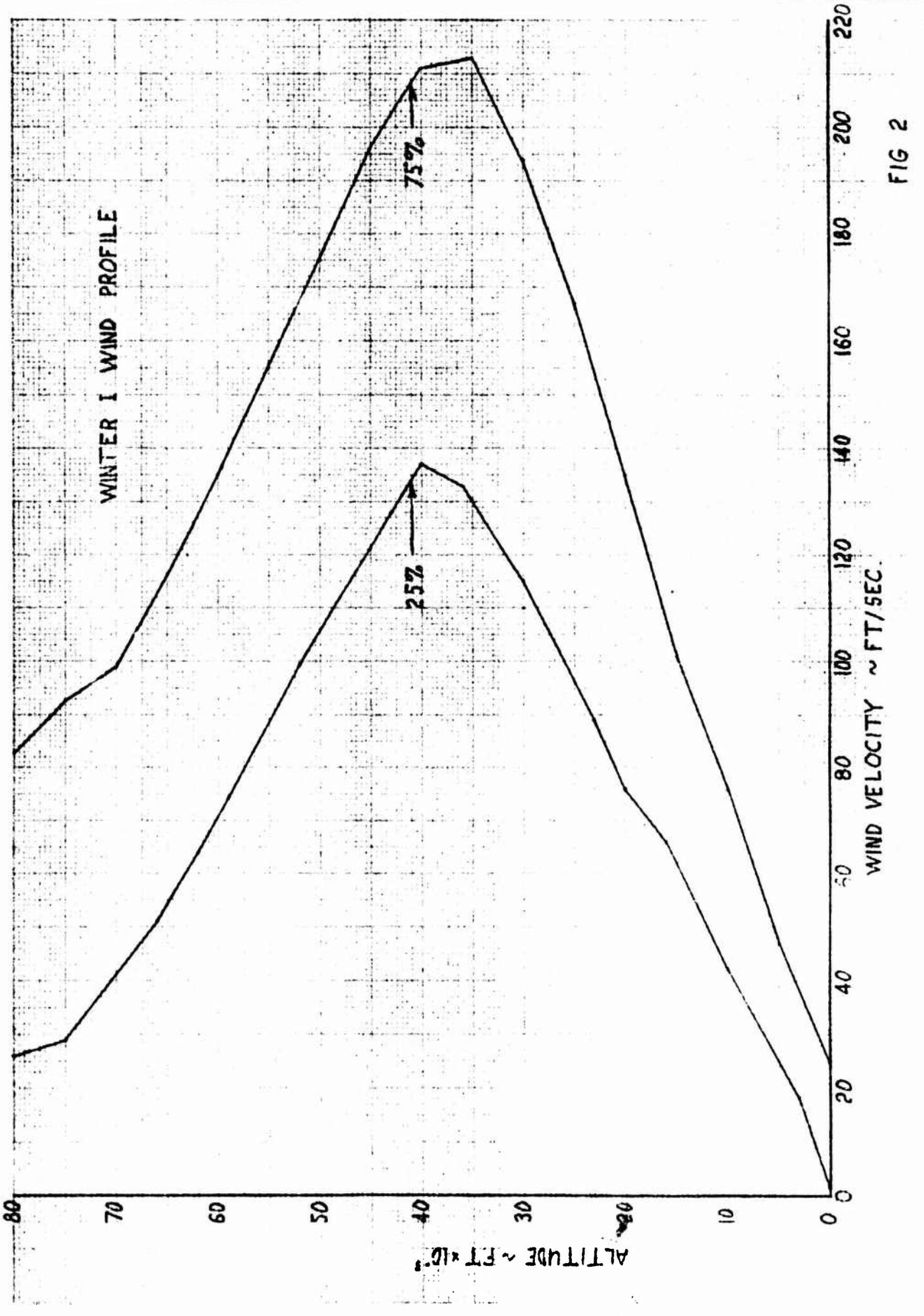

FIG 2

JR 220 (7-63)
REF: EIGSG PROCEDURE S-017

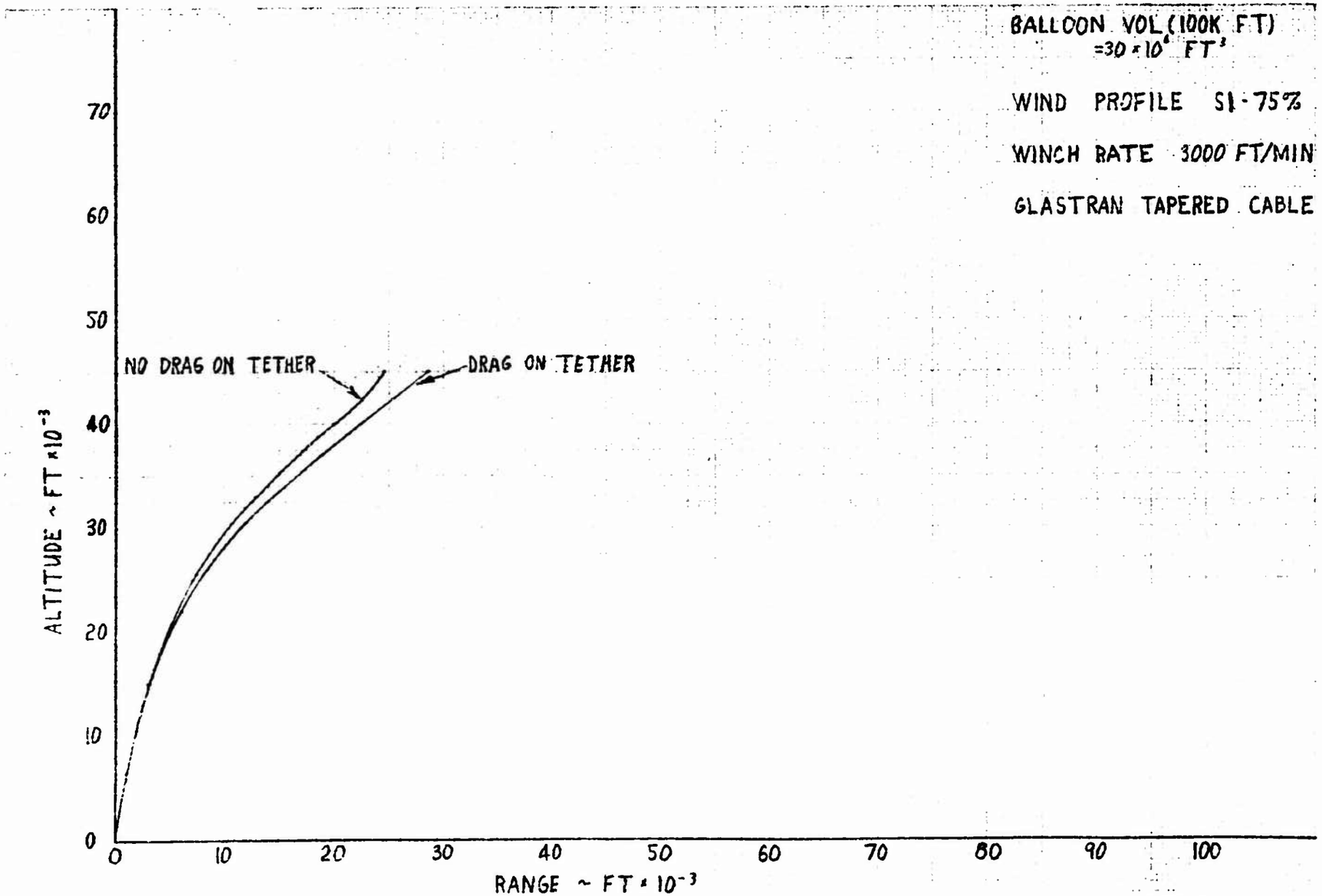

FIG 3

DATE
REV DATE
REV DATE

GOODYEAR AEROSPACE
CORPORATION
AKRON 15, OHIO

PAGE 12
GER. 13714
CODE IDENT NO. 25500

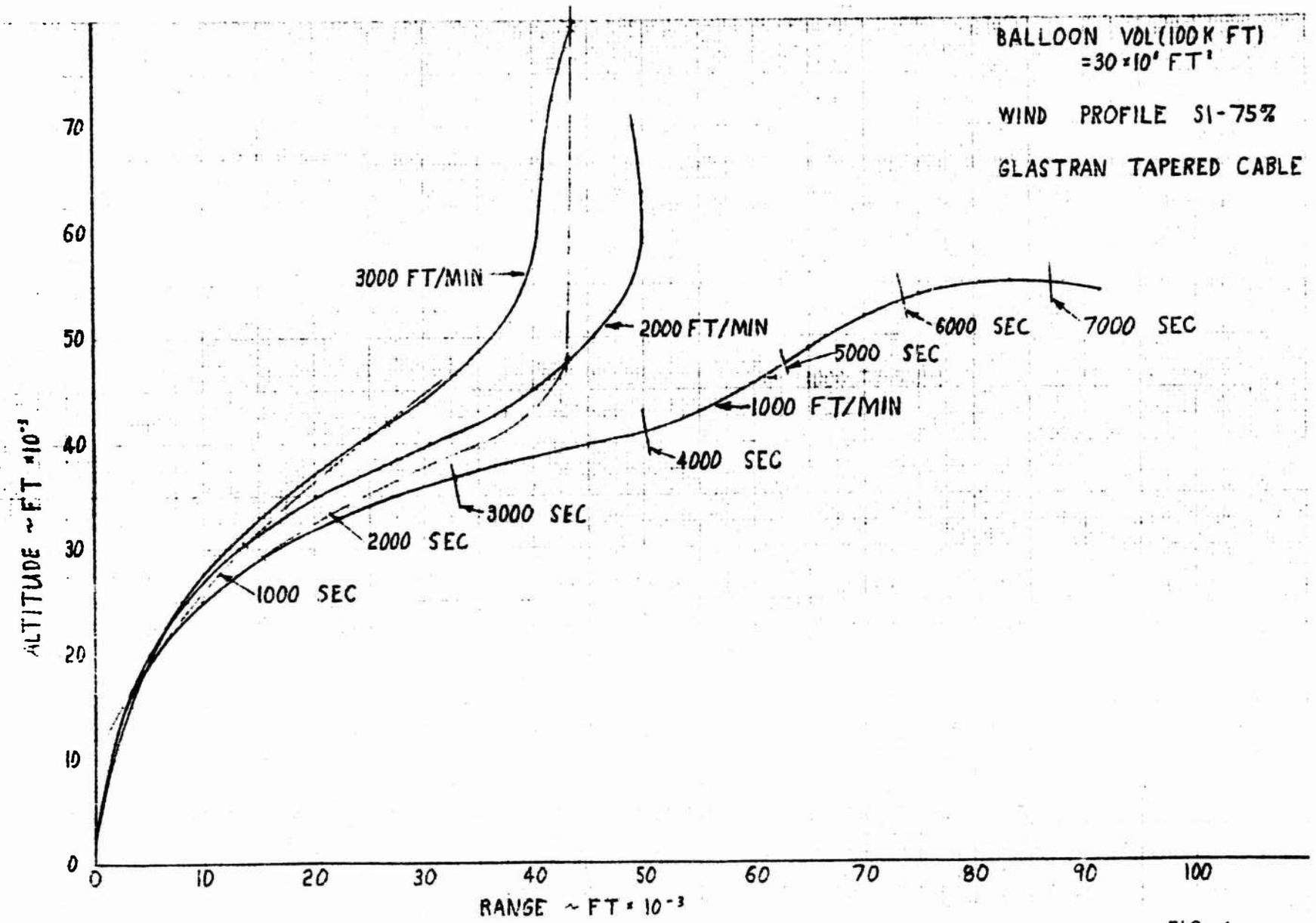

FIG 4

DATE
REV DATE
REV DATE

GOODYEAR AEROSPACE CORPORATION
AKRON 15, OHIO

PAGE 13
GER. 13711
CODE IDENT NO. 25500

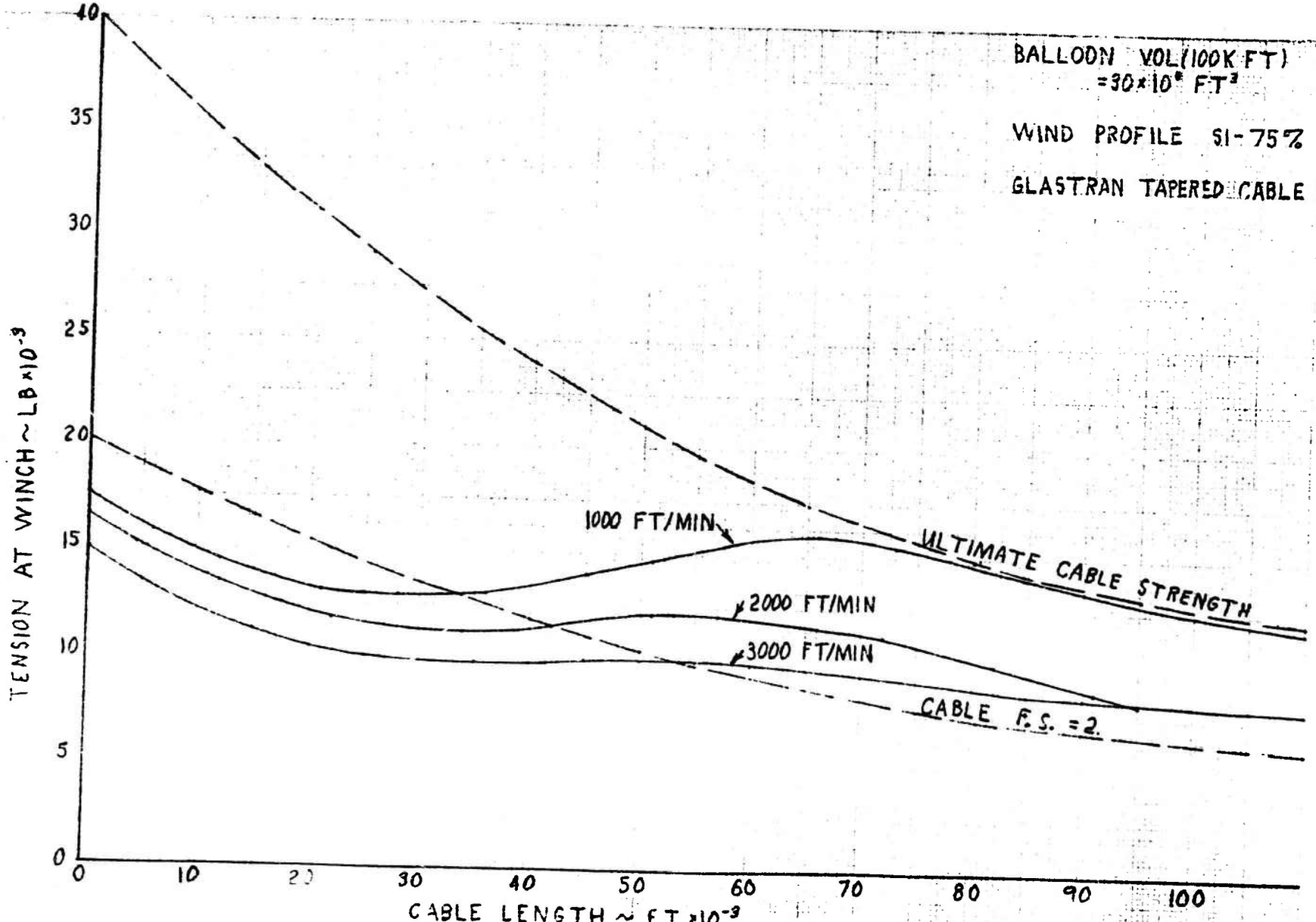

FIG 5

DATE
REV DATE
REV DATE

GOODYEAR AEROSPACE
CORPORATION
AKRON 15, OHIO

PAGE 14
GER. 13714
CODE IDENT NO. 25500

GOODYEAR AEROSPACE
CORPORATION
AKRON 15, OHIO

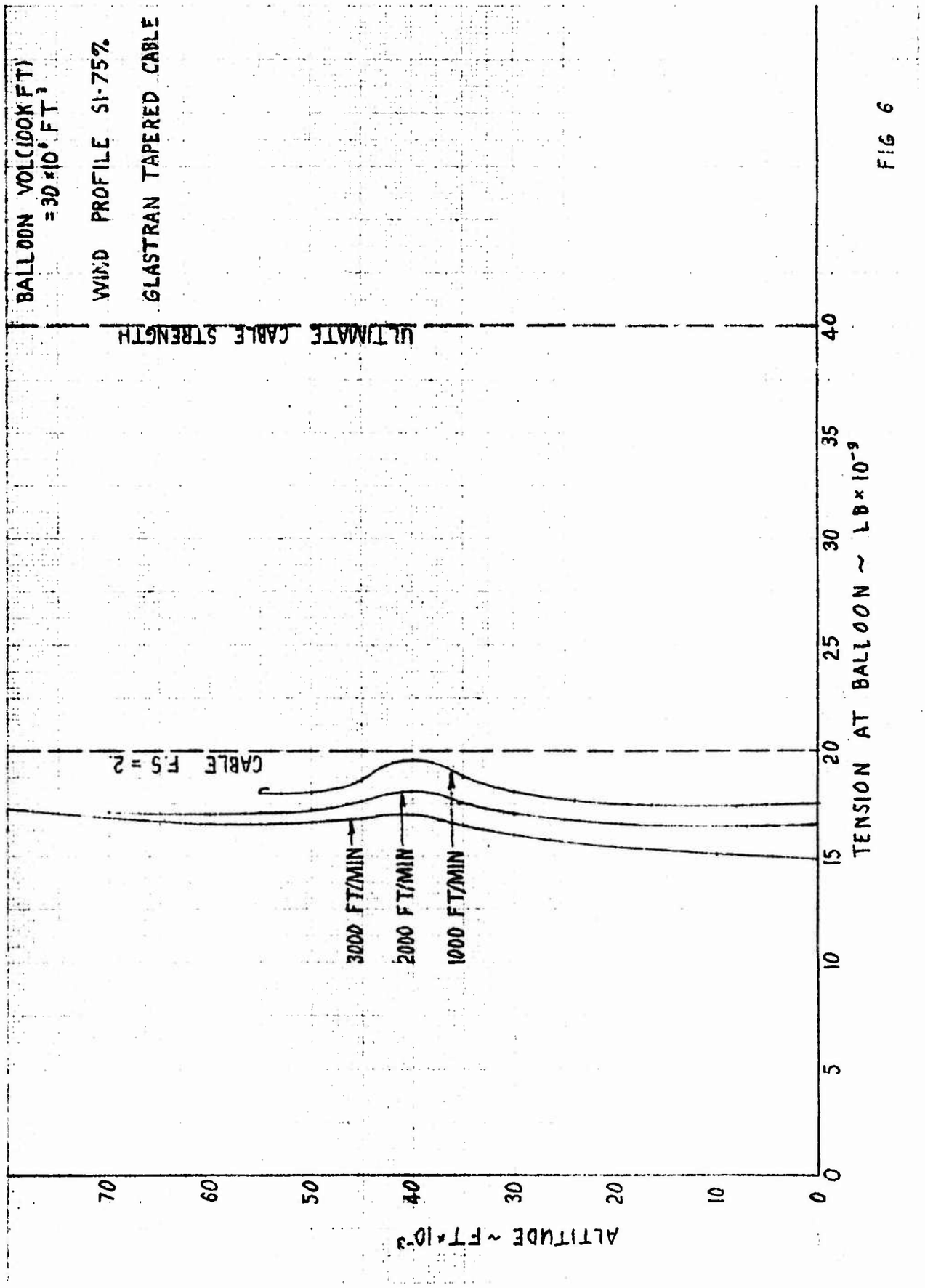

FIG 6

JE 230 (7-63)
REF: ENGRG PROCEDURE 5-017

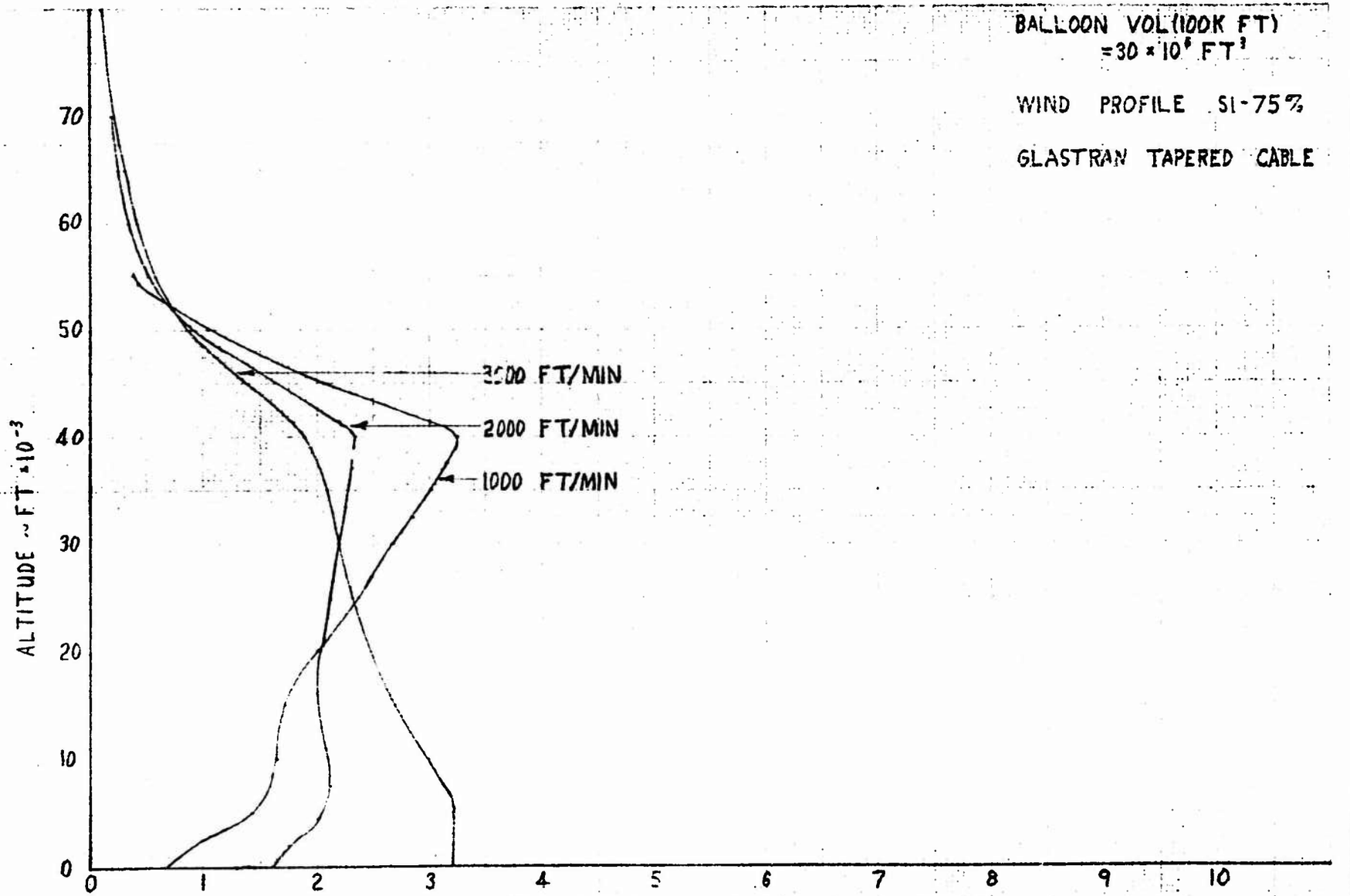

FIG 7

DATE
REV DATE
REV DATE

GOODYEAR AEROSPACE
CORPORATION
AKRON 15, OHIO

PAGE 16
GER. 13714
CODE IDENT NO. 25500

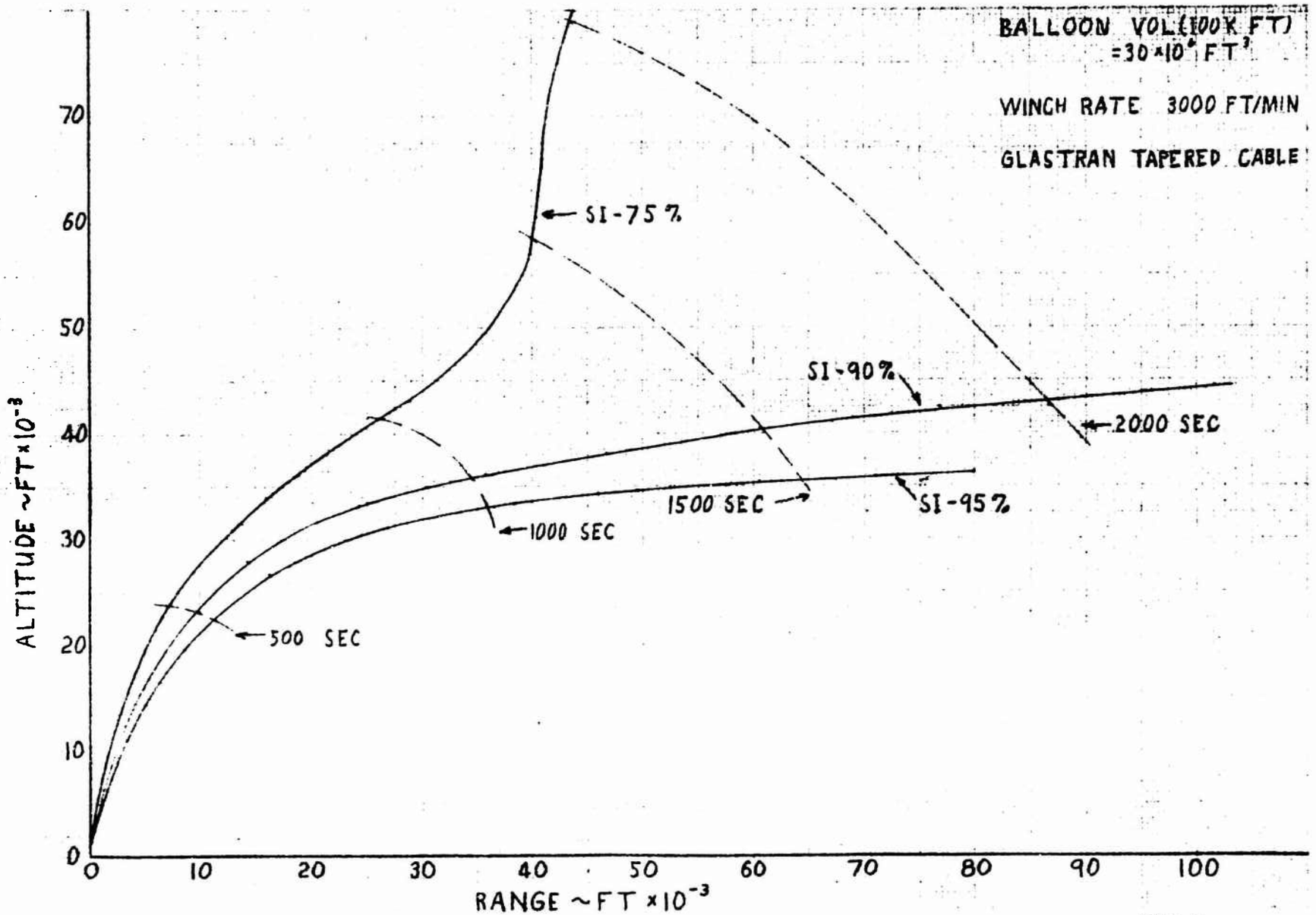

FIG 8

DATE
REV DATE
REV DATE

GOODYEAR AEROSPACE
CORPORATION
AKRON 11, OHIO

PAGE 17
GER. 13711
CODE IDENT NO. 25500

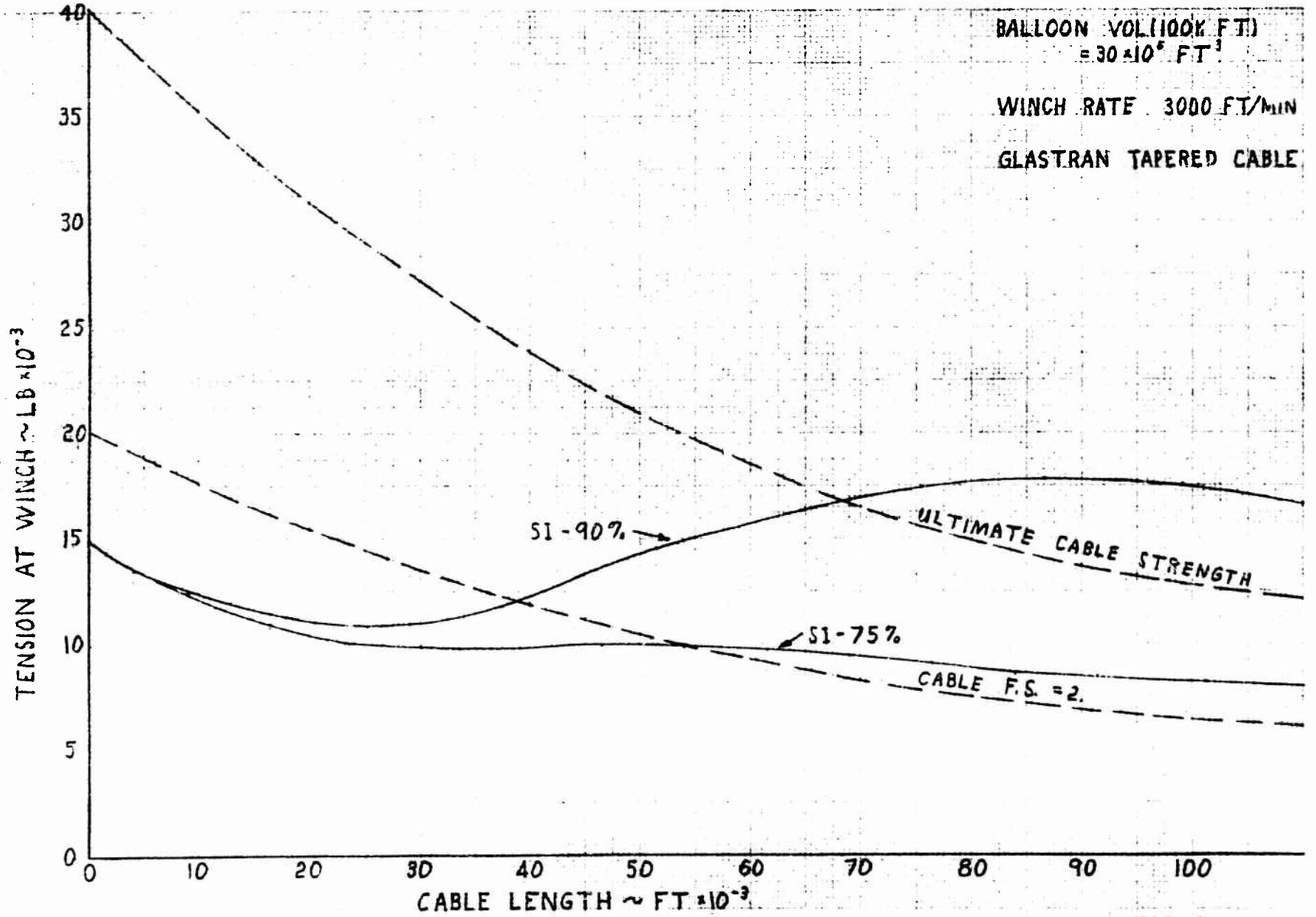

FIG 9

DATE
REV DATE
REV DATE

GOODYEAR AEROSPACE
CORPORATION
AKRON 15, OHIO

PAGE 18
GER. 13711
CODE IDENT NO. 25500

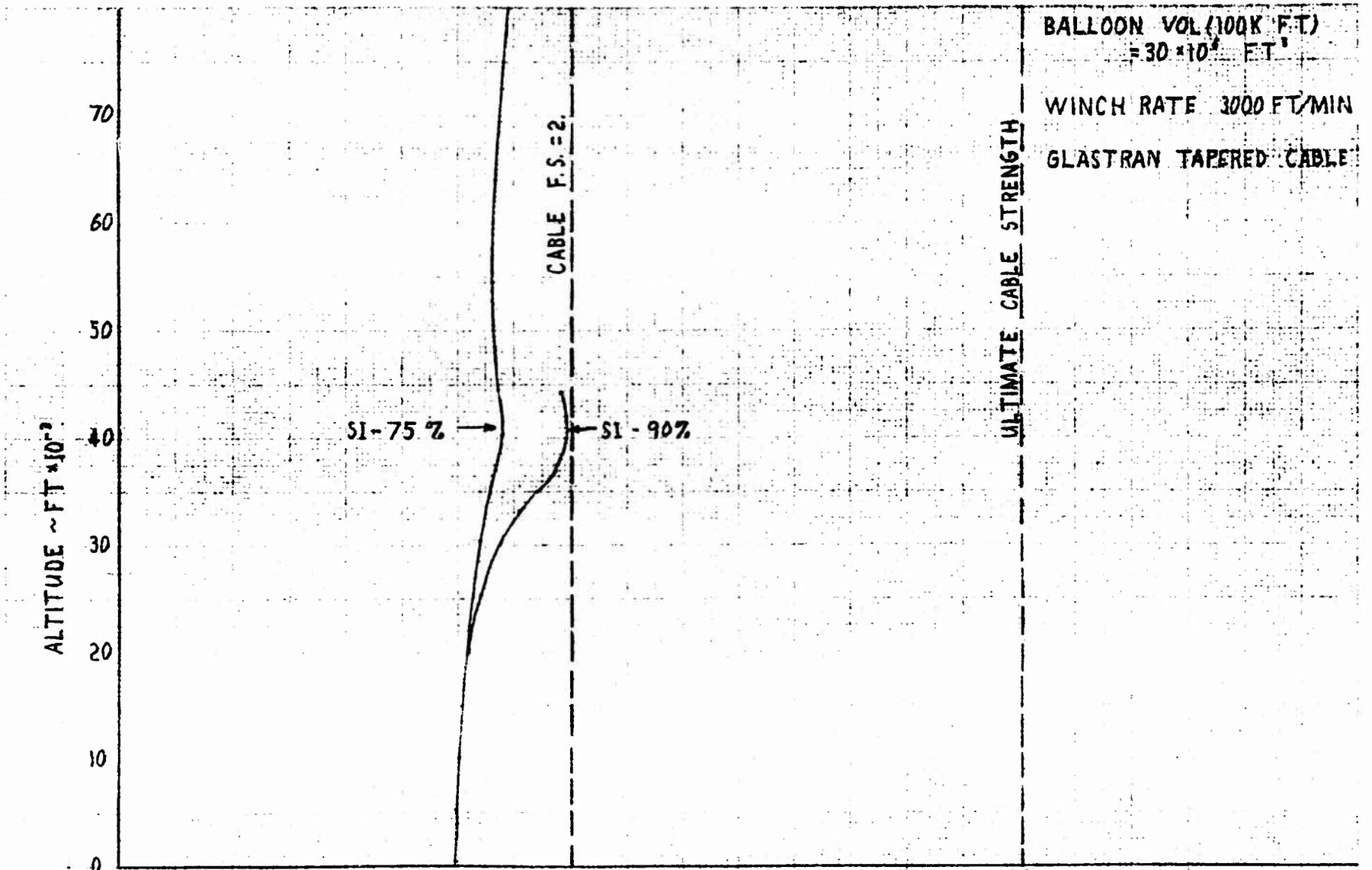

FIG 10

DATE
REV DATE
REV DATE

GOODYEAR AEROSPACE
CORPORATION
AKRON 15, OHIO

PAGE 19
GER- 13714
CODE IDENT NO. 25500

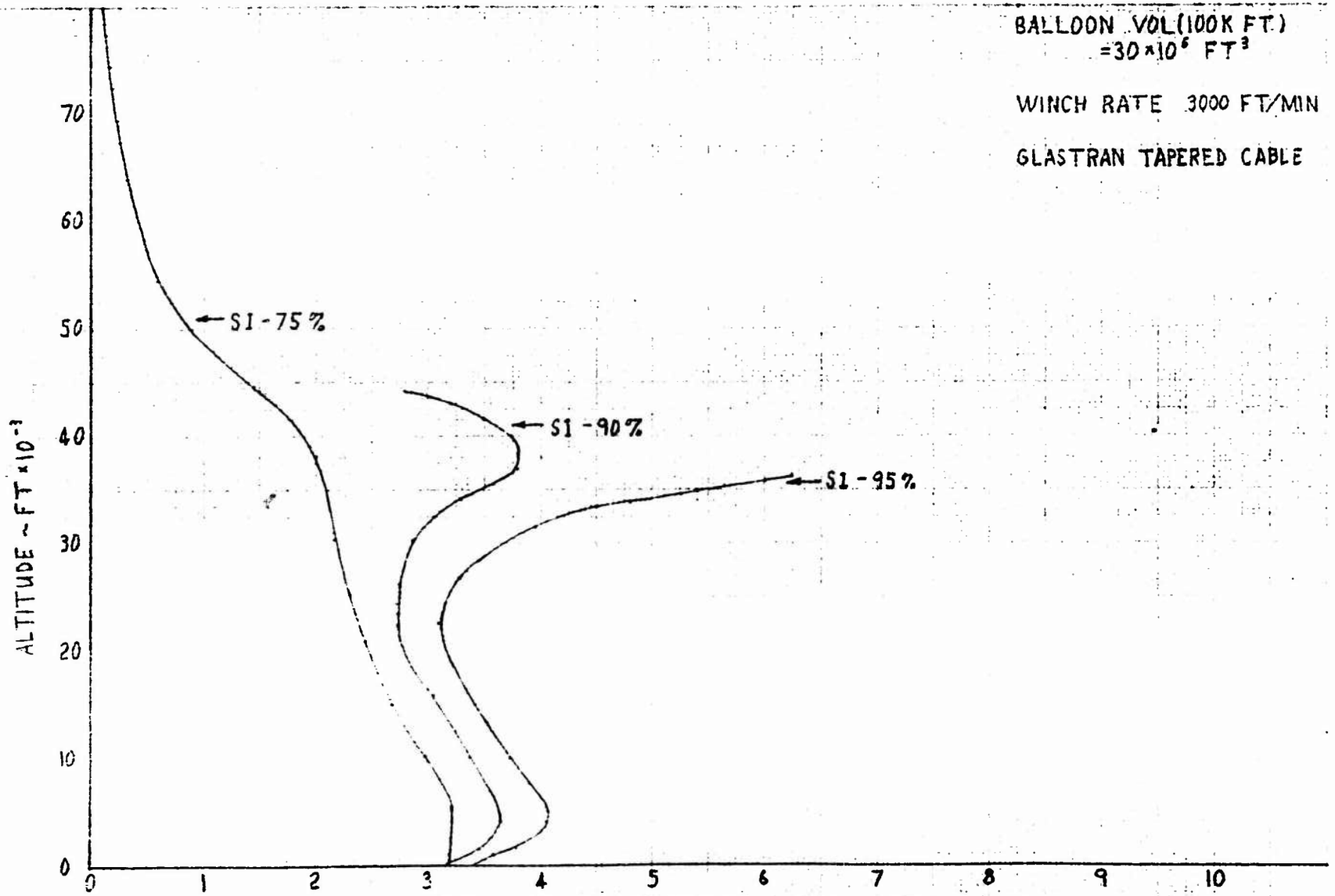

FIG 11

DATE
REV DATE
REV DATE
GOODYEAR AEROSPACE CORPORATION
PAGE 20
GER. 13711
CODE IDENT NO. 25500

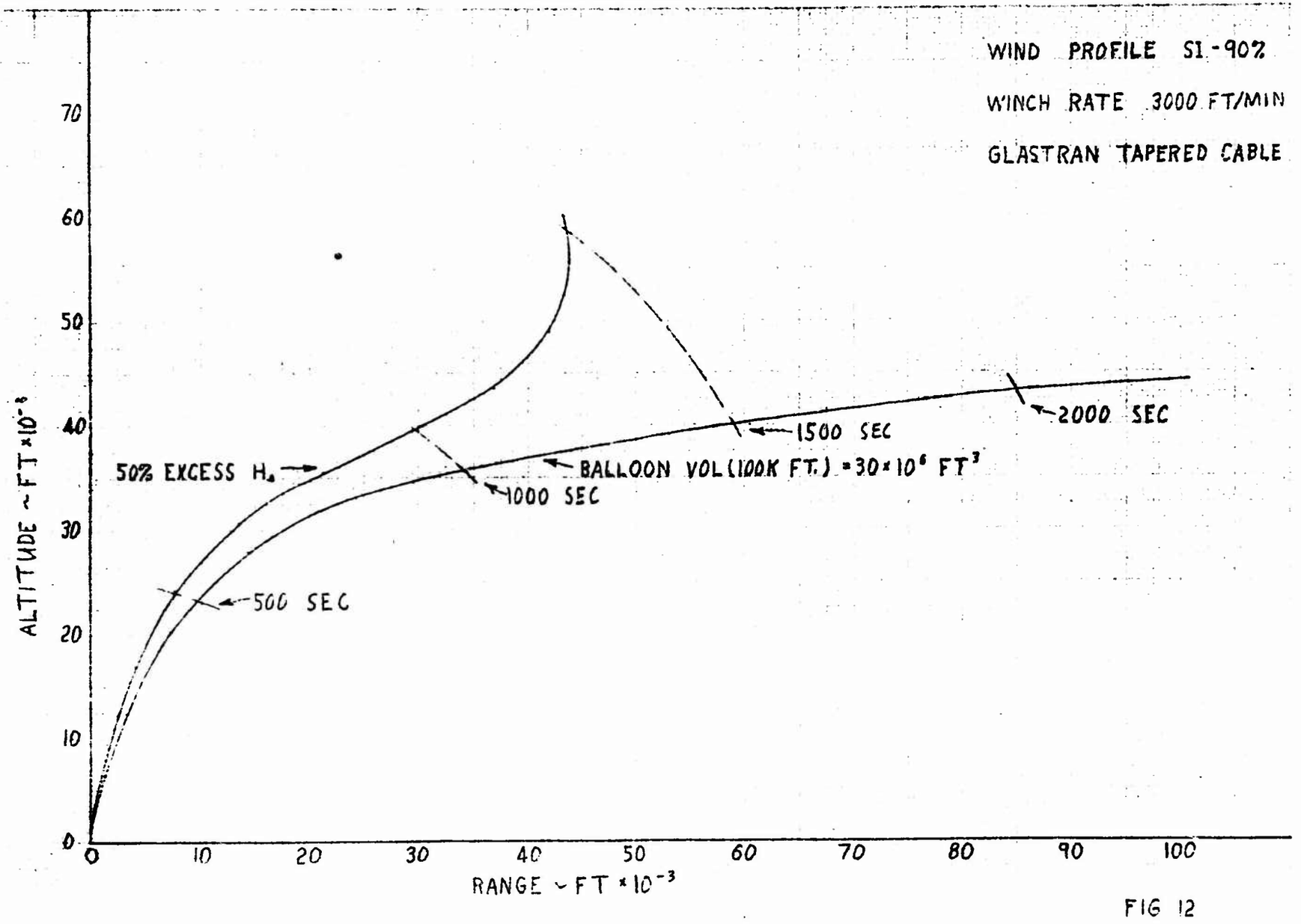

FIG 12

DATE
REV DATE
REV DATE

GOODYEAR AEROSPACE CORPORATION
AKRON 15, OHIO

PAGE 21
GER. 13714
CODE IDENT NO. 25500

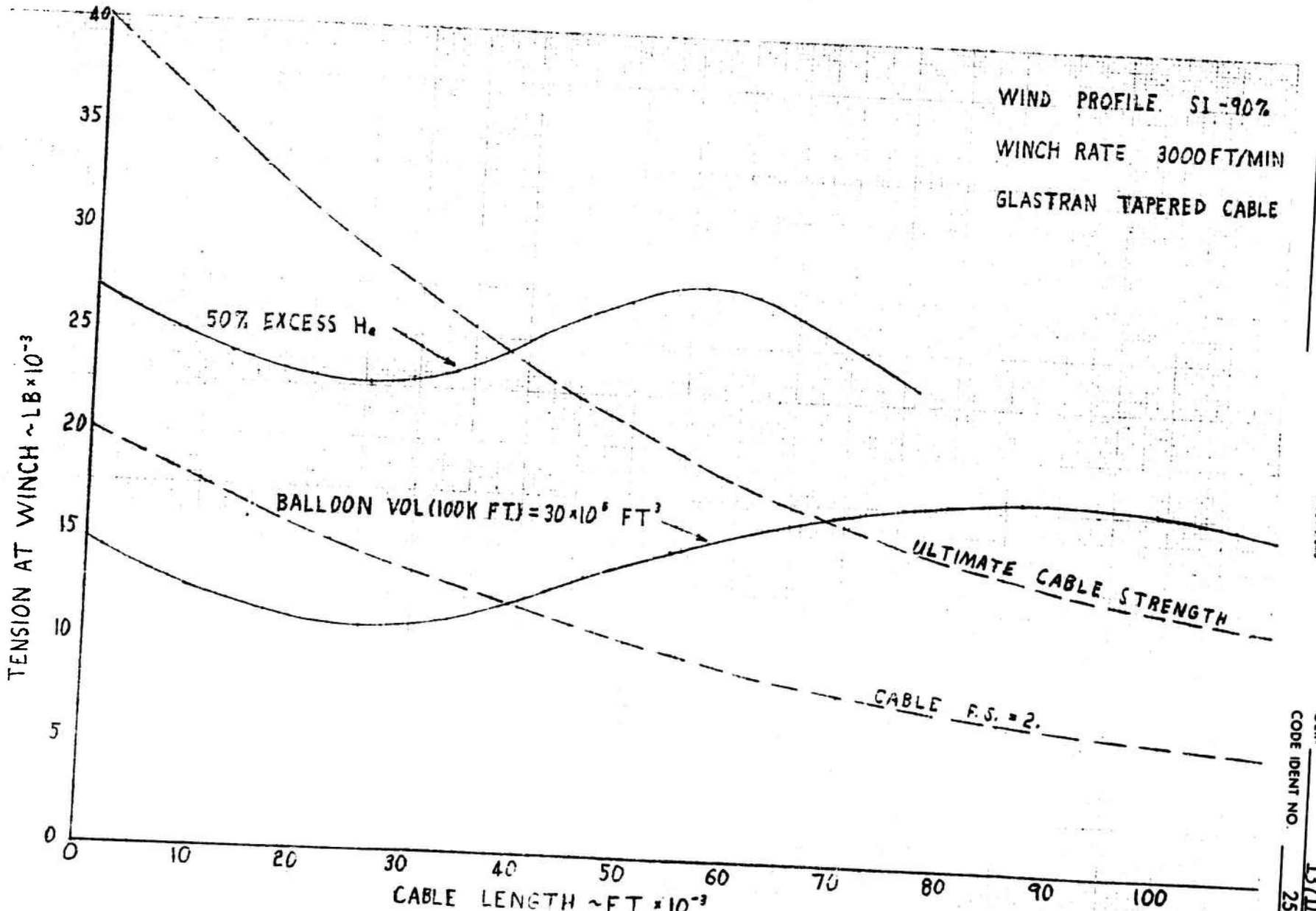

FIG 13

DATE
REV DATE
REV DATE

GOODYEAR AEROSPACE
CORPORATION
AKRON 15, OHIO

PAGE 22
GER. 13714
CODE IDENT NO. 25500

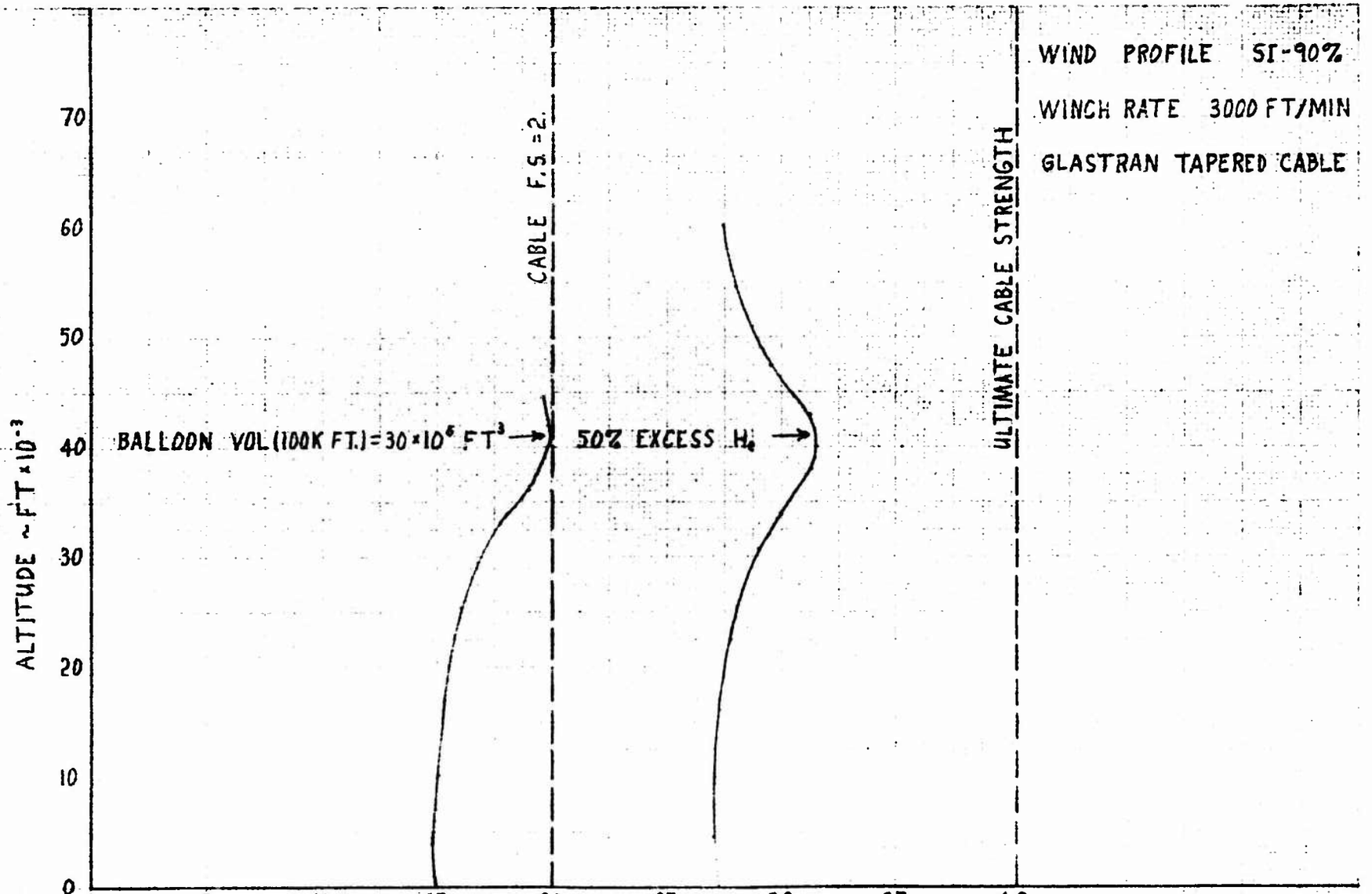

FIG 14

DATE
REV DATE
REV DATE

GOODYEAR AEROSPACE
CORPORATION
AKRON 15, OHIO

PAGE 23
GER. 13714
CODE IDENT NO. 25500

JR 220 (7-63)

REF: ENGRG PROCEDURE S-017

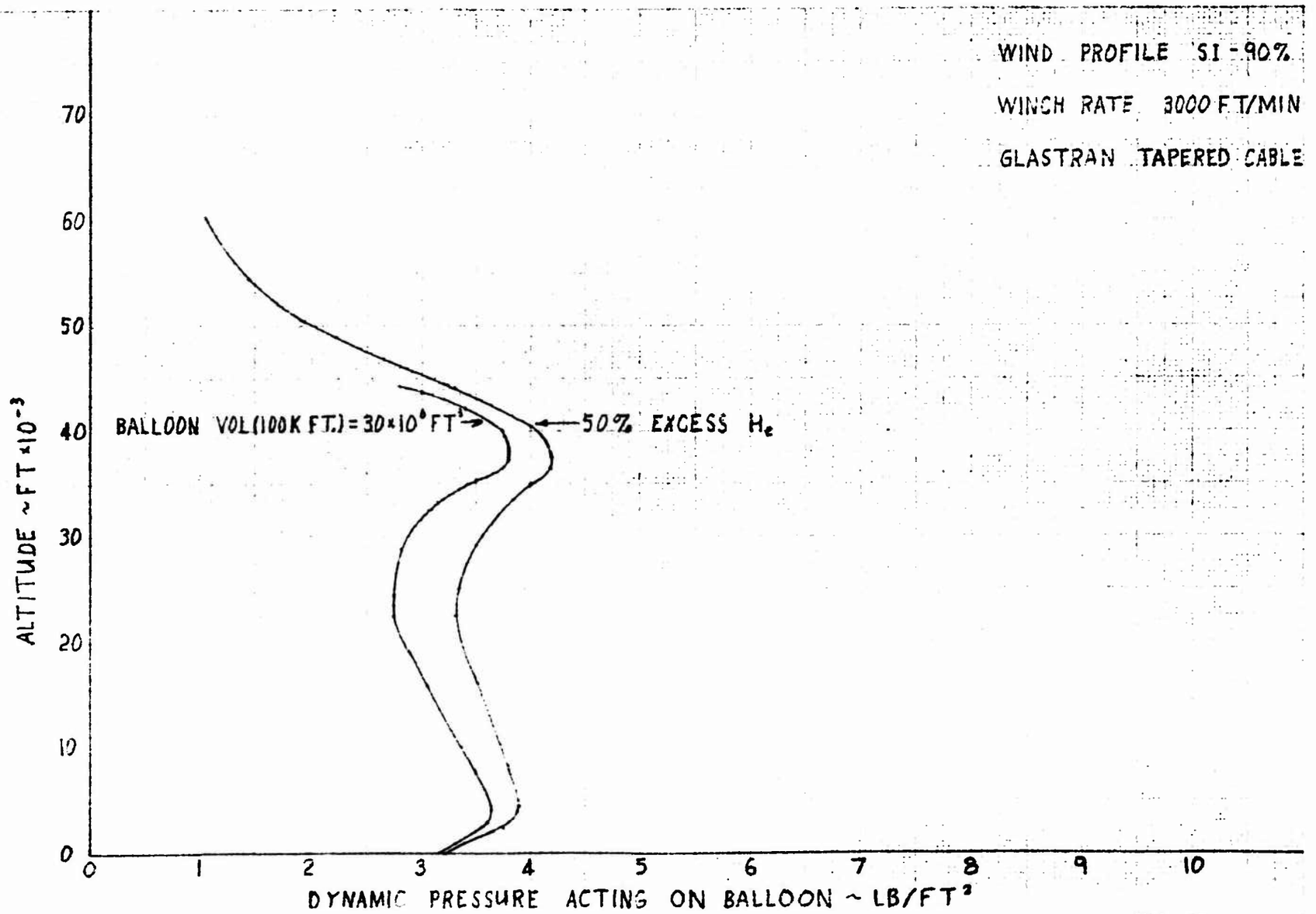

FIG 15

DATE

REV DATE

REV DATE

GOODYEAR AEROSPACE CORPORATION AKRON 15, OHIO

PAGE 24

GER 13714

CODE IDENT NO. 25500

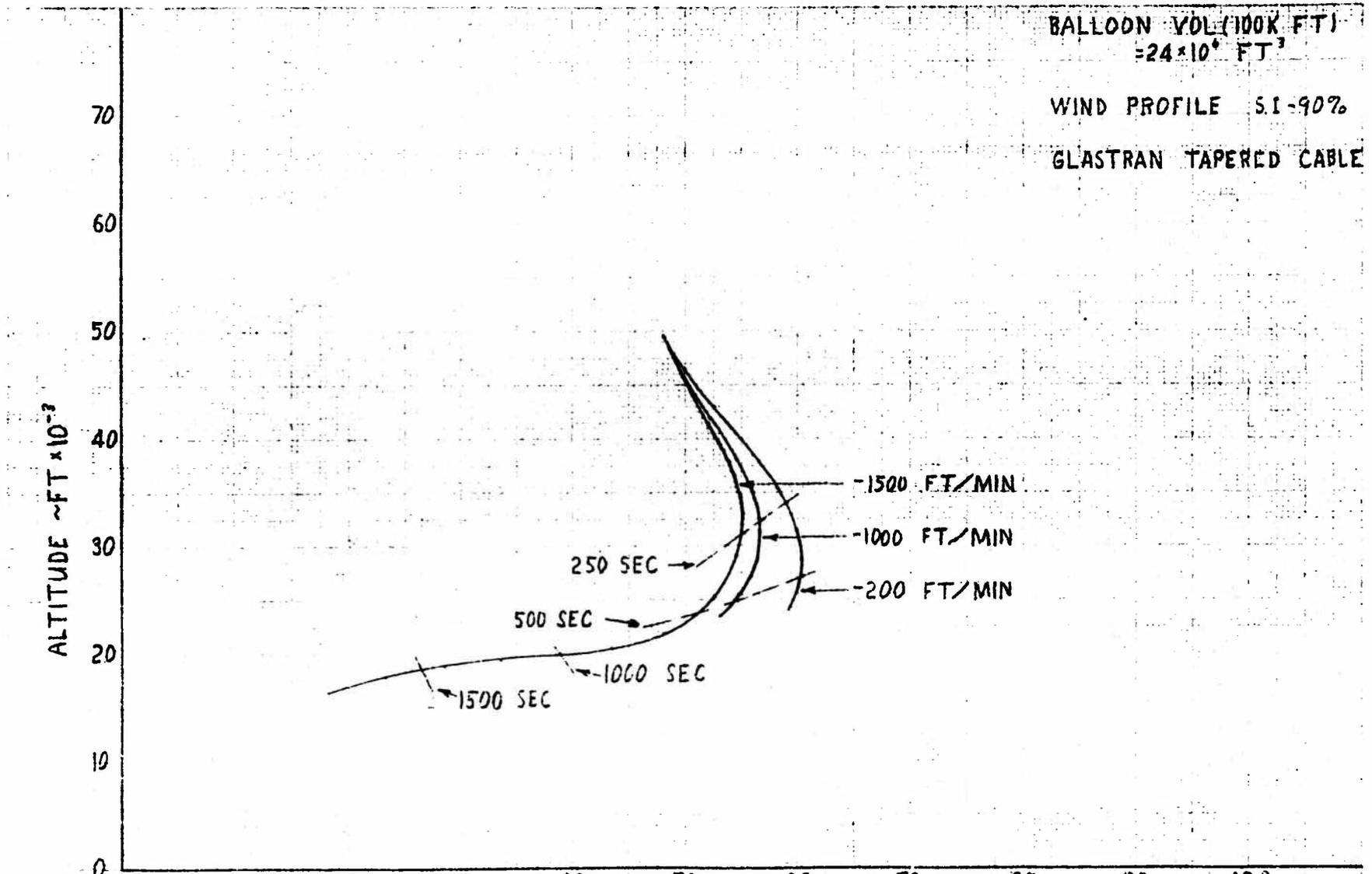

FIG 16

DATE
REV DATE
REV DATE

GOODYEAR AEROSPACE CORPORATION
AKRON 15, OHIO

PAGE 25
GER- 13711
CODE IDENT NO. 25500

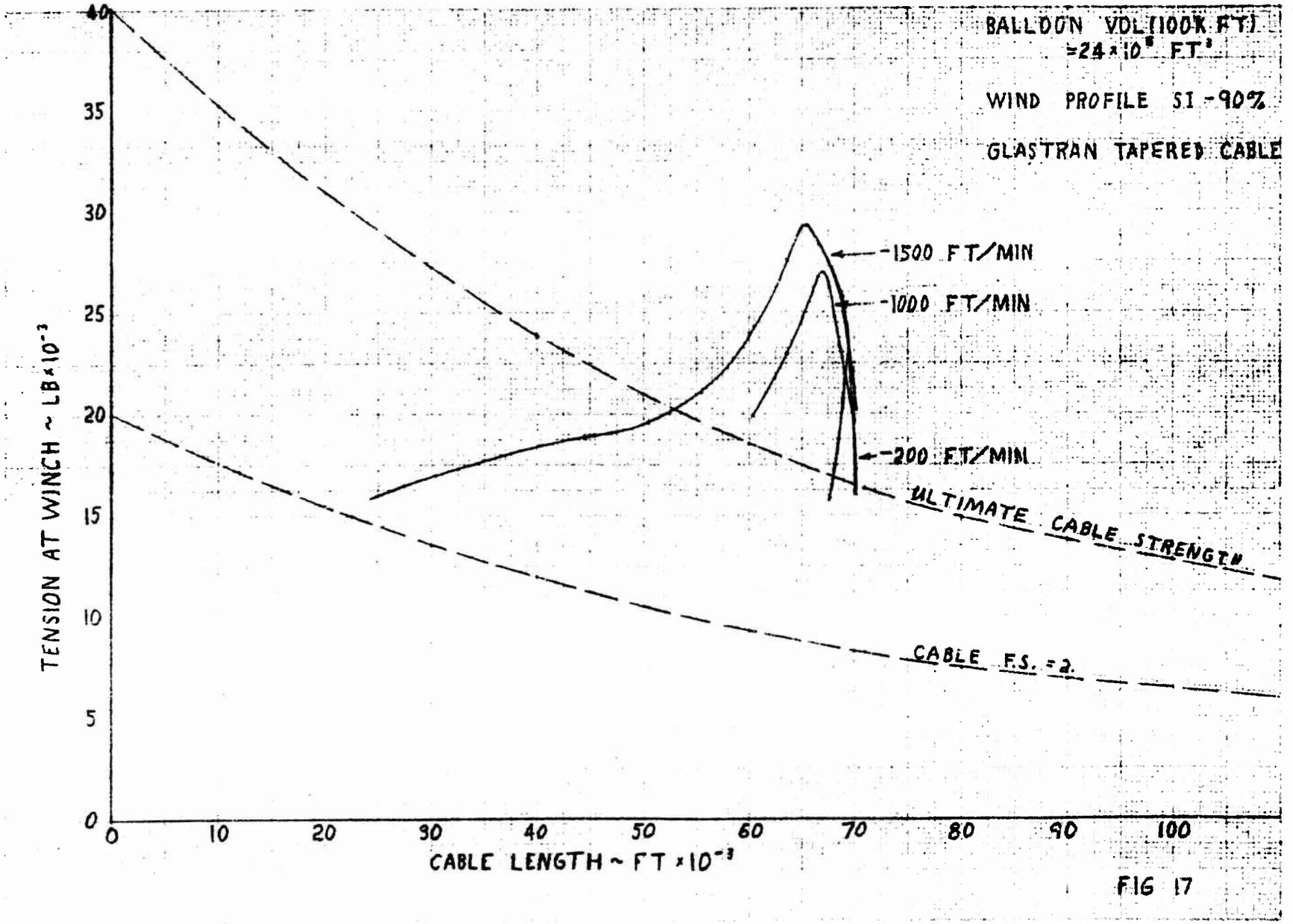

FIG 17

DATE
REV DATE
REV DATE

GOODYEAR AEROSPACE
CORPORATION
AKRON 15, OHIO

PAGE 26
GER. 13714
CODE IDENT NO. 25500

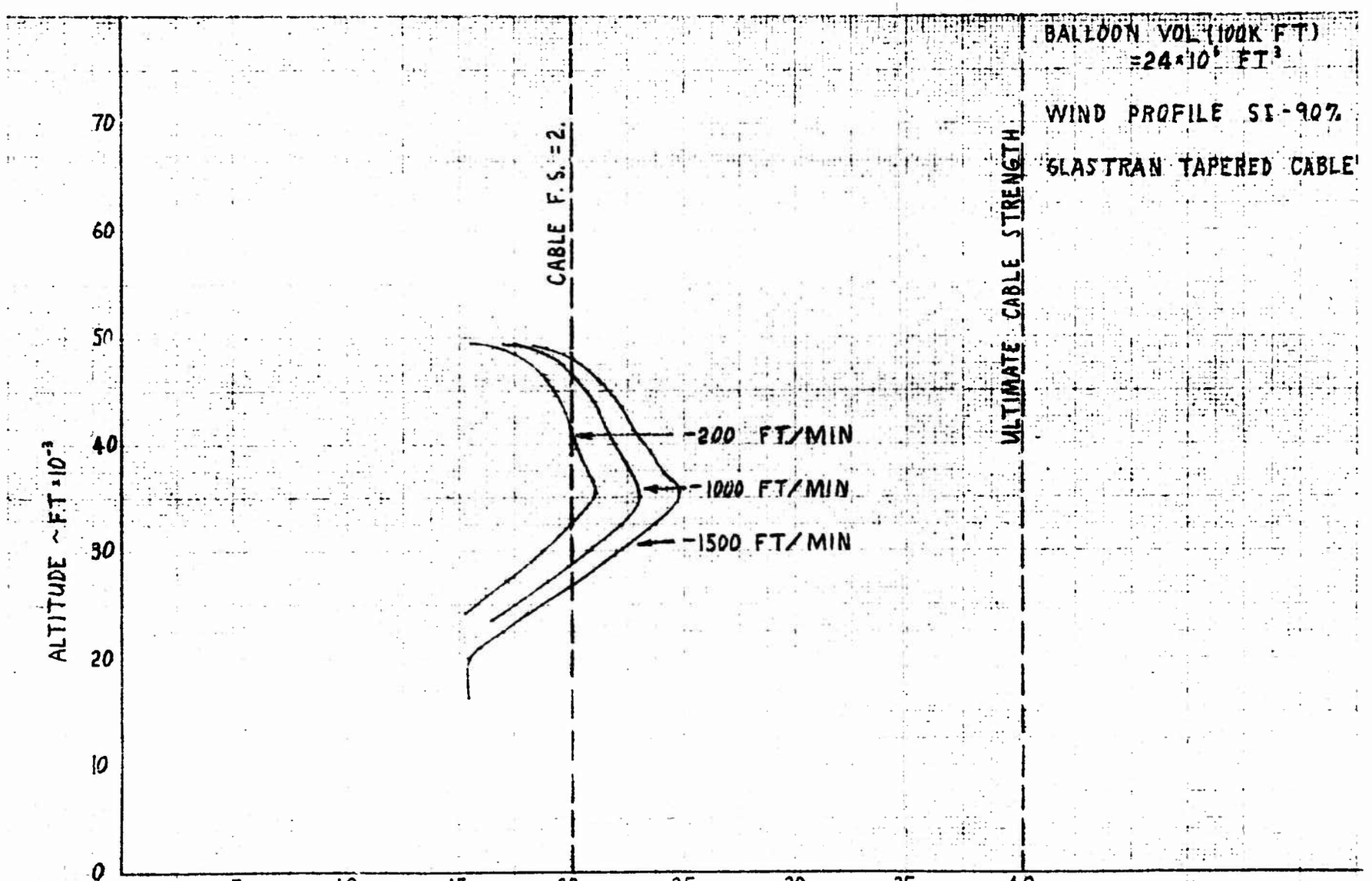

FIG 18

DATE
REV DATE
REV DATE

GOODYEAR AEROSPACE
CORPORATION
AKRON 15, OHIO

PAGE 27
GER. 13714
CODE IDENT NO. 25500

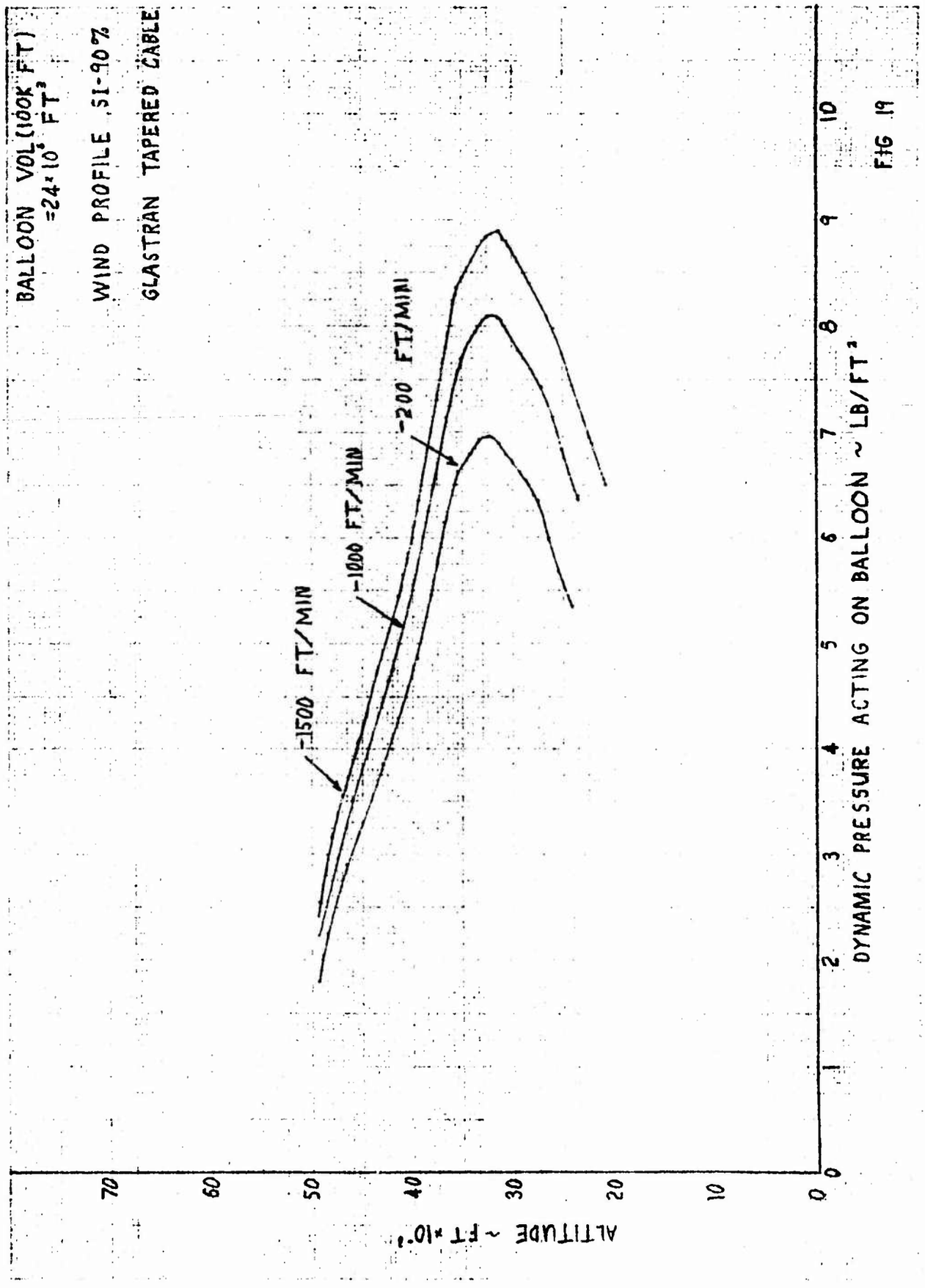

FIG 19

JR 220 (7-63)
REF: ENGRG PROCEDURE S-017

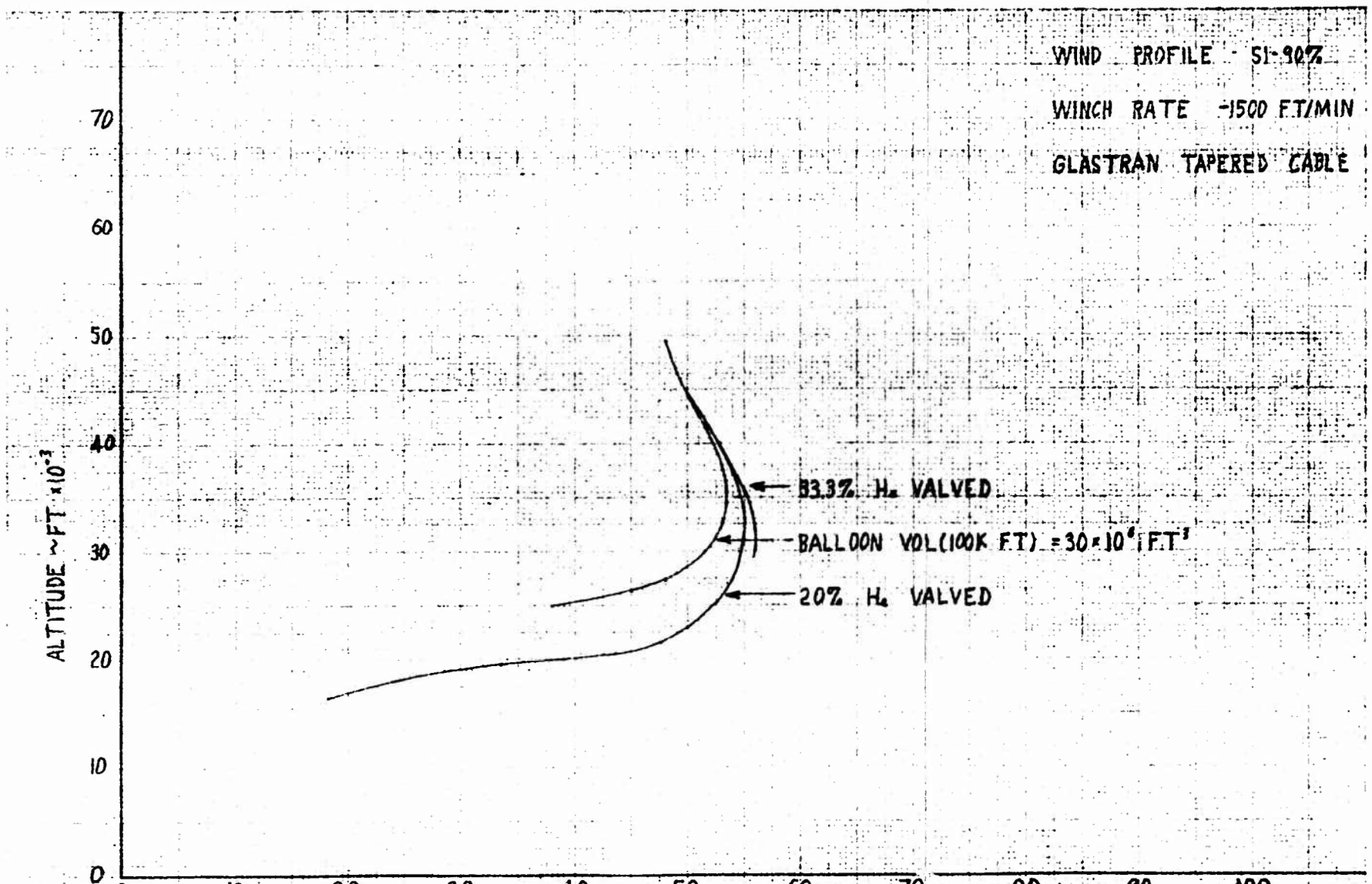

FIG 20

DATE
REV DATE
REV DATE

GOODYEAR AEROSPACE CORPORATION

PAGE 29
GER. 13714
CODE IDENT NO. 25500

JR 220 (7-63)

REF: ENGRG PROCEDURE S-017

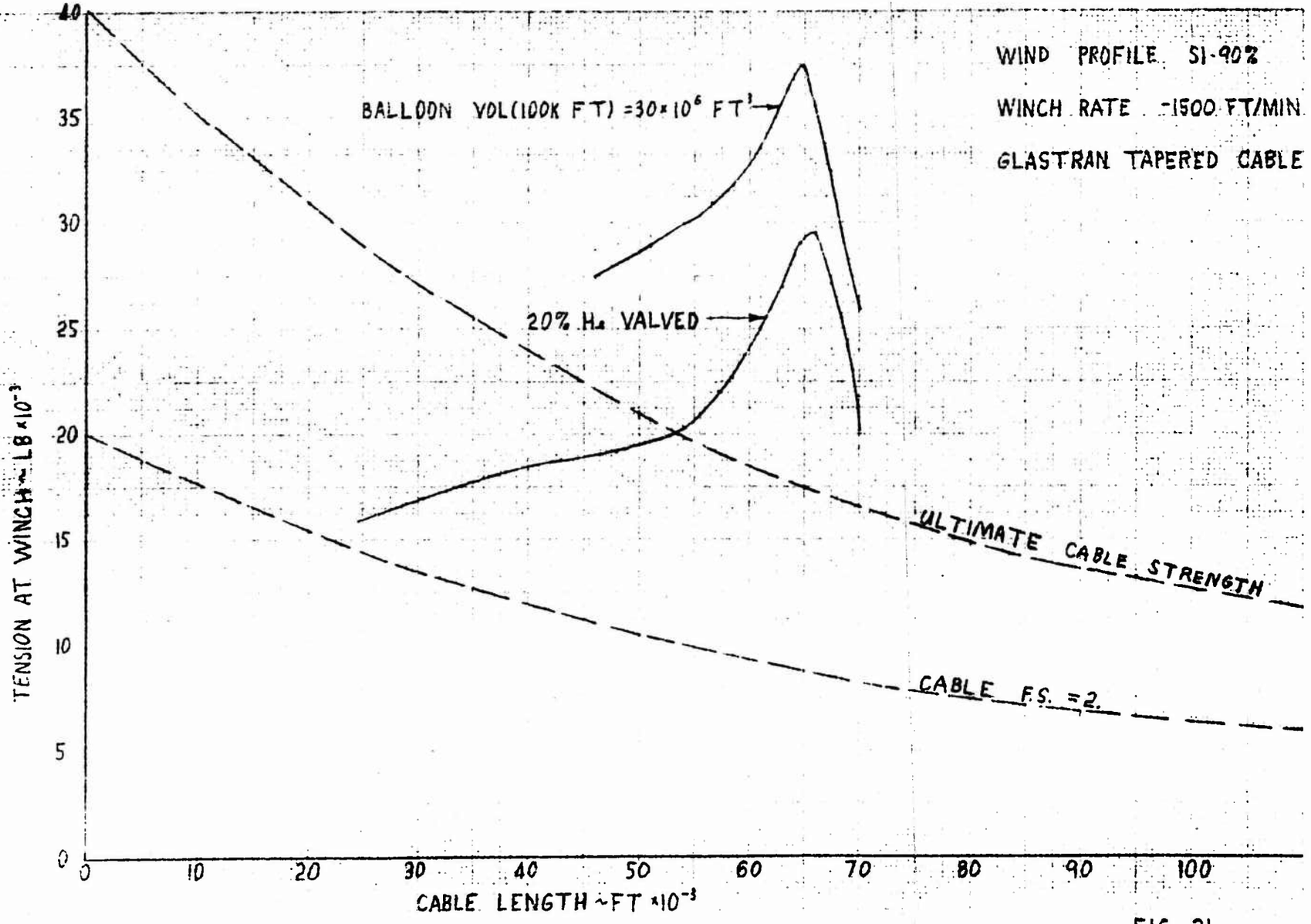

FIG 21

DATE
REV DATE
REV DATE

GOODYEAR AEROSPACE CORPORATION
AKRON 15, OHIO

PAGE 30
GER- 13714
CODE IDENT NO. 25500

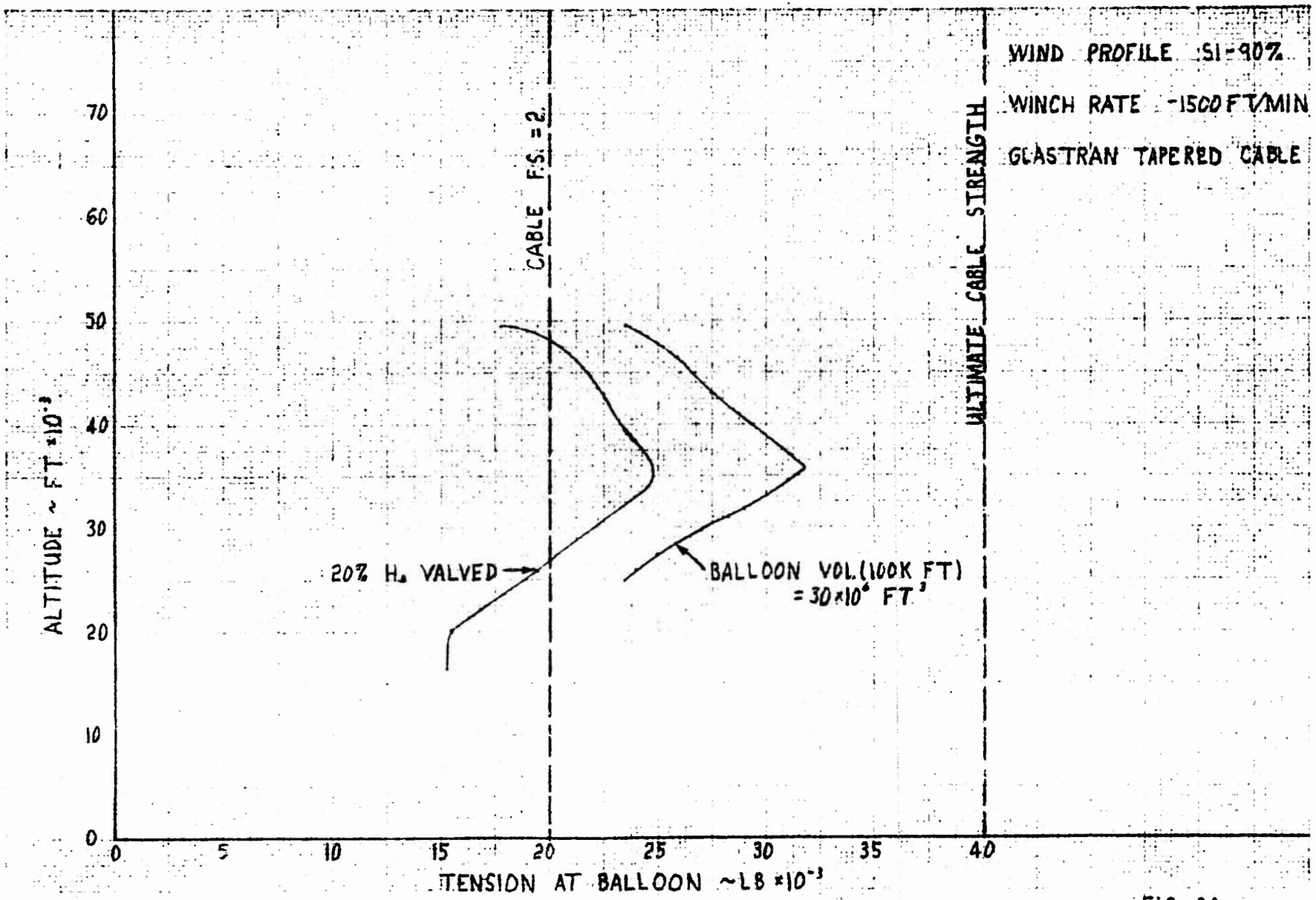

FIG 22

DATE
REV DATE
REV DATE

GOODYEAR AEROSPACE CORPORATION
AKRON, OHIO

PAGE 31
GER. 13714
CODE IDENT NO. 25500

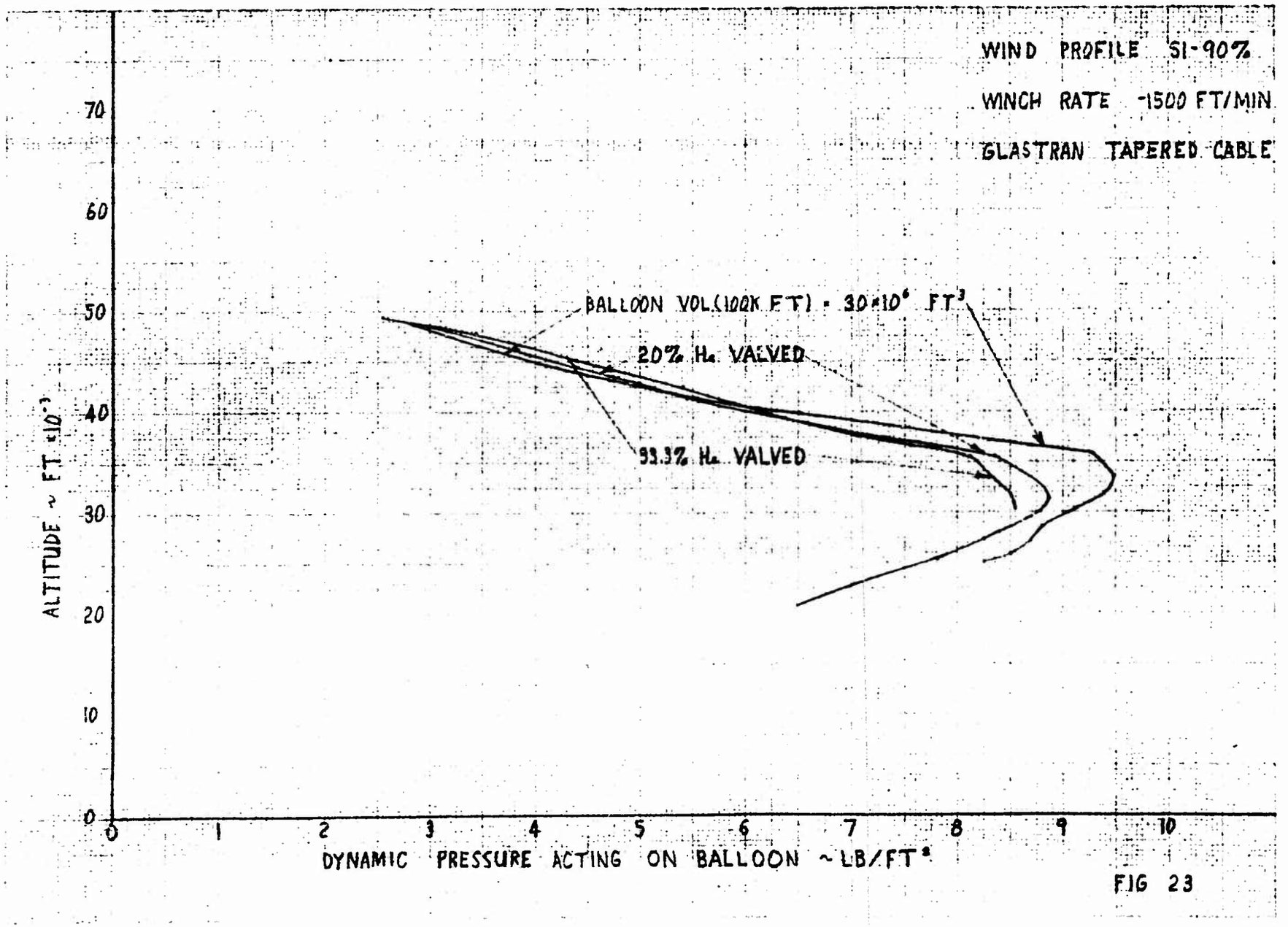

FIG 23

DATE
REV DATE
REV DATE

GOODYEAR AEROSPACE
CORPORATION
AKRON 15, OHIO

PAGE 32
GER. 13714
CODE IDENT NO. 25500

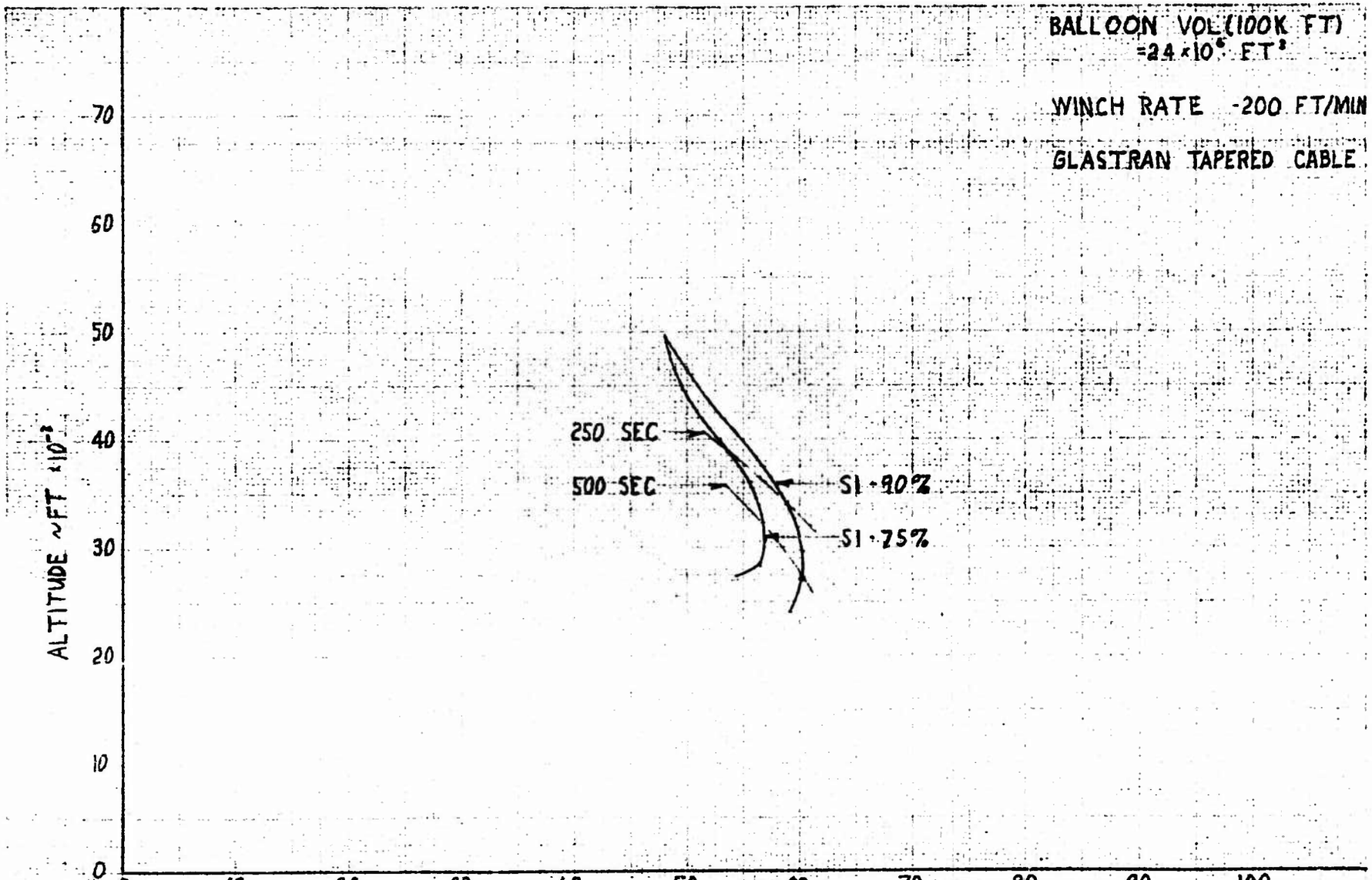

FIG 24

DATE
REV DATE
REV DATE
GOODYEAR AEROSPACE
CORPORATION
AKRON 15, OHIO
PAGE 33
GER. 13714
CODE IDENT NO. 25500

JB 220 (7-63)

REF: ENGBG PROCEDURE S-017

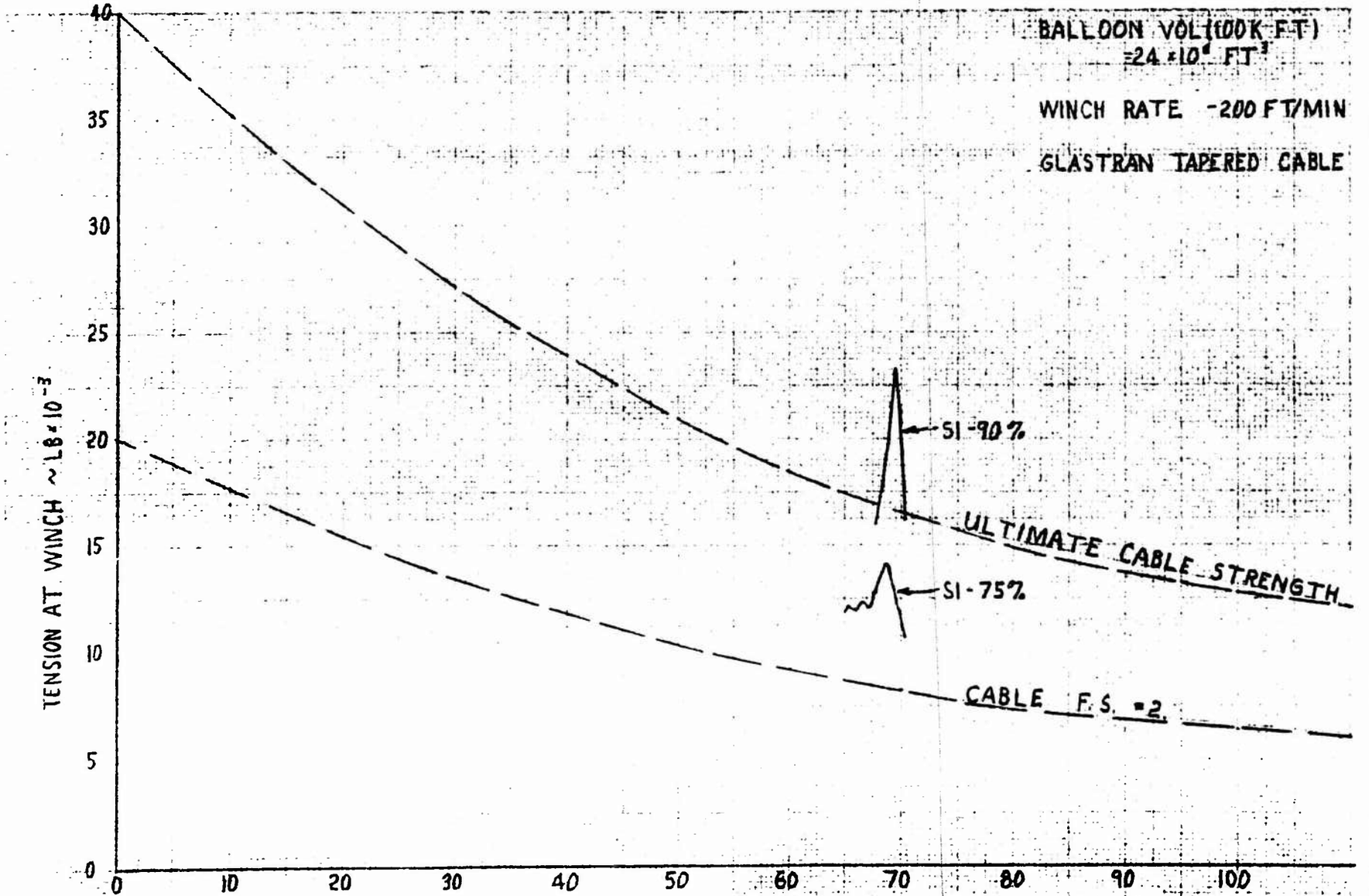

FIG 25

DATE
REV DATE
REV DATE

GOODYEAR AEROSPACE
CORPORATION
AKRON 15, OHIO

PAGE 34
GER. 13714
CODE IDENT NO. 25500

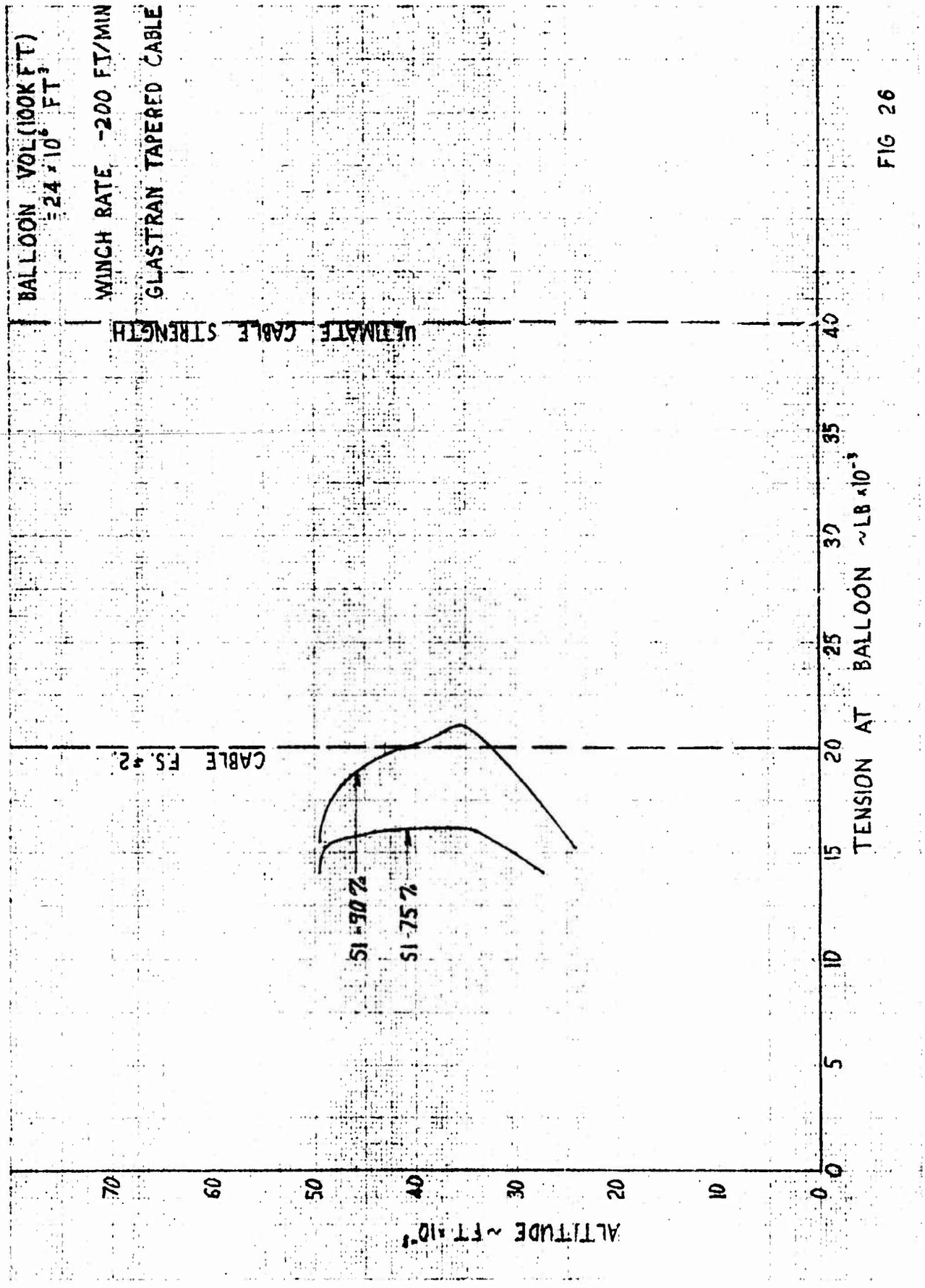

FIG 26

IR 230 (7-63)
REF: DGBG PROCEDURE S-017

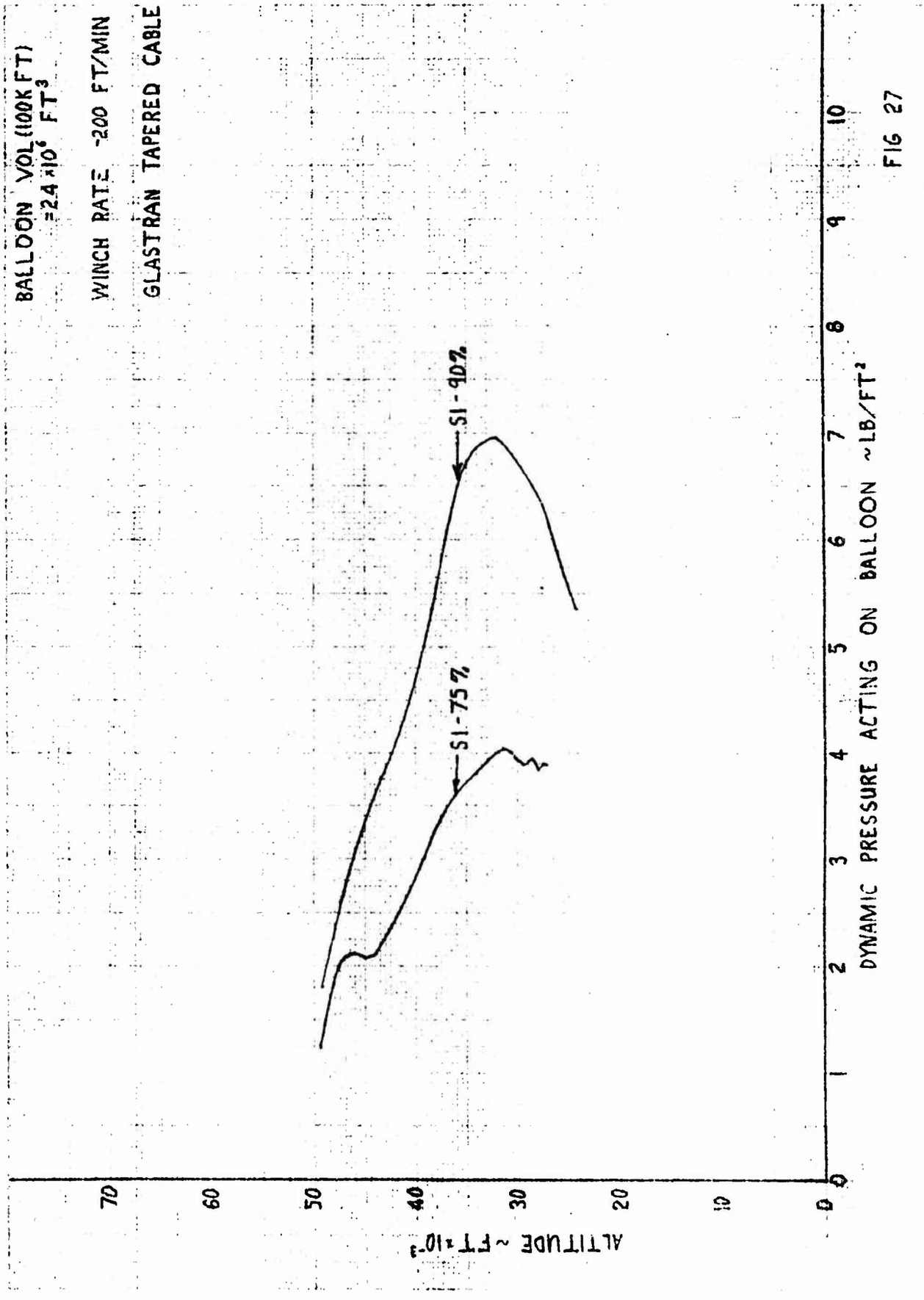
BALLOON VOL (100K FT)
=2.4 ×10⁶ FT³
WINCH RATE -200 FT/MIN
GLASTRAN TAPERED CABLE
S1-90%
S1-75%
ALTITUDE ~ FT ×10⁻³
0
10
20
30
40
50
60
70
DYNAMIC PRESSURE ACTING ON BALLOON ~LB/FT²
0
1
2
3
4
5
6
7
8
9
10

FIG 27

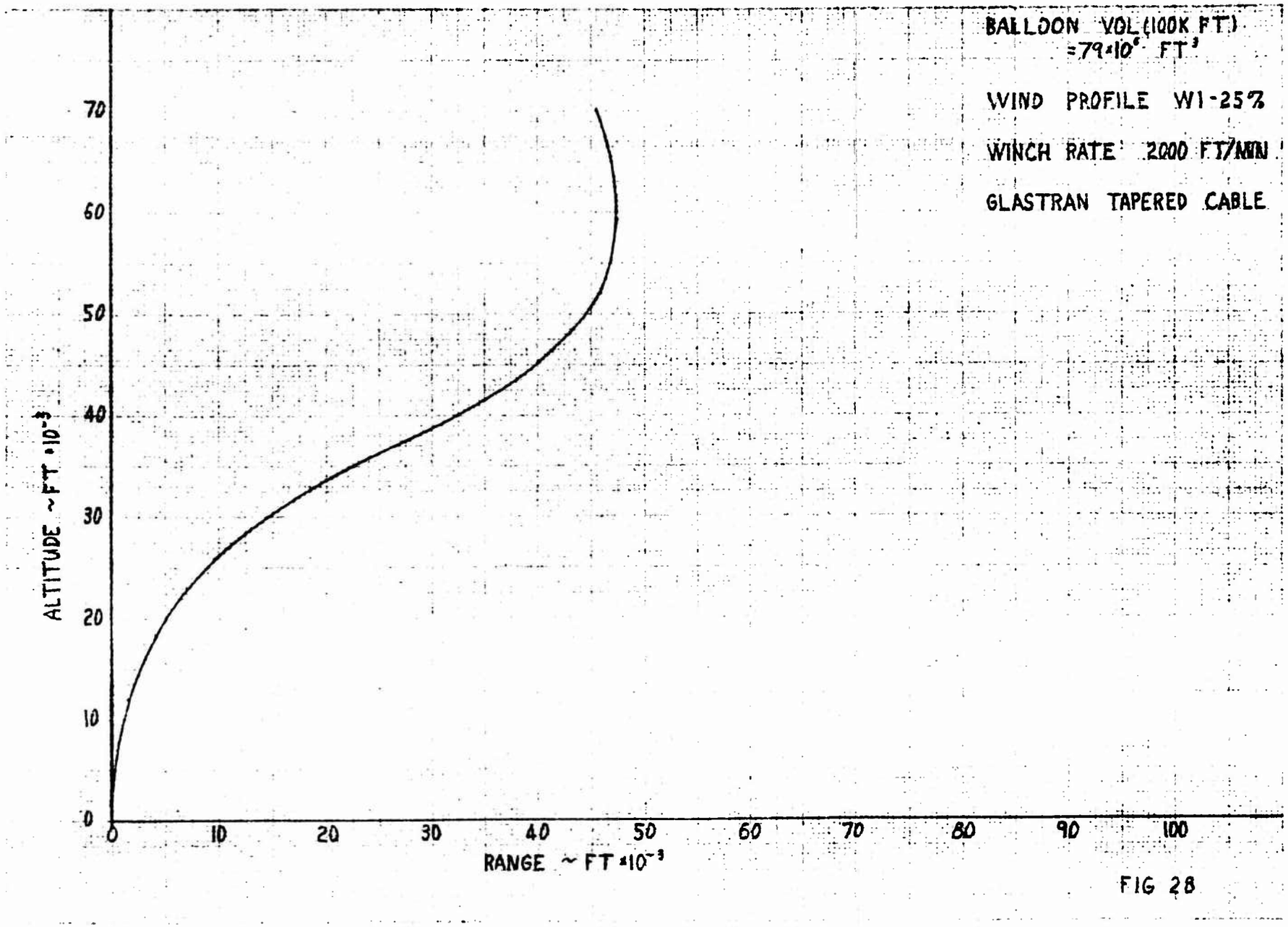

FIG 28

DATE
REV DATE
REV DATE

GOODYEAR AEROSPACE CORPORATION AKRON 15, OHIO

PAGE 37
GER. 13714
CODE IDENT NO. 25500

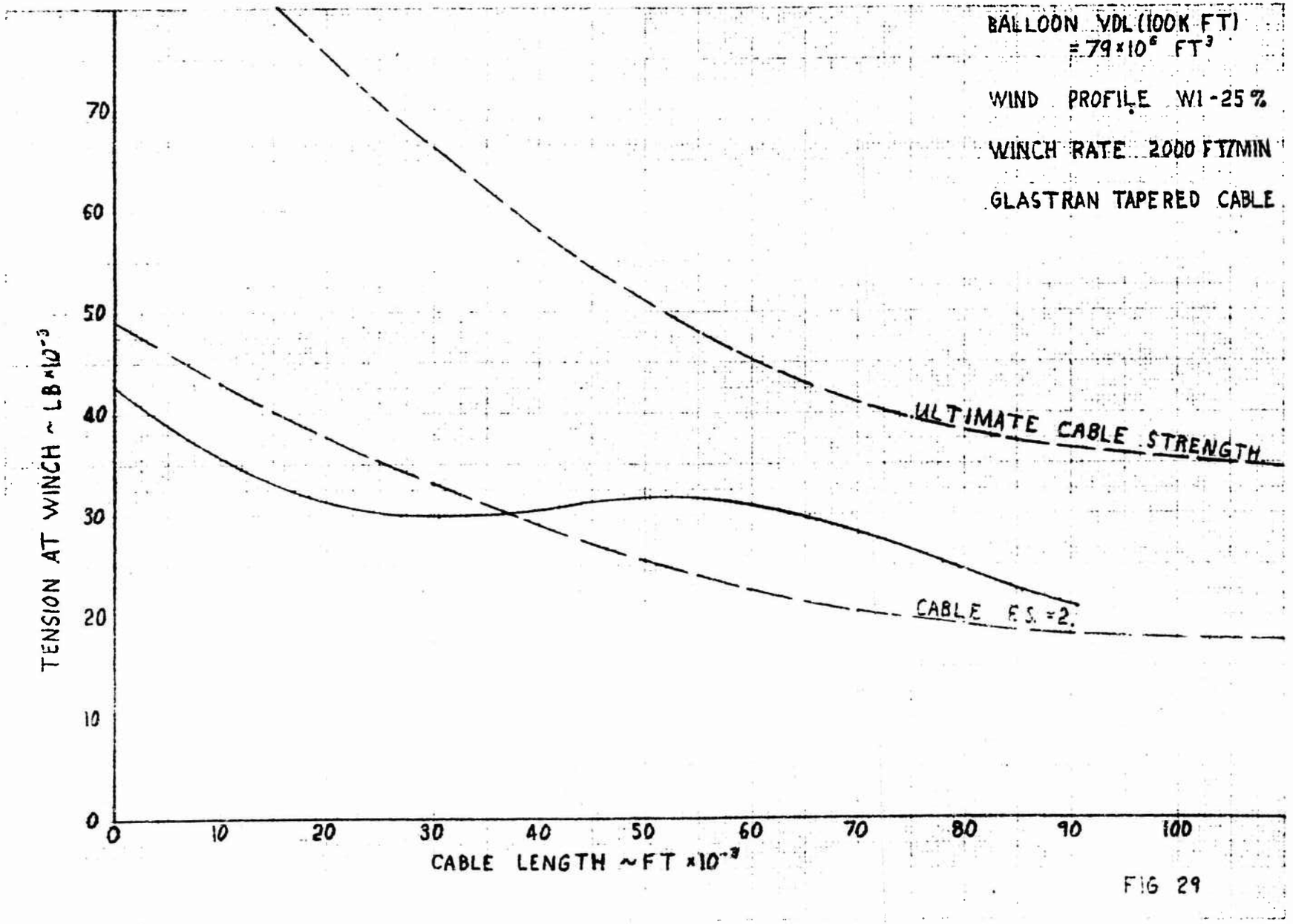

FIG 29

DATE
REV DATE
REV DATE

GOODYEAR AEROSPACE
CORPORATION

PAGE 38
GER. 13714
CODE IDENT NO. 25500

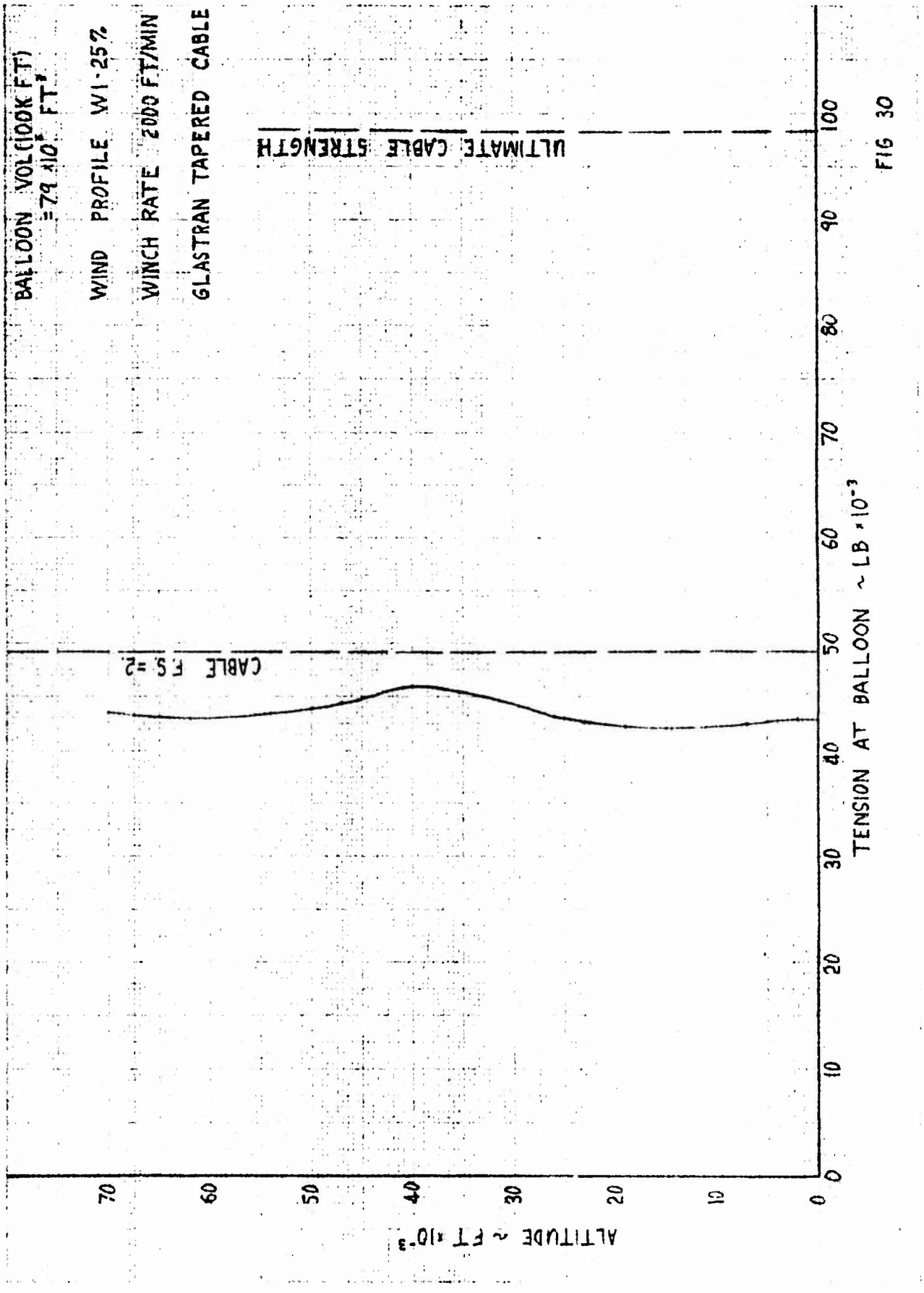
BALLOON VOL(100K FT)
=.79 x10⁸ FT³
WIND PROFILE WI-25%
WINCH RATE 2000 FT/MIN
GLASTRAN TAPERED CABLE
ULTIMATE CABLE STRENGTH
CABLE F.S.=2
TENSION AT BALLOON ~ LB x10⁻³
ALTITUDE ~ FT x10⁻³
0
10
20
30
40
50
60
70
80
90
100

FIG 30

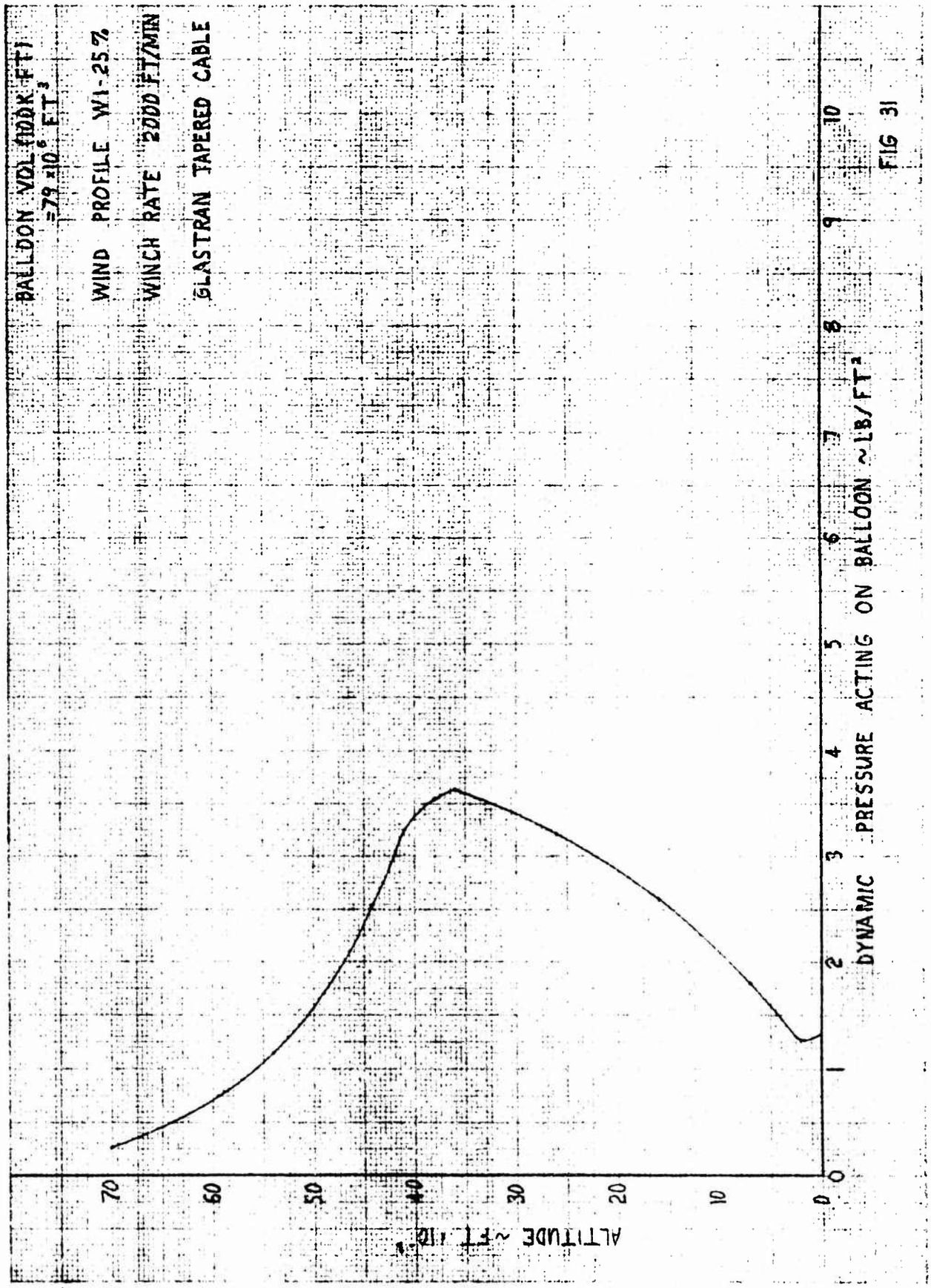
BALLOON VOLUME (100K FT)
=79 x10⁶ FT³
WIND PROFILE W1-25%
WINCH RATE 2000 FT/MIN
GLASTRAN TAPERED CABLE
ALTITUDE ~ FT x 10³
0
10
20
30
40
50
60
70
1
2
3
4
5
6
7
8
9
10
DYNAMIC PRESSURE ACTING ON BALLOON ~ LB/FT²

FIG 31

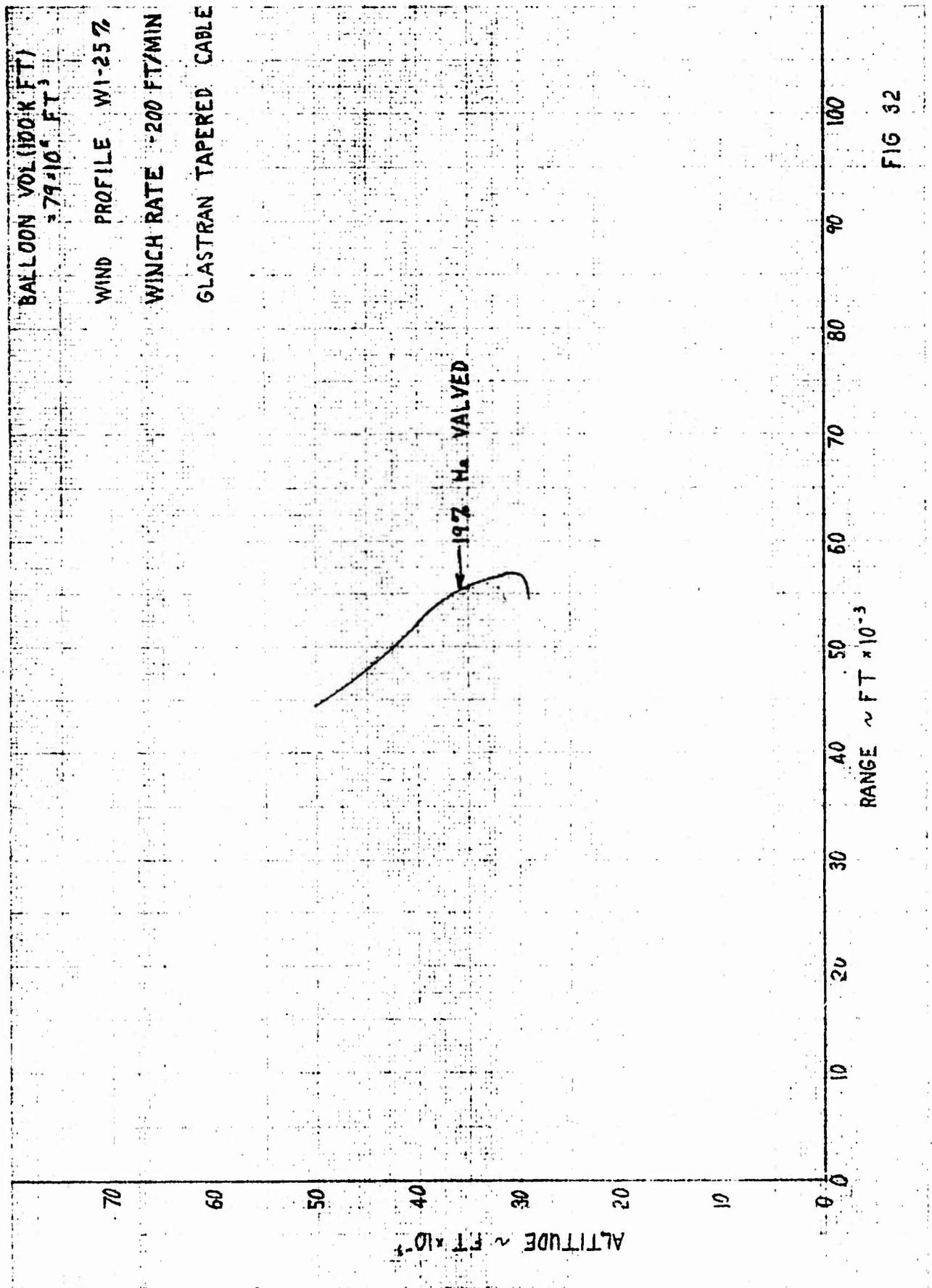
BALLOON VOL (100 K FT)
= 79 x 10⁶ FT³
WIND PROFILE W1-25%
WINCH RATE -200 FT/MIN
GLASTRAN TAPERED CABLE
19% He VALVED
ALTITUDE ~ FT x 10⁻³
RANGE ~ FT x 10⁻³
0
10
20
30
40
50
60
70
80
90
100

FIG 32

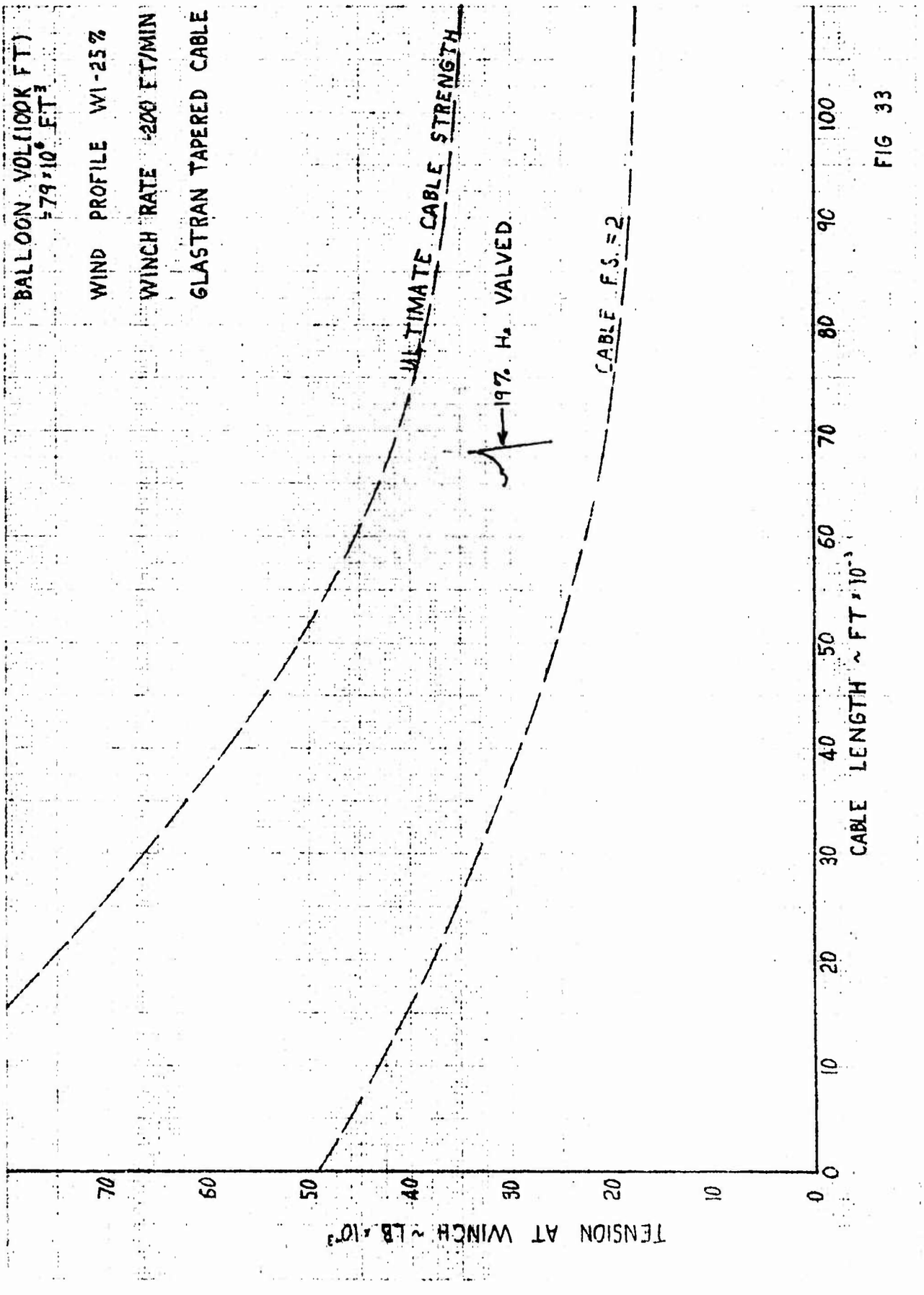
BALLOON VOL (100K FT)
~79*10^6 FT^3
WIND PROFILE WI-25%
WINCH RATE ~200 FT/MIN
GLASTRAN TAPERED CABLE
ULTIMATE CABLE STRENGTH
19% H2 VALVED
CABLE F.S.=2
TENSION AT WINCH ~ LB *10^3
CABLE LENGTH ~ FT * 10^-3
0
10
20
30
40
50
60
70
80
90
100

FIG 33

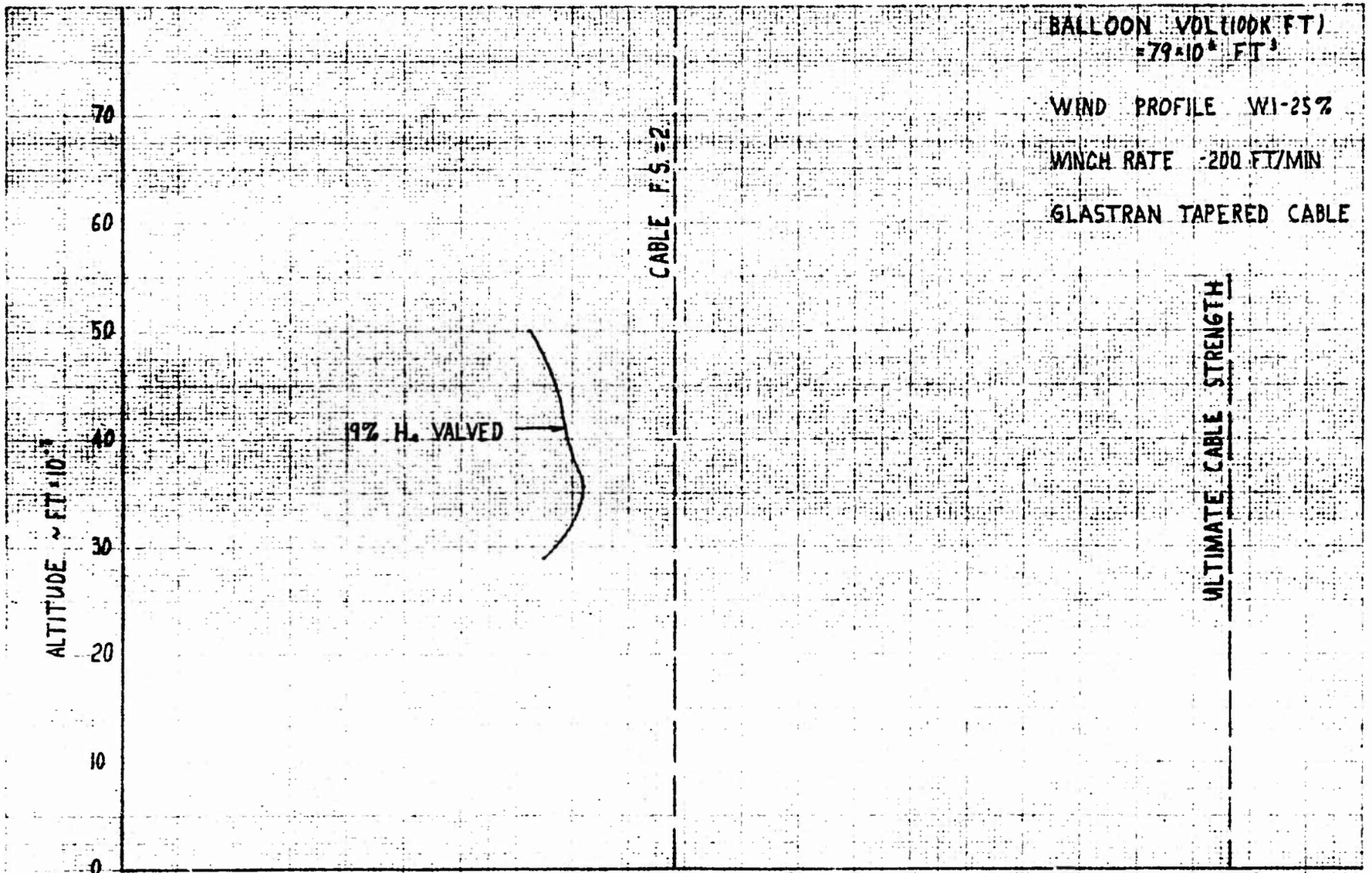

FIG 34

DATE
REV DATE
REV DATE

GOODYEAR AEROSPACE CORPORATION
AKRON 15, OHIO

PAGE 43
GER. 13714
CODE IDENT NO. 25500

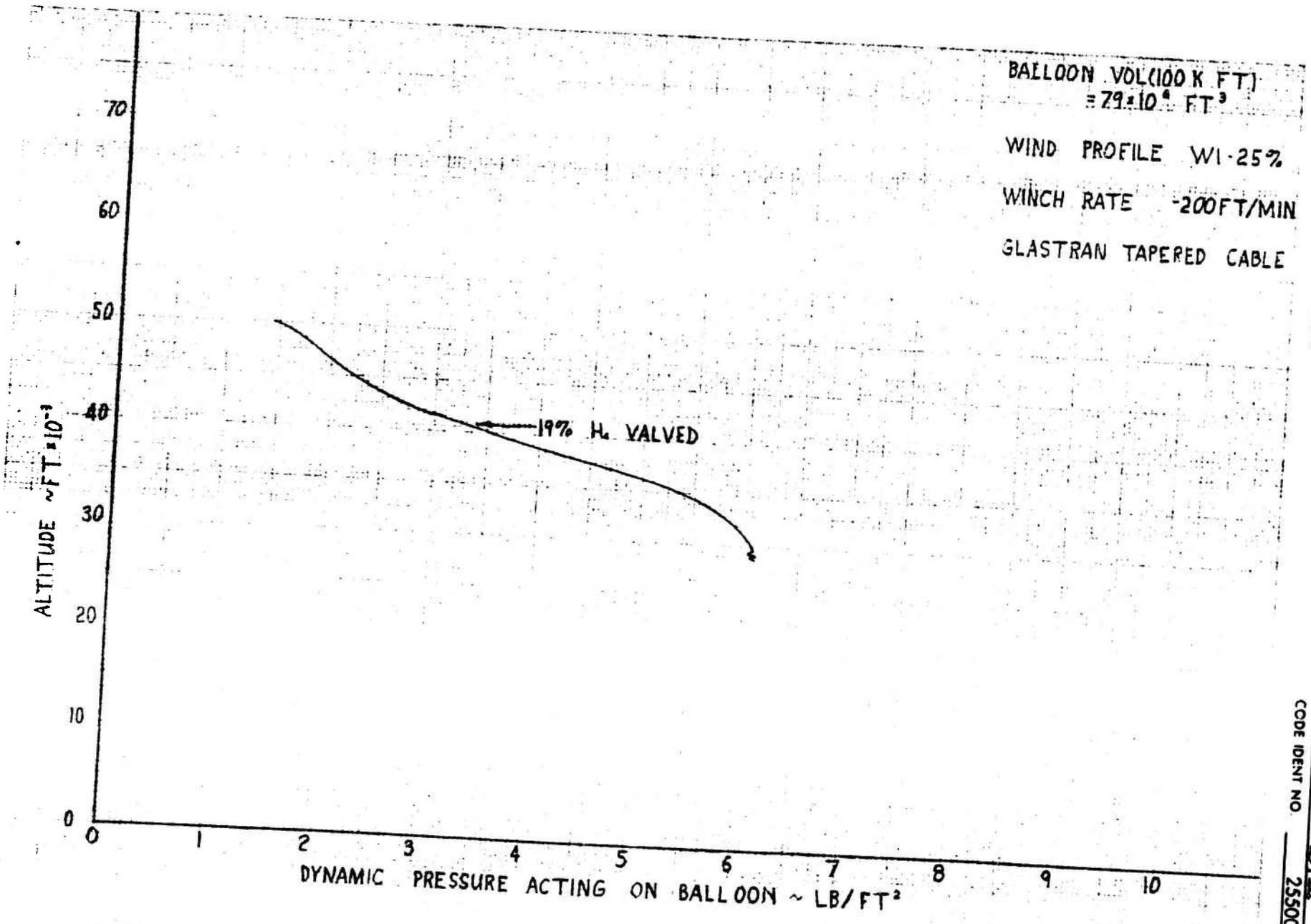

FIG 35

DATE
REV DATE
REV DATE

GOODYEAR AEROSPACE
CORPORATION
AKRON 15, OHIO

PAGE 44
GER. 13714
CODE IDENT NO 25500

SECTION V - REFERENCES

1. Dynamics of Tethered Balloon in the Longitudinal Plane, Odin R. Elnan, Ph.D., and Carl T. Evert, Ph.D., Goodyear Engineering Report 12901, October 1966.

2. Classical Mechanics, H. Goldstein, Ph.D., Addison-Wesley, Cambridge, Mass., 1950.

3. High-Altitude Tethered Balloon Systems Study, James A. Menke, Goodyear Aerospace Corporation, Contract F19628-67-C-0145, May 10, 1967.

4. AFCRL Memorandum, dated 20 December 1967, "Wind Data," from Edward J. Young, Captain USAF to J. J. Vorachek.

5. High-Altitude Tethered Balloon Systems Study, Jerome J. Vorachek, Goodyear Engineering Report 13552, November 30, 1967.

REF: ENGINEERING PROCEDURE S-017

APPENDIX A

Equations of Motion

1. General

Using Lagrangian techniques and assuming the system can be simulated by a tether of "N" straight links with a balloon hinged to the top link, two differential equations can be derived. The position of the winch on a flat non-rotating earth is considered to be the origin of an inertia coordinate system. The first equation expresses the motion of the balloon about its hinge point; and the second expresses the motion of any link about its lower connection point. The derivation and notation follow very closely the work of Professors Odin R. Elnan and Carl T. Evert (Reference 1).

Lagrange's differential equations of motion (Reference 2) for the system are:

$$\frac{d}{dt}\left(\frac{\partial T}{\partial \dot{\theta}}\right) - \frac{\partial T}{\partial \theta} = F_{\theta} \tag{1}$$

$$\frac{d}{dt}\left(\frac{\partial T}{\partial \dot{\phi}_r}\right) - \frac{\partial T}{\partial \phi_r} = F_{\phi_r} \tag{2}$$

where the generalized coordinates are θ and ϕ_r (r = 1, ..., N), the generalized forces are F_{θ} and F_{ϕ_r} (r = 1, ..., N) and T is the total

REF: ENGINEERING PROCEDURE S.017

kinetic energy of the system. It should be noted that the coordinate θ could be chosen as ϕ_{N+1}.

2. Cable Representation

The tether (as shown in Figure A-1) is represented by "N" links, each of constant length. However, the length as well as the mass of each link is assumed to be a function of the winching rate and cable profile. Each link is considered rigid, and each hinge frictionless. Therefore, all forces but no moments can be transferred through a hinge.

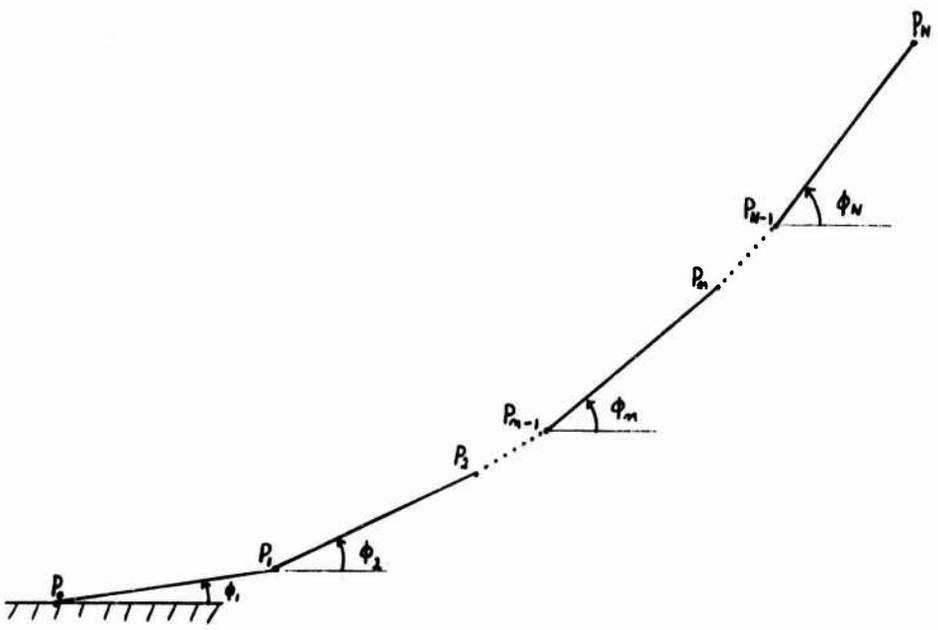

Figure A-1 - Tether Model

REF: ENGINEERING PROCEDURE S-017
54)(77

The angle that each link makes with the horizontal (measured positive for counterclockwise rotations) is ϕ_i (i = 1, ..., N). It is assumed that all external forces acting on a link can be concentrated at the geometric center of the link. This introduces an obvious error for both the aerodynamic and gravitational forces. However, since the ability to locate the center of pressure and center of mass for each link contributes to the complexity of the derivation and computer simulation, it seems reasonable to ignore the error at this point.

A typical link is shown in Figure A-2.

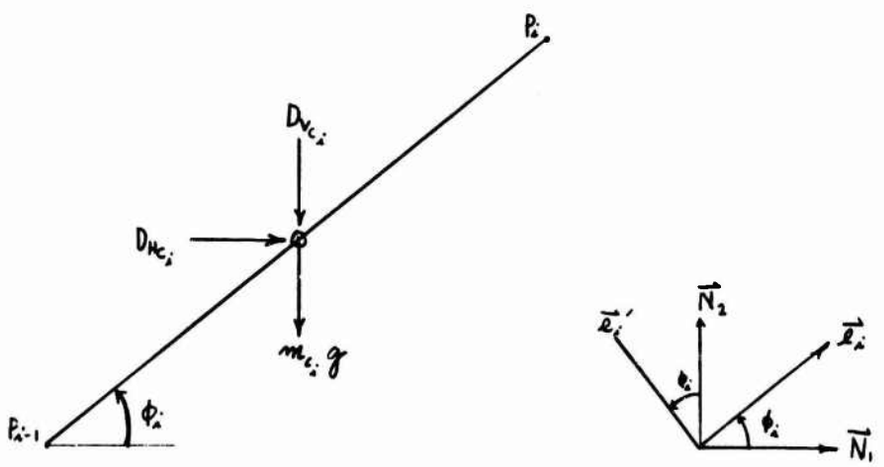

Figure A-2 - A Typical Link

REF: ENGINEERING PROCEDURE S.017

P_i^* denotes the mass center of the "i"th link and is assumed to be a distance of $\ell_c/2$ from the hinge point P_{i-1}.

For one link:

$$\vec{r}_1 = \frac{\ell_{c_1}}{2}\,\vec{e}_1 \tag{3}$$

$$\dot{\vec{r}}_1 = \vec{V}^{P_1^*} = \frac{\ell_{c_1}}{2}\,\dot{\phi}_1\,\vec{e}_1' + \frac{\dot{\ell}_{c_1}}{2}\,\vec{e}_1 \tag{4}$$

$$\vec{V}^{P_1} = \ell_{c_1}\,\dot{\phi}_1\,\vec{e}_1' + \dot{\ell}_{c_1}\,\vec{e}_1 \tag{5}$$

where $\vec{r}_i$ is the position vector from P_o to P_i^*.

For two links:

$$\dot{\vec{r}}_2 = \vec{V}^{P_2^*} = \vec{V}^{P_1} + \vec{V}^{P_2^*/P_1} \tag{6}$$

where $\vec{V}^{P_i^*/P_{i-1}}$ denotes the velocity of P_i^* relative to P_{i-1}

$$\vec{V}^{P_2^*/P_1} = \frac{\ell_{c_2}}{2}\,\dot{\phi}_2\,\vec{e}_2' + \frac{\dot{\ell}_{c_2}}{2}\,\vec{e}_2 \tag{7}$$

$$\vec{V}^{P_2^*} = \ell_{c_1}\,\dot{\phi}_1\,\vec{e}_1' + \dot{\ell}_{c_1}\,\vec{e}_1 + \frac{\ell_{c_2}}{2}\,\dot{\phi}_2\,\vec{e}_2' + \frac{\dot{\ell}_{c_2}}{2}\,\vec{e}_2 \tag{8}$$

In general:

$$\dot{\vec{r}}_n = \vec{V}^{P_n^*} = \sum_{i=1}^{n-1} \ell_{c_i}\,\dot{\phi}_i\,\vec{e}_i' + \sum_{i=1}^{n-1} \dot{\ell}_{c_i}\,\vec{e}_i + \frac{\ell_{c_n}}{2}\,\dot{\phi}_n\,\vec{e}_n' + \frac{\dot{\ell}_{c_n}}{2}\,\vec{e}_n \tag{9}$$

REF: ENGINEERING PROCEDURE S.017

$$\vec{V}^{P_n} = \sum_{i=1}^{n} \ell_{c_i} \dot{\phi}_i \vec{e}_i' + \sum_{i=1}^{n} \dot{\ell}_{c_i} \vec{e}_i \tag{10}$$

Therefore, the kinetic energy of the tether is:

$$T_c = \sum_{n=1}^{N} \left[\tfrac{1}{2} m_{c_n} (\vec{V}^{P_n *})^2 + \tfrac{1}{2} I_{c_n} \dot{\phi}_n^2 \right] \tag{11}$$

If each link is assumed to be a uniform thin rod the moment of inertia is:

$$I_{c_n} = m_{c_n} \frac{\ell_{c_n}^2}{12} \tag{12}$$

$$T_c = \sum_{n=1}^{N} \left[\tfrac{1}{2} m_{c_n} (\vec{V}^{P_n *})^2 + \frac{1}{24} m_{c_n} \ell_{c_n}^2 \dot{\phi}_n^2 \right] \tag{13}$$

Other useful relations to be used later are:

$$\frac{\partial \vec{V}^{P_n *}}{\partial \dot{\phi}_r} = \begin{cases} 0 & n < r \\ \ell_{c_r} \vec{e}_r' /2 & n = r \\ \ell_{c_r} \vec{e}_r' & n > r \end{cases} \tag{14}$$

$$\frac{\partial \vec{V}^{P_n *}}{\partial \phi_r} = \begin{cases} 0 & n < r \\ -\ell_{c_r} \dot{\phi}_r \vec{e}_r /2 + \dot{\ell}_{c_r} \vec{e}_r' /2 & n = r \\ -\ell_{c_r} \dot{\phi}_r \vec{e}_r + \dot{\ell}_{c_r} \vec{e}_r' & n > r \end{cases} \tag{15}$$

REF: ENGINEERING PROCEDURE S.017

3. Balloon and Harness Representation

The balloon harness (denoted by ℓ_h = radius of balloon) is considered to be normal to the balloon's longitudinal axis at all times. The balloon has "directional mass" M_1 and M_2 along and normal to the harness and concentrated at the center of gravity of the balloon (Q). Since the balloon is assumed to be an expanding sphere, the "directional mass" M_1 and M_2 are equal and concentrated at the geometric center of the sphere as shown in Figure A-3.

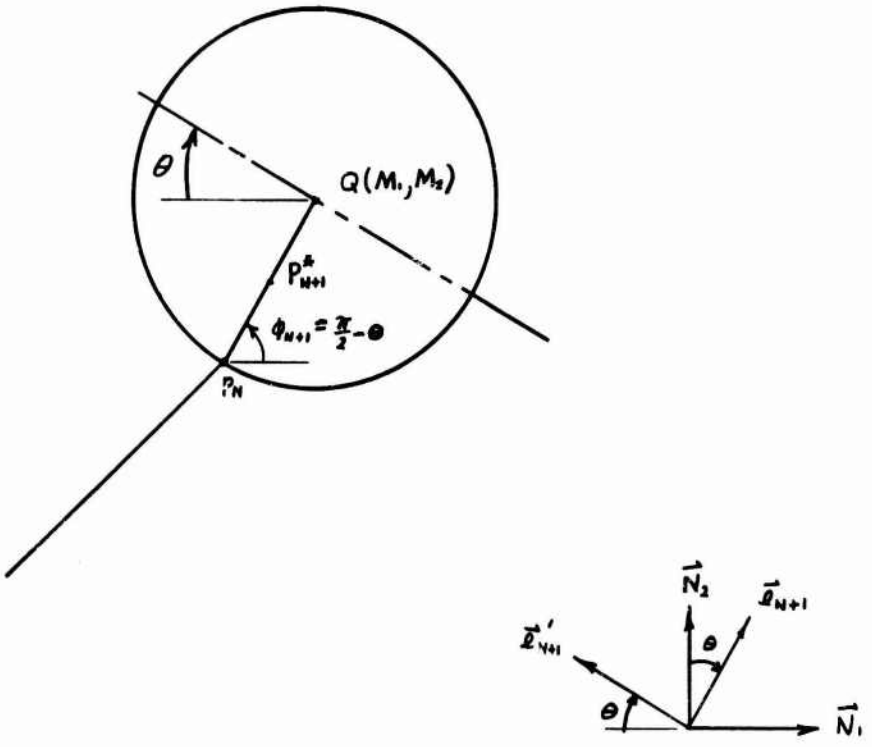

Figure A-3 - Balloon and Harness

E-ID-15(7-68)(77-10)
REF: ENGINEERING PROCEDURE S-017

The kinetic energy of the harness plus balloon is:

$$T_b = m_h \frac{\ell_h^2}{24} \dot{\theta}^2 + \tfrac{1}{2} m_h (\vec{V}^{P^*_{N+1}})^2 + \tfrac{1}{2} M_1 (\vec{V}^Q \cdot \vec{e}_{N+1})^2 + \tfrac{1}{2} M_2 (\vec{V}^Q \cdot \vec{e}'_{N+1})^2 + \tfrac{1}{2} I_B \dot{\theta}^2 \tag{16}$$

where $\vec{V}^Q$ is the velocity of Q and I_B is the mass moment of inertia of the balloon about Q.

It follows that:

$$\vec{V}^{P^*_{N+1}} = \vec{V}^{P_N} + \tfrac{1}{2}\ell_h \dot{\phi}_{N+1} \vec{e}'_{N+1} = \sum_{i=1}^{N} \ell_{c_i} \dot{\phi}_i \vec{e}'_i + \sum_{i=1}^{N} \dot{\ell}_{c_i} \vec{e}_i - \tfrac{1}{2}\ell_h \dot{\theta} \vec{e}'_{N+1}$$

$$\vec{V}^Q = \sum_{i=1}^{N} \ell_{c_i} \dot{\phi}_i \vec{e}'_i + \sum_{i=1}^{N} \dot{\ell}_{c_i} \vec{e}_i - \ell_h \dot{\theta} \vec{e}'_{N+1} \tag{17}$$

$$\tag{18}$$

$$\left.\begin{aligned}
&\frac{\partial \vec{V}^{P^*_{N+1}}}{\partial \dot{\phi}_r} = \ell_{c_r} \vec{e}'_r && \frac{\partial \vec{V}^Q}{\partial \dot{\phi}_r} = \ell_{c_r} \vec{e}'_r \\
&\frac{\partial \vec{V}^{P^*_{N+1}}}{\partial \dot{\theta}} = -\tfrac{1}{2}\ell_h \vec{e}'_{N+1} && \frac{\partial \vec{V}^Q}{\partial \dot{\theta}} = -\ell_h \vec{e}'_{N+1} \\
&\frac{\partial \vec{V}^{P^*_{N+1}}}{\partial \phi_r} = -\ell_{c_r} \dot{\phi}_r \vec{e}_r + \dot{\ell}_{c_r} \vec{e}'_r && \frac{\partial \vec{V}^Q}{\partial \phi_r} = -\ell_{c_r} \dot{\phi}_r \vec{e}_r + \dot{\ell}_{c_r} \vec{e}'_r \\
&\frac{\partial \vec{V}^{P^*_{N+1}}}{\partial \theta} = -\tfrac{1}{2}\ell_h \dot{\theta} \vec{e}_{N+1} && \frac{\partial \vec{V}^Q}{\partial \theta} = -\ell_h \dot{\theta} \vec{e}_{N+1}
\end{aligned}\right\} \tag{19}$$

E-ID-15(7-64)(77-10)
REF: ENGINEERING PROCEDURE 5.017

4. The Inertia Terms

The total kinetic energy is given by the sum of equations (13) and (16):

$$T = \sum_{n=1}^{N} \left[\tfrac{1}{2} m_{c_n} (\vec{V}^{P_n^*})^2 + m_{c_n} \frac{\ell_{c_n}^2}{24} \dot{\phi}_n^2 \right] + m_h \frac{\ell_h^2}{24} \dot{\theta}^2$$

$$+ \tfrac{1}{2} m_h (\vec{V}^{P_{N+1}^*})^2 + \tfrac{1}{2} M_1 (\vec{V}^Q \cdot \vec{e}_{N+1})^2 + \tfrac{1}{2} M_2 (\vec{V}^Q \cdot \vec{e}'_{N+1})^2 + \tfrac{1}{2} I_B \dot{\theta}^2 \qquad (20)$$

$$\frac{\partial T}{\partial \dot{\phi}_r} = \sum_{n=r+1}^{N} \Big[m_{c_n} \vec{V}^{P_n^*} \cdot \ell_{c_r} \vec{e}'_r + m_{c_r} \vec{V}^{P_r^*} \cdot \frac{\ell_{c_r}}{2} \vec{e}'_r + m_{c_r} \frac{\ell_{c_r}^2}{12} \dot{\phi}_r$$

$$+ m_h \ell_{c_r} \vec{e}'_r \vec{V}^{P_{N+1}^*} + M_1 \vec{V}^Q \cdot \vec{e}_{N+1} \ell_{c_r} \vec{e}'_r \cdot \vec{e}_{N+1} + M_2 \vec{V}^Q \cdot \vec{e}'_{N+1} \ell_{c_r} \vec{e}'_r \cdot \vec{e}'_{N+1} \qquad (21)$$

Note that the following relations exist between the unit vectors.

$$\left.\begin{array}{ll}
\vec{e}'_n = \vec{N}_2 \cos\phi_n - \vec{N}_1 \sin\phi_n & \vec{e}_n = \vec{N}_1 \cos\phi_n + \vec{N}_2 \sin\phi_n \\
\vec{e}'_i = \vec{N}_2 \cos\phi_i - \vec{N}_1 \sin\phi_i & \vec{e}_i = \vec{N}_1 \cos\phi_i + \vec{N}_2 \sin\phi_i \\
\vec{e}'_r = \vec{N}_2 \cos\phi_r - \vec{N}_1 \sin\phi_r & \vec{e}_r = \vec{N}_1 \cos\phi_r + \vec{N}_2 \sin\phi_r \\
\vec{e}'_{N+1} = \vec{N}_2 \sin\theta - \vec{N}_1 \cos\theta & \vec{e}_{N+1} = \vec{N}_1 \sin\theta + \vec{N}_2 \cos\theta
\end{array}\right\} \qquad (22)$$

E-ID-15(7-64)(77-10)
REF: ENGINEERING PROCEDURE 5.017

Using equations (9) and (22)

$$\vec{V}^{P_n^*} \cdot \vec{e}_r' = \sum_{i=1}^{n-1} \ell_{c_i} \dot{\phi}_i \cos(\phi_i - \phi_r) + \sum_{i=1}^{n-1} \dot{\ell}_{c_i} \sin(\phi_i - \phi_r)$$

$$+ \frac{\ell_{c_n}}{2} \dot{\phi}_n \cos(\phi_n - \phi_r) + \frac{\dot{\ell}_{c_n}}{2} \sin(\phi_n - \phi_r) \qquad (23)$$

$$\vec{V}^{P_r^*} \cdot \vec{e}_r' = \sum_{i=1}^{r-1} \ell_{c_i} \dot{\phi}_i \cos(\phi_i - \phi_r) + \sum_{i=1}^{r-1} \dot{\ell}_{c_i} \sin(\phi_i - \phi_r) + \frac{\ell_{c_r}}{2} \dot{\phi}_r \qquad (24)$$

Using equations (17) and (22)

$$\vec{V}^{P_{N+1}^*} \cdot \vec{e}_r' = \sum_{i=1}^{N} \ell_{c_i} \dot{\phi}_i \cos(\phi_i - \phi_r) + \sum_{i=1}^{N} \dot{\ell}_{c_i} \sin(\phi_i - \phi_r) - \tfrac{1}{2} \ell_h \dot{\theta} \sin(\theta + \phi_r) \qquad (25)$$

Using equations (18) and (22)

$$\vec{V}^{Q} \cdot \vec{e}_{N+1} = \sum_{i=1}^{N} \ell_{c_i} \dot{\phi}_i \cos(\phi_i + \theta) + \sum_{i=1}^{N} \dot{\ell}_{c_i} \sin(\theta + \phi_i) \qquad (26)$$

$$\vec{V}^{Q} \cdot \vec{e}_{N+1}' = \sum_{i=1}^{N} \ell_{c_i} \dot{\phi}_i \sin(\phi_i + \theta) - \sum_{i=1}^{N} \dot{\ell}_{c_i} \cos(\theta + \phi_i) - \ell_h \dot{\theta} \qquad (27)$$

Also:

$$\left.\begin{aligned} \vec{e}_r' \cdot \vec{e}_{N+1} &= \cos(\theta + \phi_r) \\ \vec{e}_r' \cdot \vec{e}_{N+1}' &= \sin(\theta + \phi_r) \end{aligned}\right\} \qquad (28)$$

B-ID-15(7-64)(77-10) REF: ENGINEERING PROCEDURE S-017

Therefore $\frac{\partial T}{\partial \dot{\phi}_r}$ may be written as:

$$\frac{\partial T}{\partial \dot{\phi}_r} = \sum_{n=r+1}^{N}\left\{m_{c_n} \ell_{c_r}\left[\sum_{i=1}^{n-1} \ell_{c_i} \dot{\phi}_i \cos(\phi_i - \phi_r) + \sum_{i=1}^{n-1} \dot{\ell}_{c_i} \sin(\phi_i - \phi_r)\right.\right.$$

$$\left.\left. + \frac{\ell_{c_n}}{2} \dot{\phi}_n \cos(\phi_n - \phi_r) + \frac{\dot{\ell}_{c_n}}{2} \sin(\phi_n - \phi_r)\right]\right\}$$

$$+ m_{c_r} \frac{\ell_{c_r}}{2}\left[\sum_{i=1}^{r-1} \ell_{c_i} \dot{\phi}_i \cos(\phi_i - \phi_r) + \sum_{i=1}^{r-1} \dot{\ell}_{c_i} \sin((\phi_i - \phi_r) + \frac{\ell_{c_r}}{2} \dot{\phi}_r\right] + m_{c_r} \frac{\ell_{c_r}^2}{12} \dot{\phi}_r$$

$$+ m_h \ell_{c_r}\left[\sum_{i=1}^{N} \ell_{c_i} \dot{\phi}_i \cos(\phi_i - \phi_r) + \sum_{i=1}^{N} \dot{\ell}_{c_i} \sin(\phi_i - \phi_r) - \tfrac{1}{2} \ell_h \dot{\theta} \sin(\theta + \phi_r)\right]$$

$$+ M_1 \ell_{c_r}\left[\cos(\theta + \phi_r)\left\{\sum_{i=1}^{N} \ell_{c_i} \dot{\phi}_i \cos(\phi_i + \theta) + \sum_{i=1}^{N} \dot{\ell}_{c_i} \sin(\theta + \phi_i)\right\}\right]$$

$$+ M_2 \ell_{c_r}\left[\sin(\theta + \phi_r)\left\{\sum_{i=1}^{N} \dot{\ell}_{c_i} \dot{\phi}_i \sin(\theta + \phi_i) - \sum_{i=1}^{N} \dot{\ell}_{c_i} \cos(\theta + \phi_i) - \ell_h \dot{\theta}\right\}\right] \tag{29}$$

Likewise:

$$\frac{\partial T}{\partial \dot{\theta}} = m_h \frac{\ell_h^2}{12} \dot{\theta} + m_h \vec{V}^{P^*_{N+1}} \cdot \frac{\partial \vec{V}^{P^*_{N+1}}}{\partial \theta} + M_1 \vec{V}^{Q} \cdot \vec{e}_{N+1} \frac{\partial \vec{V}^{Q}}{\partial \theta} \cdot \vec{e}_{N+1}$$

$$+ M_2 \vec{V}^{Q} \cdot \vec{e}'_{N+1} \frac{\partial \vec{V}^{Q}}{\partial \theta} \cdot \vec{e}'_{N+1} + I_B \dot{\theta} \tag{30}$$

E-ID-15(7-64)(77-10)
REF: ENGINEERING PROCEDURE S.017

or

$$\frac{\partial T}{\partial \dot{\theta}} = \dot{\theta}\left\{I_B + \frac{m_h}{3}\ell_h^2 + M_2\ell_h^2\right\} - \sum_{i=1}^{N} \ell_h \ell_{c_i} \dot{\phi}_i \sin(\phi_i + \theta)\left\{\frac{m_h}{2} + M_2\right\}$$
$$+ \sum_{i=1}^{N} \ell_h \dot{\ell}_{c_i} \cos(\phi_i + \theta)\left\{\frac{m_h}{2} + M_2\right\} \qquad (31)$$

The time derivative of equation (29) is:

$$\frac{d}{dt}\left(\frac{\partial T}{\partial \dot{\phi}_r}\right) = \sum_{n=r+1}^{N}\left\{\dot{m}_{c_n}\ell_{c_r}\left[\sum_{i=1}^{n-1}\ell_{c_i}\dot{\phi}_i\cos(\phi_i - \phi_r) + \sum_{i=1}^{n-1}\dot{\ell}_{c_i}\sin(\phi_i - \phi_r)\right.\right.$$
$$\left. + \frac{\ell_{c_n}}{2}\dot{\phi}_n\cos(\phi_n - \phi_r) + \frac{\dot{\ell}_{c_n}}{2}\sin(\phi_n - \phi_r)\right]$$
$$+ m_{c_n}\dot{\ell}_{c_r}\left[\sum_{i=1}^{n-1}\ell_{c_i}\dot{\phi}_i\cos(\phi_i - \phi_r) + \sum_{i=1}^{n-1}\dot{\ell}_{c_i}\sin(\phi_i - \phi_r)\right.$$
$$\left. + \frac{\ell_{c_n}}{2}\dot{\phi}_n\cos(\phi_n - \phi_r) + \frac{\dot{\ell}_{c_n}}{2}\sin(\phi_n - \phi_r)\right]$$
$$+ m_{c_n}\ell_{c_r}\left[\sum_{i=1}^{n-1}\dot{\ell}_{c_i}\dot{\phi}_i\cos(\phi_i - \phi_r) + \sum_{i=1}^{n-1}\ell_{c_i}\ddot{\phi}_i\cos(\phi_i - \phi_r)\right.$$
$$\left.\left. - \sum_{i=1}^{n-1}\ell_{c_i}\dot{\phi}_i\sin(\phi_i - \phi_r)(\dot{\phi}_i - \dot{\phi}_r)\right]\right.$$

(continued on next page)

E-ID-15(7-64)(77-10)
REF: ENGINEERING PROCEDURE S.017

$$+ m_{c_n} \ell_{c_r} \left[\sum_{i=1}^{n-1} \ddot{\ell}_{c_i} \sin(\phi_i - \phi_r) + \sum_{i=1}^{n-1} \dot{\ell}_{c_i} \cos(\phi_i - \phi_r)(\dot{\phi}_i - \dot{\phi}_r) \right.$$

$$\left. + \frac{\ddot{\ell}_{c_n}}{2} \sin(\phi_n - \phi_r) + \frac{\dot{\ell}_{c_n}}{2} \cos(\phi_n - \phi_r)(\dot{\phi}_n - \dot{\phi}_r) \right]$$

$$+ m_{c_n} \ell_{[illegible]} \left[\frac{\dot{\ell}_{c_n}}{2} \dot{\phi}_n \cos(\phi_n - \phi_r) + \frac{\ell_{c_n}}{2} \ddot{\phi}_n \cos(\phi_n - \phi_r) \right.$$

$$\left. - \frac{\ell_{c_n}}{2} \dot{\phi}_n \sin(\phi_n - \phi_r)(\dot{\phi}_n - \dot{\phi}_r) \right] \Bigg\}$$

$$+ \dot{m}_{c_r} \frac{\ell_{c_r}}{2} \left[\sum_{i=1}^{r-1} \ell_{c_i} \dot{\phi}_i \cos(\phi_i - \phi_r) + \sum_{i=1}^{r-1} \dot{\ell}_{c_i} \sin(\phi_i - \phi_r) \right]$$

$$+ m_{c_r} \frac{\dot{\ell}_{c_r}}{2} \left[\sum_{i=1}^{r-1} \ell_{c_i} \dot{\phi}_i \cos(\phi_i - \phi_r) + \sum_{i=1}^{r-1} \dot{\ell}_{c_i} \sin(\phi_i - \phi_r) \right]$$

$$+ m_{c_r} \frac{\ell_{c_r}}{2} \left[\sum_{i=1}^{r-1} \ell_{c_i} \ddot{\phi}_i \cos(\phi_i - \phi_r) - \sum_{i=1}^{r-1} \ell_{c_i} \dot{\phi}_i \sin(\phi_i - \phi_r)(\dot{\phi}_i - \dot{\phi}_r) \right.$$

$$\left. + \sum_{i=1}^{r-1} \dot{\ell}_{c_i} \dot{\phi}_i \cos(\phi_i - \phi_r) + \sum_{i=1}^{r-1} \ddot{\ell}_{c_i} \sin(\phi_i - \phi_r) + \sum_{i=1}^{r-1} \dot{\ell}_{c_i} \cos[illegible](\dot{\phi}_i - \dot{\phi}_r) \right]$$

$$+ \dot{m}_{c_r} \frac{\ell_{c_r}^2}{3} \dot{\phi}_r + m_{c_r} \frac{\ell_{c_r}^2}{3} \ddot{\phi}_r + 2 m_{c_r} \frac{\ell_{c_r}}{3} \dot{\ell}_{c_r} \dot{\phi}_r$$

$$+ m_h \dot{\ell}_{c_r} \left[\sum_{i=1}^{N} \ell_{c_i} \dot{\phi}_i \cos(\phi_i - \phi_r) + \sum_{i=1}^{N} \dot{\ell}_{c_i} \sin(\phi_i - \phi_r) - \tfrac{1}{2} \ell_h \dot{\theta} \sin(\theta + \phi_r) \right.$$

(continued on next page)

E-ID-15(7-64)(77-10)
REF: ENGINEERING PROCEDURE 5-017

$$+ m_h \ell_{c_r} \left[\sum_{i=1}^{N} \dot{\ell}_{c_i} \dot{\phi}_i \cos(\phi_i - \phi_r) + \sum_{i=1}^{N} \ell_{c_i} \ddot{\phi}_i \cos(\phi_i - \phi_r) \right.$$

$$\left. - \sum_{i=1}^{N} \ell_{c_i} \dot{\phi}_i \sin(\phi_i - \phi_r)(\dot{\phi}_i - \dot{\phi}_r) \right]$$

$$+ m_h \ell_{c_r} \left[\sum_{i=1}^{N} \ddot{\ell}_{c_i} \sin(\phi_i - \phi_r) + \sum_{i=1}^{N} \dot{\ell}_{c_i} \cos(\phi_i - \phi_r)(\dot{\phi}_i - \dot{\phi}_r) - \tfrac{1}{2} \ell_h \ddot{\theta} \sin(\theta + \phi_r) \right.$$

$$\left. - \tfrac{1}{2} \ell_h \dot{\theta} \cos(\theta + \phi_r)(\dot{\theta} + \dot{\phi}_r) \right]$$

$$+ M_1 \dot{\ell}_{c_r} \left[\cos(\theta + \phi_r) \left\{ \sum_{i=1}^{N} \ell_{c_i} \dot{\phi}_i \cos(\phi_i + \theta) + \sum_{i=1}^{N} \dot{\ell}_{c_i} \sin(\theta + \phi_i) \right\} \right]$$

$$+ M_1 \ell_{c_r} \left[- \sin(\theta + \phi_r)(\dot{\theta} + \dot{\phi}_r) \left\{ \sum_{i=1}^{N} \ell_{c_i} \dot{\phi}_i \cos(\phi_i + \theta) + \sum_{i=1}^{N} \dot{\ell}_{c_i} \sin(\theta + \phi_i) \right\} \right]$$

$$+ M_1 \ell_{c_r} \left[\cos(\theta + \phi_r) \left\{ \sum_{i=1}^{N} \dot{\ell}_{c_i} \dot{\phi}_i \cos(\phi_i + \theta) + \sum_{i=1}^{N} \ell_{c_i} \ddot{\phi}_i \cos(\phi_i + \theta) \right. \right.$$

$$\left. \left. - \sum_{i=1}^{N} \ell_{c_i} \dot{\phi}_i \sin(\phi_i + \theta)(\dot{\phi}_i + \dot{\theta}) \right\} \right]$$

(continued on next page)

B-ID-15(7-64)(77-10)
REF: ENGINEERING PROCEDURE S.017

$$+M_1 \ell_{c_r}\left[\cos(\theta+\phi_r)\left\{\sum_{i=1}^{N}\ddot{\ell}_{c_i}\sin(\theta+\phi_i)+\sum_{i=1}^{N}\dot{\ell}_{c_i}\cos(\theta+\phi_i)(\dot{\theta}+\dot{\phi}_i)\right\}\right]$$

$$+M_2 \dot{\ell}_{c_r}\left[\sin(\theta+\phi_r)\left\{\sum_{i=1}^{N}\ell_{c_i}\dot{\phi}_i\sin(\theta+\phi_i)=\sum_{i=1}^{N}\dot{\ell}_{c_i}\cos(\theta+\phi_i)-\ell_h\dot{\theta}\right\}\right]$$

$$+M_2 \ell_{c_r}\left[\cos(\theta+\phi_r)(\dot{\theta}+\dot{\phi}_r)\left\{\sum_{i=1}^{N}\ell_{c_i}\dot{\phi}_i\sin(\theta+\phi_i)-\sum_{i=1}^{N}\dot{\ell}_{c_i}\cos(\theta+\phi_i)-\ell_h\dot{\theta}\right\}\right]$$

$$+M_2 \ell_{c_r}\left[\sin(\theta+\phi_r)\left\{\sum_{i=1}^{N}\dot{\ell}_{c_i}\dot{\phi}_i\sin(\theta+\phi_i)+\sum_{i=1}^{N}\ell_{c_i}\ddot{\phi}_i\sin(\theta+\phi_i)\right.\right.$$

$$\left.\left.+\sum_{i=1}^{N}\ell_{c_i}\dot{\phi}_i\cos(\theta+\phi_i)(\dot{\theta}+\dot{\phi}_i)\right\}\right]$$

$$+M_2 \ell_{c_r}\left[\sin(\theta+\phi_r)\left\{-\sum_{i=1}^{N}\ddot{\ell}_{c_i}\cos(\theta+\phi_i)+\sum_{i=1}^{N}\dot{\ell}_{c_i}\sin(\theta+\phi_i)(\dot{\theta}+\dot{\phi}_i)-\ell_h\ddot{\theta}\right\}\right]. \tag{32}$$

It should be noted that the time derivative of ℓ_h and m_h has been excluded in equation (32). Since ℓ_h is the radius of the balloon, its mass is zero and therefore, also its time derivative. The radius does change, however; but its time derivative is small when compared to $\dot{\ell}_c$ and is therefore ignored.

REF: ENGINEERING PROCEDURE 5.017
E-ID-1x(7-60)(77-10)

The time derivative of equation (31) is:

$$\frac{d}{dt}\left(\frac{\partial T}{\partial \dot{\theta}}\right) = \ddot{\theta}\left\{I_B + \ell_h^2\left[\frac{m_h}{3} + M_2\right]\right\} + \dot{\theta}\,\dot{I}_B$$

$$-\left[\frac{m_h}{2} + M_2\right]\left\{\sum_{i=1}^{N} \ell_h\,\dot{\ell}_{c_i}\,\dot{\phi}_i \sin(\phi_i + \theta) + \sum_{i=1}^{N} \ell_h\,\ell_{c_i}\,\ddot{\phi}_i \sin(\phi_i + \theta)\right.$$

$$\left. + \sum_{i=1}^{N} \ell_h\,\ell_{c_i}\,\dot{\phi}_i \cos(\phi_i + \theta)\,(\dot{\phi}_i + \dot{\theta})\right\}$$

$$+\left[\frac{m_h}{2} + M_2\right]\left\{\sum_{i=1}^{N} \ell_h\,\ddot{\ell}_{c_i} \cos(\phi_i + \theta) - \sum_{i=1}^{N} \ell_h\,\dot{\ell}_{c_i} \sin(\phi_i + \theta)(\dot{\phi}_i + \dot{\theta})\right\} \tag{33}$$

Referring to Figure A-3:

$$\frac{\partial \vec{e}_{N+1}}{\partial \theta} = -\vec{e}'_{N+1} \qquad \frac{\partial \vec{e}'_{N+1}}{\partial \theta} = \vec{e}_{N+1} \tag{34}$$

$$\frac{\partial T}{\partial \phi_r} = \sum_{n=1}^{N} m_{c_n}\,\vec{V}^{P_n^*} \cdot \frac{\partial \vec{V}^{P_n^*}}{\partial \phi_r} + m_h\,\vec{V}^{P_{N+1}^*} \cdot \frac{\partial \vec{V}^{P_{N+1}^*}}{\partial \phi_r} + M_1\,\vec{V}^{Q} \cdot \vec{e}_{N+1}\,\frac{\partial \vec{V}^{Q}}{\partial \phi_r} \cdot \vec{e}_{N+1}$$

$$+ M_2\,\vec{V}^{Q} \cdot \vec{e}'_{N+1}\,\frac{\partial \vec{V}^{Q}}{\partial \phi_r} \cdot \vec{e}'_{N+1} \tag{35}$$

E-ID-15(7-64)(77-10) REF: ENGINEERING PROCEDURE 5.017

Expanding all the terms in equation (35) results in:

$$\frac{\partial T}{\partial \phi_r} = \sum_{n=r+1}^{N} m_{c_n} \left[\sum_{i=1}^{n-1} \ell_{c_i} \dot{\phi}_i \ell_{c_r} \dot{\phi}_r \sin(\phi_i - \phi_r) + \sum_{i=1}^{n-1} \ell_{c_i} \dot{\ell}_{c_r} \dot{\phi}_i \cos(\phi_i - \phi_r) \right.$$

$$- \sum_{i=1}^{n-1} \dot{\ell}_{c_i} \ell_{c_r} \dot{\phi}_r \cos(\phi_i - \phi_r) + \sum_{i=1}^{n-1} \dot{\ell}_{c_i} \dot{\ell}_{c_r} \sin(\phi_i - \phi_r)$$

$$+ \frac{\ell_{c_n}}{2} \dot{\phi}_n \ell_{c_r} \dot{\phi}_r \sin(\phi_n - \phi_r) + \frac{\ell_{c_n}}{2} \dot{\phi}_n \dot{\ell}_{c_r} \cos(\phi_n - \phi_r)$$

$$\left. - \frac{\dot{\ell}_{c_n}}{2} \ell_{c_r} \dot{\phi}_r \cos(\phi_n - \phi_r) + \frac{\dot{\ell}_{c_n}}{2} \dot{\ell}_{c_r} \sin(\phi_n - \phi_r) \right]$$

$$+ m_{c_r} \sum_{i=1}^{r-1} \ell_{c_i} \dot{\phi}_i \frac{\ell_{c_r}}{2} \dot{\phi}_r \sin(\phi_i - \phi_r) + m_{c_r} \sum_{i=1}^{r-1} \ell_{c_i} \dot{\phi}_i \frac{\dot{\ell}_{c_r}}{2} \cos(\phi_i - \phi_r)$$

$$- m_{c_r} \sum_{i=1}^{r-1} \dot{\ell}_{c_i} \frac{\ell_{c_r}}{2} \dot{\phi}_r \cos(\phi_i - \phi_r) + m_{c_r} \sum_{i=1}^{r-1} \dot{\ell}_{c_i} \frac{\dot{\ell}_{c_r}}{2} \sin(\phi_i - \phi_r)$$

$$+ m_h \left[- \left(\sum_{i=1}^{N} \ell_{c_i} \dot{\phi}_i \ell_{c_r} \dot{\phi}_r + \sum_{i=1}^{N} \dot{\ell}_{c_i} \dot{\ell}_{c_r} \right) \sin(\phi_r - \phi_i) \right.$$

$$+ \left(\sum_{i=1}^{N} \ell_{c_i} \dot{\phi}_i \dot{\ell}_{c_r} - \sum_{i=1}^{N} \dot{\ell}_{c_i} \ell_{c_r} \dot{\phi}_r \right) \cos(\phi_i - \phi_r) - \tfrac{1}{2} \ell_h \dot{\theta} \ell_{c_r} \dot{\phi}_r \cos(\phi_r + \theta)$$

$$\left. - \tfrac{1}{2} \ell_h \dot{\theta} \dot{\ell}_{c_r} \sin(\theta + \phi_r) \right]$$

(continued on next page)

E-TD-15(7-64)(77-10)
REF: ENGINEERING PROCEDURE 5.017

$$+M_1\Bigg[-\sum_{i=1}^{N} \ell_{c_i}\dot{\phi}_i \cos(\phi_i+\theta)\,\ell_{c_r}\dot{\phi}_r \sin(\theta+\phi_r)$$

$$-\sum_{i=1}^{N} \dot{\ell}_{c_i} \sin(\theta+\phi_i)\,\ell_{c_r}\dot{\phi}_r \sin(\theta+\phi_r)$$

$$+\sum_{i=1}^{N} \ell_{c_i}\dot{\phi}_i \cos(\phi_i+\theta)\,\dot{\ell}_{c_r} \cos(\theta+\phi_r)$$

$$+\sum_{i=1}^{N} \dot{\ell}_{c_i} \sin(\theta+\phi_i)\,\dot{\ell}_{c_r} \cos(\theta+\phi_r)\Bigg]$$

$$+M_2\Bigg[\sum_{i=1}^{N} \ell_{c_i}\dot{\phi}_i \sin(\phi_i+\theta)\,\ell_{c_r}\dot{\phi}_r \cos(\theta+\phi_r)$$

$$-\sum_{i=1}^{N} \dot{\ell}_{c_i} \cos(\theta+\phi_i)\,\ell_{c_r}\dot{\phi}_r \cos(\theta+\phi_r) - \ell_h\dot{\theta}\,\ell_{c_r}\dot{\phi}_r \cos(\theta+\phi_r)$$

$$+\sum_{i=1}^{N} \ell_{c_i}\dot{\phi}_i \sin(\phi_i+\theta)\,\dot{\ell}_{c_r} \sin(\theta+\phi_r) - \sum_{i=1}^{N} \dot{\ell}_{c_i} \cos(\theta+\phi_i)\,\dot{\ell}_{c_r} \sin(\theta+\phi_r)$$

$$-\ell_h\dot{\theta}\,\dot{\ell}_{c_r} \sin(\theta+\phi_r)\Bigg] \qquad (36)$$

E-ID-15(7-60)(77-10)
REF: ENGINEERING PROCEDURE S.017

Similarly,

$$\frac{\partial T}{\partial \theta} = m_h \vec{V}^{P^*_{N+1}} \cdot \frac{\partial \vec{V}^{P^*_{N+1}}}{\partial \theta} + M_1 \vec{V}^{Q} \cdot \vec{e}_{N+1}\left[\frac{\partial \vec{V}^{Q}}{\partial \theta} \cdot \vec{e}_{N+1} + \vec{V}^{Q} \cdot \frac{\partial \vec{e}_{N+1}}{\partial \theta}\right]$$

$$+ M_2 \vec{V}^{Q} \cdot \vec{e}'_{N+1}\left[\frac{\partial \vec{V}^{Q}}{\partial \theta} \cdot \vec{e}'_{N+1} + \vec{V}^{Q} \cdot \frac{\partial \vec{e}'_{N+1}}{\partial \theta}\right] \qquad (37)$$

Expanding all the terms in equation (37) gives:

$$\frac{\partial T}{\partial \theta} = m_h\left[-\sum_{i=1}^{N} \ell_{c_i} \dot{\phi}_i \frac{\ell_h}{2} \dot{\theta} \cos(\theta + \phi_i) - \sum_{i=1}^{N} \dot{\ell}_{c_i} \frac{\ell_h}{2} \dot{\theta} \sin(\theta + \phi_i)\right]$$

$$+M_1\left[\left(\sum_{i=1}^{N} \ell_{c_i} \dot{\phi}_i \cos(\phi_i + \theta)\right)\left(-\sum_{i=1}^{N} \ell_{c_i} \dot{\phi}_i \sin(\theta + \phi_i)\right)\right.$$

$$+\left(\sum_{i=1}^{N} \dot{\ell}_{c_i} \sin(\theta + \phi_i)\right)\left(\sum_{i=1}^{N} -\ell_{c_i} \dot{\phi}_i \sin(\theta + \phi_i)\right)$$

$$+\left(\sum_{i=1}^{N} \ell_{c_i} \dot{\phi}_i \cos(\theta + \phi_i)\right)\left(\sum_{i=1}^{N} \dot{\ell}_{c_i} \cos(\theta + \phi_i)\right)$$

$$\left.+\left(\sum_{i=1}^{N} \dot{\ell}_{c_i} \sin(\theta + \phi_i)\right)\left(\sum_{i=1}^{N} \dot{\ell}_{c_i} \cos(\theta + \phi_i)\right)\right]$$

$$+M_2\left[\left(\sum_{i=1}^{N} \ell_{c_i} \dot{\phi}_i \sin(\phi_i + \theta)\right)\left(\sum_{i=1}^{N} \ell_{c_i} \dot{\phi}_i \cos(\theta + \phi_i)\right)\right.$$

(continued on next page)

B-ID-15(7-64)(77-10) REF: ENGINEERING PROCEDURE 5.017

$$+\left(\sum_{i=1}^{N} \ell_{c_i}\, \dot{\phi}_i \sin(\phi_i + \theta)\right)\left(\sum_{i=1}^{N} \dot{\ell}_{c_i} \sin(\theta + \phi_i)\right)$$

$$-\left(\sum_{i=1}^{N} \dot{\ell}_{c_i} \cos(\theta + \phi_i)\right)\left(\sum_{i=1}^{N} \ell_{c_i}\, \dot{\phi}_i \cos(\theta + \phi_i)\right)$$

$$-\left(\sum_{i=1}^{N} \dot{\ell}_{c_i} \cos(\theta + \phi_i)\right)\left(\sum_{i=1}^{N} \dot{\ell}_{c_i} \sin(\theta + \phi_i)\right)$$

$$-\ell_h\, \dot{\theta}\left(\sum_{i=1}^{N} \ell_{c_i}\, \dot{\phi}_i \cos(\theta + \phi_i) + \sum_{i=1}^{N} \dot{\ell}_{c_i} \sin(\theta + \phi_i)\right)\Bigg] \qquad (38)$$

Substituting equations (33) and (38) into equation (1), cancelling like terms and solving for $\ddot{\theta}$ yields:

$$\ddot{\theta} = \Bigg\{ F_\theta - \dot{\theta}\, \dot{I}_B + \left[M_2 + \frac{m_h}{2}\right]\left[\ell_h \ell_c \left(\sum_{i=1}^{N} \dot{\phi}_i^{\,2} \cos(\phi_i + \theta) + \sum_{i=1}^{N} \ddot{\phi}_i \sin(\phi_i + \theta)\right)\right]$$

$$+\left[2 M_2 \ell_h \dot{\ell}_c + \dot{\ell}_c m_h \ell_h\right] \sum_{i=1}^{N} \dot{\phi}_i \sin(\theta + \phi_i) + \left[M_2 - M_1\right] \cdot$$

$$\left[\ell_c \sum_{i=1}^{N} \dot{\phi}_i \sin(\theta + \phi_i)\left(\ell_c \sum_{i=1}^{N} \dot{\phi}_i \cos(\phi_i + \theta) + \dot{\ell}_c \sum_{i=1}^{N} \sin(\theta + \phi_i)\right)\right.$$

(continued on next page)

E-ID-15(7-64)(77-10) REF: ENGINEERING PROCEDURE 5.017

$$-\dot{\ell}_c \sum_{i=1}^{N} \cos(\phi_i + \theta)\left(\ell_c \sum_{i=1}^{N} \dot{\phi}_i \cos(\phi_i + \theta) + \dot{\ell}_c \sum_{i=1}^{N} \sin(\theta + \phi_i)\right)\Bigg]\Bigg\}\Bigg/$$

$$\left\{I_B + \ell_h^2\left[\frac{m_h}{3} + M_2\right]\right\} \qquad (39)$$

Substituting equations (32) and (36) into equation (2), cancelling like terms and solving for $\ddot{\phi}_r$ yields:

$$\ddot{\phi}_r = \Bigg\{F_{\phi_r} - \sum_{n=r+1}^{N}\Bigg[(\dot{m}_{c_n}\ell_c^2 + 2\,m_{c_n}\ell_c\dot{\ell}_c)\sum_{i=1}^{n-1}\dot{\phi}_i\cos(\phi_i - \phi_r)$$

$$+ \dot{m}_{c_n}\ell_c\dot{\ell}_c\sum_{i=1}^{n-1}\sin(\phi_i - \phi_r) - m_{c_n}\ell_c^2\sum_{i=1}^{n-1}\dot{\phi}_i^2\sin(\phi_i - \phi_r)$$

$$+ \left(\dot{m}_{c_n}\frac{\ell_c^2}{2}\dot{\phi}_n + m_{c_n}\ell_c\dot{\ell}_c\dot{\phi}_n + m_{c_n}\frac{\ell_c^2}{2}\ddot{\phi}_n\right)\cos(\phi_n - \phi_r)$$

$$+\left(\dot{m}_{c_m}\frac{\ell_c\dot{\ell}_c}{2} - m_{c_n}\frac{\ell_c^2}{2}\dot{\phi}_n^2\right)\sin(\phi_n - \phi_r) + \ell_c^2\,m_{c_n}\sum_{i=1}^{r-1}\ddot{\phi}_i\cos(\phi_i - \phi_r)\Bigg]$$

$$-\ell_c^2\sum_{n=r+2}^{N} m_{c_n}\sum_{i=r+1}^{n-1}\ddot{\phi}_i\cos(\phi_i - \phi_r)$$

(continued on next page)

E-ID-15(7-64)(77-10)
REF: ENGINEERING PROCEDURE S.017

$$-\left(\dot{m}_{c_r}\frac{\ell_c^2}{2}+m_{c_r}\ell_c\dot{\ell}_c\right)\sum_{i=1}^{r-1}\dot{\phi}_i\cos(\phi_i-\phi_r)$$

$$-\left(m_{c_r}\frac{\ell_c^2}{2}+m_h\ell_c^2\right)\sum_{i=1}^{r-1}\ddot{\phi}_i\cos(\phi_i-\phi_r)$$

$$-\dot{m}_{c_r}\frac{\ell_c\dot{\ell}_c}{2}\sum_{i=1}^{r-1}\sin(\phi_i-\phi_r)+m_{c_r}\frac{\ell_c^2}{2}\sum_{i=1}^{r-1}\dot{\phi}_i^2\sin(\phi_i-\phi_r)$$

$$-\left(\dot{m}_{c_r}\ell_c+2m_{c_r}\dot{\ell}_c\right)\frac{\ell_c}{3}\dot{\phi}_r-2m_h\dot{\ell}_c\ell_c\sum_{i=1}^{N}\dot{\phi}_i\cos(\phi_i-\phi_r)$$

$$-m_h\ell_c^2\sum_{i=r+1}^{N}\ddot{\phi}_i\cos(\phi_i-\phi_r)+m_h\ell_c^2\sum_{i=1}^{N}\dot{\phi}_i^2\sin(\phi_i-\phi_r)$$

$$+m_h\frac{\ell_c\ell_h}{2}\ddot{\theta}\sin(\theta+\phi_r)+m_h\frac{\ell_c\ell_h}{2}\dot{\theta}^2\cos(\theta+\phi_r)$$

$$-M_1\left[\left(2\dot{\ell}_c\ell_c\cos(\theta+\phi_r)-\ell_c^2\sin(\theta+\phi_r)\dot{\theta}\right)\sum_{i=1}^{N}\dot{\phi}_i\cos(\phi_i+\theta)\right.$$

$$\left.-\ell_c\dot{\ell}_c\sin(\theta+\phi_r)\dot{\theta}\sum_{i=1}^{N}\sin(\theta+\phi_i)\right.$$

$$\left.+\ell_c^2\cos(\theta+\phi_r)\left(\sum_{i=1}^{r-1}\ddot{\phi}_i\cos(\phi_i+\theta)+\sum_{i=r+1}^{N}\ddot{\phi}_i\cos(\phi_i+\theta)\right.\right.$$

(concluded on next page)

E-2D-15(7-68)(77-20)
REF: ENGINEERING PROCEDURE S.017

$$-\sum_{i=1}^{N} \dot{\phi}_i^{\,2} \sin(\theta + \phi_i) - \dot{\theta} \sum_{i=1}^{N} \dot{\phi}_i \sin(\phi_i + \theta)\Bigg) + \ell_c \dot{\ell}_c \cos(\theta+\phi_r)\, \dot{\theta} \sum_{i=1}^{N} \cos(\theta+\phi_i)\Bigg]$$

$$-M_2\Bigg[\Bigg(2\dot{\ell}_c \ell_c \sin(\theta + \phi_r) + \ell_c^{\,2} \cos(\theta + \phi_r)\, \dot{\theta}\Bigg) \sum_{i=1}^{N} \dot{\phi}_i \sin(\theta + \phi_i)$$

$$-\ell_c \dot{\ell}_c \cos(\theta + \phi_r)\, \dot{\theta} \sum_{i=1}^{N} \cos(\theta + \phi_i) + \ell_c^{\,2} \sin(\theta + \phi_r) \cdot$$

$$\Bigg(\sum_{i=1}^{r-1} \ddot{\phi}_i \sin(\theta + \phi_r) + \sum_{i=r+1}^{N} \ddot{\phi}_i \sin(\theta + \phi_i) + \sum_{i=1}^{N} \dot{\phi}_i^{\,2} \cos(\theta + \phi_i)$$

$$+ \dot{\theta} \sum_{i=1}^{N} \dot{\phi}_i \cos(\theta + \phi_i)\Bigg) + \ell_c \dot{\ell}_c \sin(\theta+\phi_r)\, \dot{\theta} \sum_{i=1}^{N} \sin(\theta + \phi_i)$$

$$-\ell_c \ell_h \left(\dot{\theta}^2 \cos(\theta + \phi_r) + \ddot{\theta} \sin(\theta + \phi_r)\right)\Bigg]\Bigg\} \Bigg/$$

$$\Bigg\{\ell_c^{\,2} \sum_{n=r+1}^{N} m_{c_n} + \ell_c^{\,2}\left[\frac{m_{c_r}}{3} + m_h + M_1 \cos^2(\theta + \phi_r) + M_2 \sin^2(\theta + \phi_r)\right]\Bigg\} \tag{40}$$

Note that ℓ_{c_i} and $\dot{\ell}_{c_i}$ have been taken out of the summations because each link is assumed to have the same length and same time derivative. Terms

REF: ENGINEERING PROCEDURE S.017
E-TD-15(7-64)(77-10)

involving $\ddot{\ell}_{c_i}$ are set equal to zero.

5. The Generalized Forces

The generalized force F_θ is given by:

$$F_\theta = \vec{F}_{N+1} \cdot \frac{\partial \vec{V}^{P^*_{N+1}}}{\partial \dot{\theta}} + \vec{F}_Q \cdot \frac{\partial \vec{V}^{Q}}{\partial \dot{\theta}} + \sum_{n=1}^{N} \vec{F}_n \cdot \frac{\partial \vec{V}^{P_n^*}}{\partial \dot{\theta}} + M \qquad (41)$$

where

F_θ is the external torque acting on the balloon

$\vec{F}_{N+1}$ is the applied force acting on the harness

$\vec{F}_Q$ is the applied force acting on the balloon

$\vec{F}_n$ is the applied force acting on the nth link

M is the applied moment about the center of mass of the balloon

From equation (9), $\vec{V}^{P_n^*}$ is not a function of $\dot{\theta}$.

The applied moment about the center of mass is:

$$M = M_a + \frac{\partial M_a}{\partial \dot{\theta}} \dot{\theta} + M_s \qquad (42)$$

where:

M_a is the aerodynamic moment

$\frac{\partial M_a}{\partial \dot{\theta}} \dot{\theta}$ is the aerodynamic damping moment

M_s is the static moment due to buoyant lift

REF: ENGINEERING PROCEDURE 5-017
E-ID-15(7-84)(77-10)

Since the balloon is spherical, the buoyant force is concentrated at the geometric center, and $M_s = 0$. A spherical body also has a zero aerodynamic moment. If viscous effects are ignored, the aerodynamic damping moment is zero. Therefore, equation (41) simplifies to:

$$F_\theta = \vec{F}_{N+1} \cdot \frac{\partial \vec{V}^{P^*_{N+1}}}{\partial \dot{\theta}} + \vec{F}_Q \cdot \frac{\partial \vec{V}^{Q}}{\partial \dot{\theta}} \tag{43}$$

$\vec{F}_Q$ represents the force vector acting on the center of gravity of the balloon and is given by:

$$\vec{F}_Q = H\,\vec{N}_1 + B\,\vec{N}_2 \tag{44}$$

where H is the horizontal force and B is the vertical force as shown in Figure A-4.

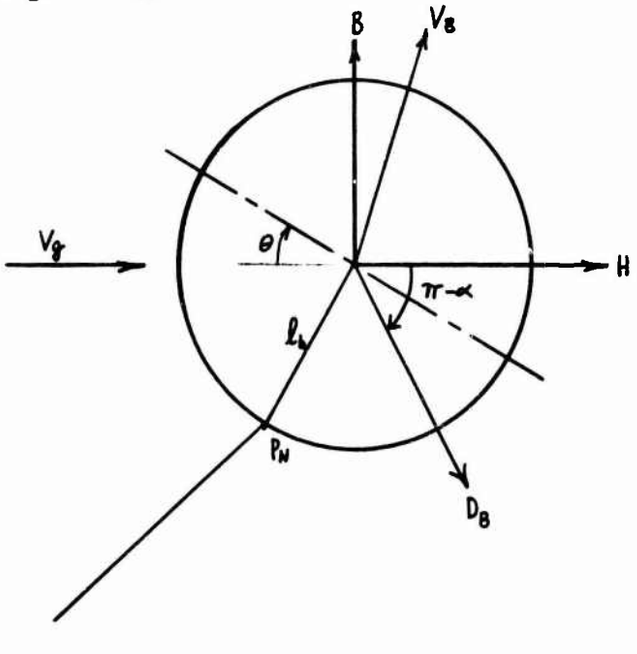

V_B = Balloon velocity

V_g = Wind velocity

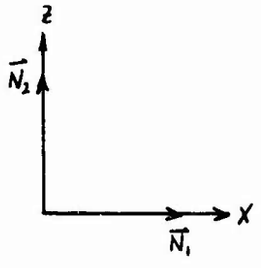

Figure A-4 - Forces Acting on Balloon

REF: ENGINEERING PROCEDURE S-017

The forces that contribute to B and H are the buoyant force, the weight of the balloon structure, the weight of the helium inside the balloon and the drag forces.

The total drag force is $D_B = C_{D_B} q_B S_B$ (45)

C_{D_B} is assumed to be constant and equal to .15

S_B varies and is equal to $\pi \ell_h^2 \sim ft^2$

q_B is the dynamic pressure acting on the balloon relative to the air $\sim lb/ft^2$

In this case, not only is the balloon moving but a variable wind is acting on it. The wind velocity is a function of altitude. At any time, the wind velocity is considered constant and equal to the velocity of the wind at the altitude of the center of gravity of the balloon. This assumption eliminates an aerodynamic moment which probably does slightly effect the motion of large balloons. If the balloon is moving vertically with a velocity $\dot{z}$ and horizontally with a velocity $\dot{x}$ and the horizontal wind velocity is V_g than the dynamic pressure is:

$$q_B = \tfrac{1}{2} \rho \left[(\dot{x} - V_g)^2 + \dot{z}^2 \right] \qquad (46)$$

The drag can now be broken into two components, one in the $\vec{N}_1$ direction and one into the $\vec{N}_2$ direction.

E-ID-15(7-60)(77-16) REF: ENGINEERING PROCEDURE 5.017

Referring to Figure A-4:

$$\alpha = \tan^{-1}\left[\dot{z}/(\dot{x} - V_g)\right] \tag{47}$$

Then the forces on the balloon are:

$$B = L_S - W_H - W_{B_S} - D_{V_B} \tag{48}$$

$$H = - D_{H_B} \tag{49}$$

where:

L_S is the buoyant force of the displaced air

W_H is the weight of the helium

W_{B_S} is the weight of the balloon structure

D_{V_B} is the drag force in the vertical direction (positive down) and is equal to:

$$D_{V_B} = q_B S_B C_{D_B} \sin\alpha \tag{50}$$

D_{H_B} is the drag force in the horizontal direction (positive to the left) and is equal to:

$$D_{H_B} = q_B S_B C_{D_B} \cos\alpha \tag{51}$$

Since the harness has no weight or aerodynamic forces acting on it,

$$\vec{F}_{N+1} = 0 \tag{52}$$

E-ID-15(7-64)(77-10) REF: ENGINEERING PROCEDURE S.017

Therefore, when substituting equations (19), (44) and (52) into (43), the generalized force on the balloon becomes:

$$F_\theta = (H \vec{N}_1 + B \vec{N}_2)(-\ell_h \vec{e}_{N+1}) \tag{53}$$

Simplifying

$$F_\theta = \ell_h \left[- B \sin \theta + H \cos \theta \right] \tag{54}$$

From Figure A-4, it is obvious that F_θ is the external torque about point P_N. (positive torque clockwise).

The generalized force F_{ϕ_r} is given by:

$$F_{\phi_r} = \sum_{i=1}^{N} \vec{F}_i \cdot \frac{\partial \vec{V}^{P_i^*}}{\partial \dot{\phi}_r} + \vec{F}_{N+1} \cdot \frac{\partial \vec{V}^{P_{N+1}^*}}{\partial \dot{\phi}_r} + \vec{F}_Q \cdot \frac{\partial \vec{V}^{Q}}{\partial \dot{\phi}_r} \tag{55}$$

The only unevaluated terms are $\sum_{i=1}^{N} \vec{F}_i$ which are the applied forces acting on ℓ_{c_i} shown in Figure A-2.

$$\vec{F}_i = \vec{F}^{P_i^*} + \vec{G}^{P_i^*} \tag{56}$$

where $\vec{G}^{P_i^*}$ is the gravitational force of ℓ_{c_i}

$$\vec{G}^{P_i^*} = - m_{c_i} g \vec{N}_2 \tag{57}$$

REF: ENGINEERING PROCEDURE S.017
E-ID-15(7-68)(77-15)

and $\vec{F}^{P_i^*}$ is the normal drag force on ℓ_{c_i}

$$\vec{F}^{P_i^*} = - D_{H_{c_i}} \sin^2 \phi_i \, \vec{e}_i' - D_{V_{c_i}} \cos^2 \phi_i \, \vec{e}_i' \tag{58}$$

As with the balloon, each link is moving and a variable wind is acting on it. At any time, the wind velocity across a link is considered constant and equal to the velocity of the wind at the altitude of the center of mass of the link. It should be remembered that the center of mass was assumed to be at the geometric center of each link. If the center of mass of a link is moving vertically with a velocity $\dot{z}_{c_i}$ and horizontally with a velocity $\dot{x}_{c_i}$ and the wind velocity at the center of mass is $V_{g_{c_i}}$, then the drag components are:

$$D_{H_{c_i}} = \tfrac{1}{2} C_{D_c} \rho_i S_{c_i} \left[V_{g_{c_i}} - \dot{x}_{c_i} \right]^2 \tag{59}$$

$$D_{V_{c_i}} = \tfrac{1}{2} C_{D_c} \rho_i S_{c_i} \left[\dot{z}_{c_i} \right]^2 \tag{60}$$

The factor $\sin^2 \phi_i$ and $\cos^2 \phi_i$ in equation (58) take into account the projected area in the horizontal and vertical directions and then rotate the horizontal and vertical drag components into the direction normal to ℓ_{c_i}.

C_{D_c} is assumed to be constant and equal to 1.2

S_{c_i} is equal to the average diameter of ℓ_{c_i} times ℓ_c

ρ_i is measured at the center of mass of ℓ_{c_i}

E-ID-15(7-64)(77-10) REF: ENGINEERING PROCEDURE 5.017

Therefore, when substituting equations (14), (44), (52) and (56) into equation (55), the generalized force on each link becomes:

$$F_{\phi_r} = \left(- D_{H_{c_r}} \sin^2 \phi_r \, \vec{e}_r' \, D_{V_{c_r}} \cos^2 \phi_r \, \vec{e}_r' - m_{c_r} g \, \vec{N}_2\right) \cdot \frac{\ell_c}{2} \, \vec{e}_r'$$

$$+ \sum_{i=r+1}^{N} \left(- D_{H_{c_i}} \sin^2 \phi_i \, \vec{e}_i' - D_{V_{c_i}} \cos^2 \phi_i \, \vec{e}_i' - m_{c_i} g \, \vec{N}_2\right) \cdot \ell_c \, \vec{e}_r'$$

$$+ (H \, \vec{N}_1 + B \, \vec{N}_2) \cdot \ell_c \, \vec{e}_r' \qquad (61)$$

Simplifying:

$$F_{\phi_r} = - \frac{\ell_c}{2} D_{H_{c_r}} \sin^2 \phi_r - \frac{\ell_c}{2} D_{V_{c_r}} \cos^2 \phi_r - m_{c_r} g \frac{\ell_c}{2} \cos \phi_r$$

$$+ \ell_c \sum_{i=r+1}^{N} \left[- D_{H_{c_i}} \sin^2 \phi_i \cos (\phi_r - \phi_i) - D_{V_{c_i}} \cos^2 \phi_i \cos (\phi_r - \phi_i)\right.$$

$$\left. - m_{c_i} g \cos \phi_r\right] + \ell_c \left[- H \sin \phi_r + B \cos \phi_r\right] \qquad (62)$$

From Figures A-1, A-2, and A-4, it can be seen that F_{ϕ_r} is the external torque acting about P_{r-1} (positive counterclockwise).

E-ID-15(7-64)(77-10)
REF: ENGINEERING PROCEDURE S.017

APPENDIX B

Computer Program

1. Wind Profile

The wind profile for any simulation is considered to be a function of altitude as shown in Figures 1 and 2. Any one of these curves can be approximated by twenty-four points and twenty-three line segments. The twenty-four points are stored in an array in the computer and the program interpolates between any two points. Since the wind profile curve is well behaved, 5,000 ft increments seem to be more than adequate. However, any altitude increment may be used, and the increments can be of varying size.

2. Tether Profile

Tether profiles used in this simulation are shown in Figure B-1. Both the diameter and weight per unit length can be approximated as a series of linear functions of length, and is therefore represented by thirty-two points and thirty-one line segments. The computer program interpolates to find the diameter and weight per unit length at each end of a link and then considers each link to be a right circular cylinder with diameter and weight found by averaging the end conditions. Obviously, the greater number of links used the more accurate the approximation. It has been calculated that a three link representation of 135,000 ft of tether overestimates the tether weight by less than 3.5%.

E-ID-15(7-60)(77-10) REF. ENGINEERING PROCEDURE 5.017

JR 220 (7-63)

REF: ENGRG PROCEDURE S-017

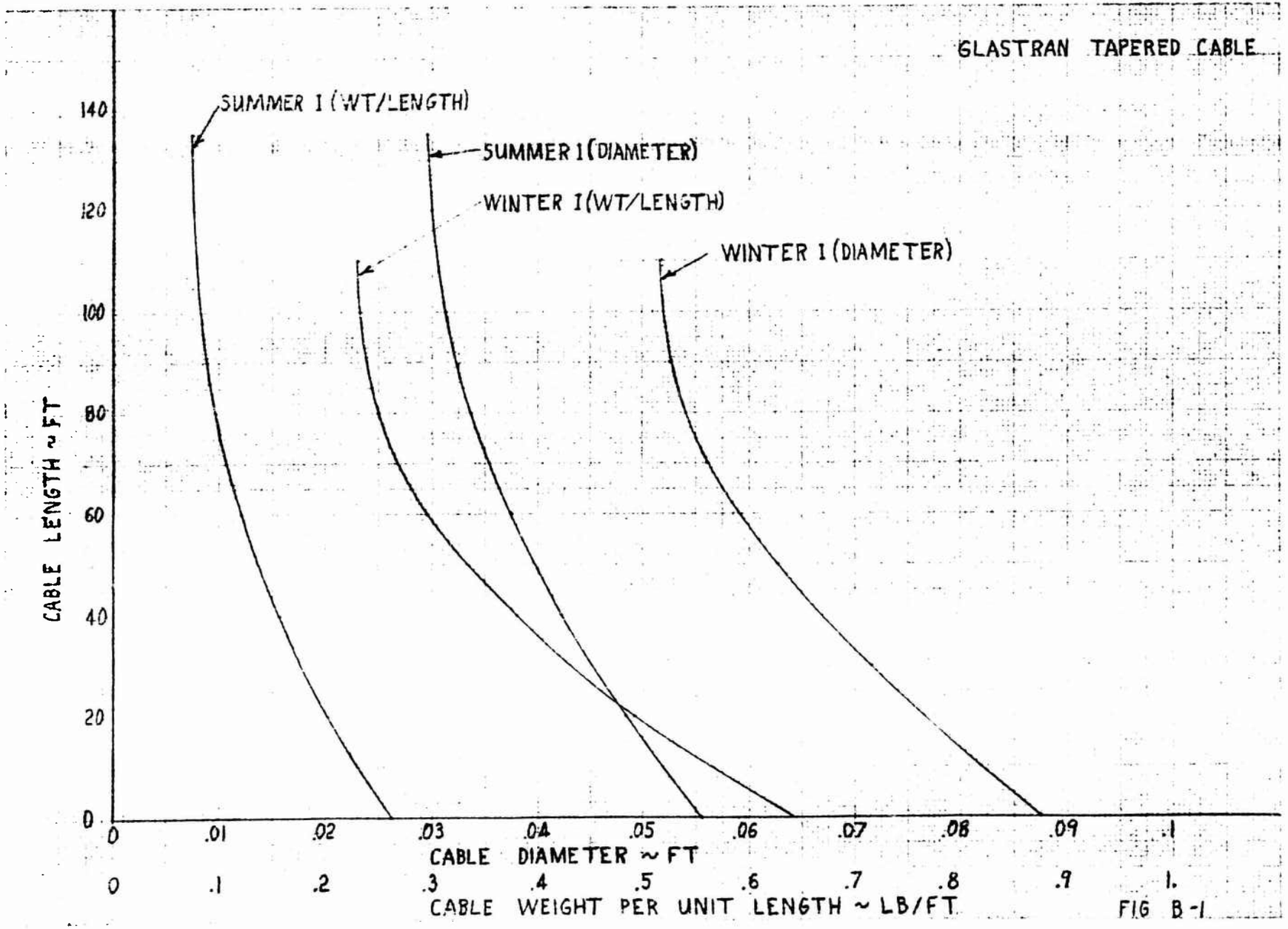

FIG B-1

DATE

REV DATE

REV DATE

GOODYEAR AEROSPACE CORPORATION AKRON 15 OHIO

PAGE B-2

GER. 18714

CODE IDENT NO. 25500

3. Winching Rate

At any time, the winching rate is considered constant. However, the program will consider discontinuous changes in the rate as a function of time as shown in Figure B-2.

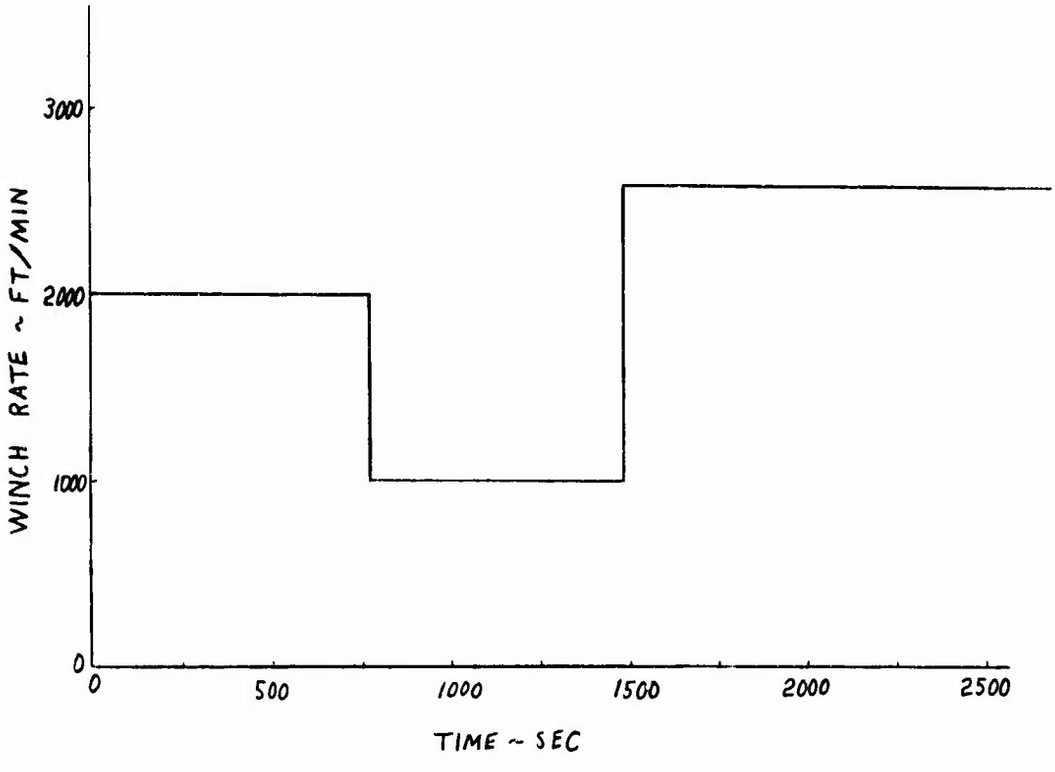

Figure B-2 - Winching Rate

E-1D-15(7-64)(77-10)
REF: ENGINEERING PROCEDURE 5-017

4. Translational Dynamics of Balloon and Tether

Although angular coordinates represent the best method of solving the equations of motion, linear coordinates must be calculated to find the forces acting on the balloon and links.

a. Balloon Dynamics

The following equations represent the linear displacements, velocities, and accelerations of the balloon:

$$x = \ell_c \sum_{i=1}^{N} \cos \phi_i + \ell_h \sin \theta \tag{63}$$

$$z = \ell_c \sum_{i=1}^{N} \sin \phi_i + \ell_h \cos \theta \tag{64}$$

$$\dot{x} = \dot{\ell}_c \sum_{i=1}^{N} \cos \phi_i - \ell_c \sum_{i=1}^{N} \sin \phi_i \dot{\phi}_i + \ell_h \cos \theta \dot{\theta} \tag{65}$$

$$\dot{z} = \dot{\ell}_c \sum_{i=1}^{N} \sin \phi_i + \ell_c \sum_{i=1}^{N} \cos \phi_i \dot{\phi}_i - \ell_h \sin \theta \dot{\theta} \tag{66}$$

B-ID-15(7-64)(77-10) REF: ENGINEERING PROCEDURE S.017

$$\ddot{z} = 2\dot{\ell}_c \sum_{i=1}^{N} \cos\phi_i \dot{\phi}_i - \ell_c \sum_{i=1}^{N} \sin\phi_i \dot{\phi}_i^2 + \ell_c \sum_{i=1}^{N} \cos\phi_i \ddot{\phi}_i$$

$$- \ell_h \cos\theta \dot{\theta}^2 - \ell_h \sin\theta \ddot{\theta} \tag{67}$$

$$\ddot{x} = -2\dot{\ell}_c \sum_{i=1}^{N} \sin\phi_i \dot{\phi}_i - \ell_c \sum_{i=1}^{N} \cos\phi_i \dot{\phi}_i^2 - \ell_c \sum_{i=1}^{N} \sin\phi_i \ddot{\phi}_i$$

$$- \ell_h \sin\theta \dot{\theta}^2 + \ell_h \cos\theta \ddot{\theta} \tag{68}$$

b. Tether Dynamics

The following equations represent the linear vertical displacement, velocities and accelerations of the geometric center of the "r"th link.

$$z_{c_r} = \ell_c \sum_{i=1}^{r-1} \sin\phi_i + \frac{\ell_c}{2} \sin\phi_r \tag{69}$$

$$\dot{x}_{c_r} = \dot{\ell}_c \sum_{i=1}^{r-1} \cos\phi_i - \ell_c \sum_{i=1}^{r-1} \sin\phi_i \dot{\phi}_i$$

$$+ \frac{\dot{\ell}_c}{2} \cos\phi_r - \frac{\ell_c}{2} \sin\phi_r \dot{\phi}_r \tag{70}$$

E-ID-15(7-66)(77-10) REF: ENGINEERING PROCEDURE 5.017

$$\dot{z}_{c_r} = \dot{\ell}_c \sum_{i=1}^{r-1} \sin \phi_i + \ell_c \sum_{i=1}^{r-1} \cos \phi_i \dot{\phi}_i$$

$$+ \frac{\dot{\ell}_c}{2} \sin \phi_r + \frac{\ell_c}{2} \cos \phi_r \dot{\phi}_r \qquad (71)$$

$$\ddot{z}_{c_r} = 2\dot{\ell}_c \sum_{i=1}^{r-1} \cos \phi_i \dot{\phi}_i + \ell_c \sum_{i=1}^{r-1} \cos \phi_i \ddot{\phi}_i - \ell_c \sum_{i=1}^{r-1} \sin \phi_i \dot{\phi}_i^2$$

$$+ \dot{\ell}_c \cos \phi_r \dot{\phi}_r + \frac{\ell_c}{2} \cos \phi_r \ddot{\phi}_r - \frac{\ell_c}{2} \sin \phi_r \dot{\phi}_r^2 \qquad (72)$$

$$\ddot{x}_{c_r} = -2\dot{\ell}_c \sum_{i=1}^{r-1} \sin \phi_i \dot{\phi}_i - \ell_c \sum_{i=1}^{r-1} \cos \phi_i \dot{\phi}_i^2 - \ell_c \sum_{i=1}^{r-1} \sin \phi_i \ddot{\phi}_i$$

$$- \dot{\ell}_c \sin \phi_r \dot{\phi}_r - \frac{\ell_c}{2} \cos \phi_r \dot{\phi}_r^2 - \frac{\ell_c}{2} \sin \phi_r \ddot{\phi}_r \qquad (73)$$

5. Tension

In an effort to show how much loading the tether must be able to accommodate, the tension at each hinge point was calculated. Referring to Figure B-3, the tension at the balloon hinge point is:

$$\sum F_z = M_1 \ddot{z} = B - PL - F_{V_N} \qquad (74)$$

$$F_{V_N} = B - PL - M_1 \ddot{z} \qquad (75)$$

B-ID-15(7-64)(77-10)
REF. ENGINEERING PROCEDURE S-017

$$\Sigma F_x = M_1 \ddot{x} = H - F_{H_N} \tag{76}$$

$$F_{H_N} = H - M_1 \ddot{x} \tag{77}$$

$$T_N = \sqrt{(F_{H_N})^2 + (F_{V_N})^2} \tag{78}$$

where:

ΣF_z and ΣF_x are the sum of the vertical and horizontal forces respectively acting on the balloon.

F_{V_N} and F_{H_N} are the vertical and horizontal components of tension on the Nth link.

PL is the payload weight in lbs.

T_N is the tension in the tether at the balloon hinge.

E-ID-15(7-64)(77-10)
REF: ENGINEERING PROCEDURE S.017

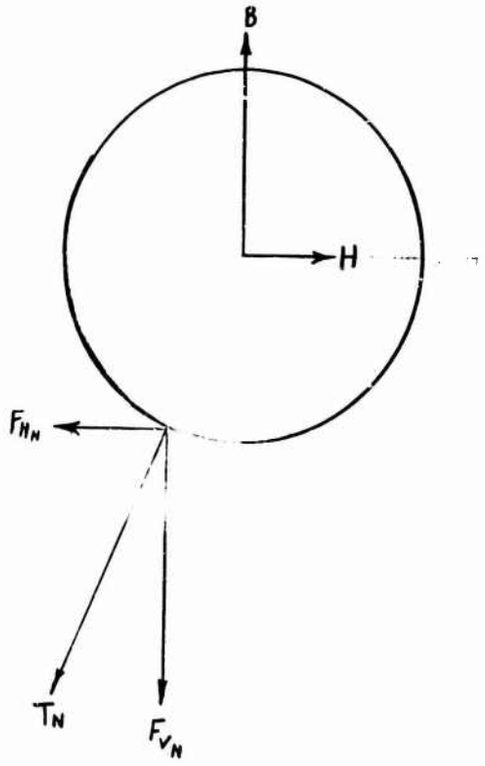

Figure B-3 - Horizontal and Vertical Forces Acting on Balloon

Figure B-4 shows the "N"th link and all the forces acting on it.

$$\sum F_{z_N} = m_{c_N} \ddot{z}_{c_N} = F_{V_N} - D_{V_N} - WT_N - F_{V_{N-1}} \tag{79}$$

$$F_{V_{N-1}} = F_{V_N} - D_{V_N} - WT_N - m_{c_N} \ddot{z}_{c_N} \tag{80}$$

$$\sum F_{x_N} = m_{c_N} \ddot{x}_{c_N} = F_{H_N} + D_{H_N} - F_{H_{N-1}} \tag{81}$$

$$F_{H_{N-1}} = F_{H_N} + D_{H_N} - m_{c_N} \ddot{x}_{c_N} \tag{82}$$

E-ID-15(7-64)(77-10)
REF: ENGINEERING PROCEDURE S.017

$$T_{N-1} = \sqrt{(F_{V_{N-1}})^2 + (F_{H_{N-1}})^2} \qquad (83)$$

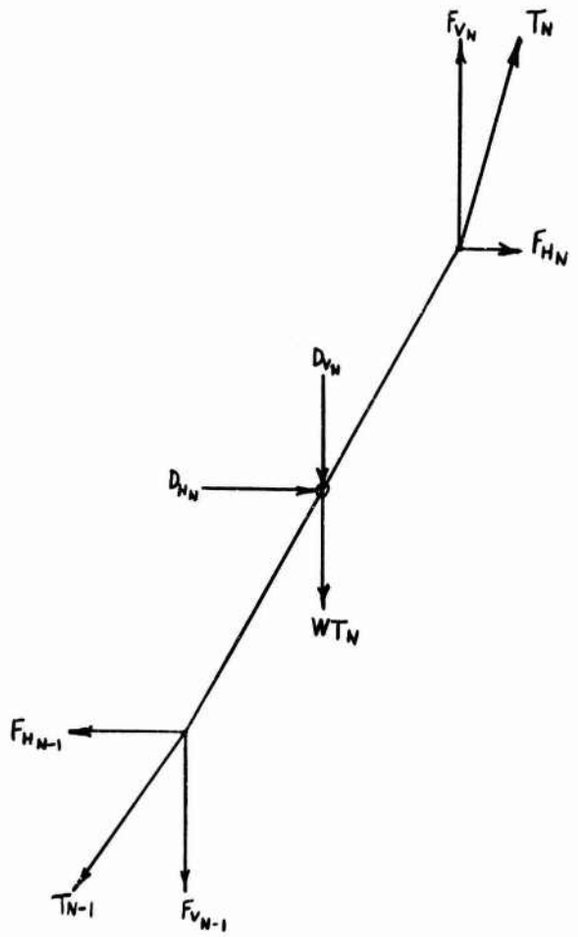

Figure B-4 - Horizontal and Vertical Forces Acting On "N"th Link

E-ID-15(7-70)(77-10)
REF: ENGINEERING PROCEDURE S-017

where:

ΣF_{z_N} and ΣF_{x_N} are the sum of the vertical and horizontal forces respectively acting on the "N"th link.

$F_{V_{N-1}}$ and $F_{H_{N-1}}$ are the vertical and horizontal components of tension at the top of the "N-1" link.

WT_N is the weight of the "N"th link in lbs.

In general for the "r"th link

$$F_{H_{r-1}} = F_{H_r} + D_{H_r} - m_{c_r} \ddot{x}_{c_r} \tag{84}$$

$$F_{V_{r-1}} = F_{V_r} - D_{V_r} - WT_r - m_{c_r} \ddot{z}_{c_r} \tag{85}$$

$$T_{r-1} = \sqrt{(F_{V_{r-1}})^2 + (F_{H_{r-1}})^2} \tag{86}$$

The tension at the winch is found by setting r=1

$$F_{H_o} = F_{H_1} + D_{H_1} - m_{c_1} \ddot{x}_{c_1} \tag{87}$$

$$F_{V_o} = F_{V_1} - D_{V_1} - WT_1 - m_{c_1} \ddot{z}_{c_1} \tag{88}$$

$$T_W = \sqrt{(F_{V_o})^2 + (F_{H_o})^2} \tag{89}$$

6. Physical Aspects of the Balloon

As mentioned previously, the balloon is considered to be a thin spherical shell expanding as it ascends. Two basic balloon sizes were used. The first one expanded to 30×10^6 ft^3 at 100,000 ft altitude, and the second, to 79×10^6 ft^3 at the same altitude. The structural weights of the balloons

E-ID-15(7-60)(77-10) REF: ENGINEERING PROCEDURE S.017

are 8600 lbs and 24,600 lbs respectively. The volume at any altitude is equal to the volume at sea level divided by the atmospheric density ratio. The weight of helium (96.5% pure) in the balloon is equal to the weight density of helium times the volume of the balloon. For the 30 million ft^3 balloon, the weight is:

$$W_H = (.01297)\ (419000) = 5430 \text{ lbs} \tag{90}$$

For the 79 million ft^3 balloon, the weight is:

$$W_H = (.01297)\ (1,102,000) = 14,300 \text{ lbs.} \tag{91}$$

The payload is assumed to be attached to the balloon at the tether hinge point. The moment of inertia about the c.g. of the balloon takes into account the payload but not the helium inside the balloon or any of the air outside the balloon. This assumes that the shear forces are negligible.

$$I_B = (2/3\ W_{B_S} + PL)\ \ell_h^2/g \tag{92}$$

The directional masses of the balloon (M_1, M_2) are

$$M_1 = M_2 = (W_H + W_{B_S} + PL)/g + \tfrac{1}{2}\rho_o V_o \tag{93}$$

where:

$\frac{1}{2}\rho_o V_o$ is the apparent mass of the balloons

ρ_o is the atmospheric density at sea level

V_o is the balloon volume at sea level

M_1 and M_2 are equal because the balloon is spherical.

7. Numerical Integration Technique

The two dynamical equations that must be solved are (39) and (40). These equations can be written in the form:

$$\ddot{\theta} = f(\dot{\theta}, \theta, \ddot{\phi}_1, \ldots, \ddot{\phi}_N, \dot{\phi}_1, \ldots, \dot{\phi}_N, \phi_1, \ldots, \phi_N, t)$$
$$\ddot{\phi}_r = g(\ddot{\theta}, \dot{\theta}, \theta, \ddot{\phi}_1, \ldots \ddot{\phi}_{r-1}, \ddot{\phi}_{r+1}, \ldots, \ddot{\phi}_N, \dot{\phi}_1, \ldots, \dot{\phi}_N, \phi_1, \ldots \phi_N, t) \quad (94)$$

It is clearly seen that equations (94) are strongly coupled. To reduce the complexity of the numerical integration, all coupling terms of second order are eliminated. Preliminary computer runs show that angular accelerations are one order of magnitude less than angular velocities. Therefore, equations (94) reduce to the following:

$$\left.\begin{aligned} \ddot{\theta} &= f_1(\dot{\theta}, \theta, \dot{\phi}_1, \ldots, \dot{\phi}_N, \phi_1, \ldots, \phi_N, t) \\ \ddot{\phi}_r &= g_1(\dot{\theta}, \theta, \dot{\phi}_1, \ldots, \dot{\phi}_N, \phi_1, \ldots, \phi_N, t) \end{aligned}\right\} \quad (95)$$

Equations (95) are solved by Runge-Kutta (4th order accuracy) numerical integration techniques. Due to the long running times, it is advantageous to use a large time increment. It has been found that an increase in the degrees of freedom requires a reduction in the time increment. To help

B-ID-15(7-64)(77-10) REF: ENGINEERING PROCEDURE S.017

alleviate this problem, the balloon's pitch angle is held constant. This affect on the dynamics of the tether was hardly noticeable. No graphs were constructed to show this because the differences were in the fourth significant figure.

8. Determination of Number of Links

As stated previously, an increase in the degrees of freedom decreases the magnitude of the time increment which will allow a stable simulation. Also the computer time increases linearly with an increase in the number of links simply because each extra link involves one more equation of the form of equation (40) which must be integrated. Therefore, an effort was made to determine the least number of links which would present a good simulation. To this end, a tether was payed-out in a summer I-90% wind. A winching rate of 3000 ft/min was used for 1500 sec. This allowed the balloon to pass through the high dynamic pressure region. Figure B-5 shows the altitude versus range of the balloon for both three links and five links. Figure B-6 shows the tether profile at 500 sec, 1000 sec, and 1500 sec. These comparisons justify the use of three links in all future runs unless a wind profile containing severe cross winds is used. The conclusions that three links is adequate for the simulation was also reached by Professors Elnan and Evert in Reference 1.

E-ID-15(7-64)(77-10)
REF: ENGINEERING PROCEDURE 5-017

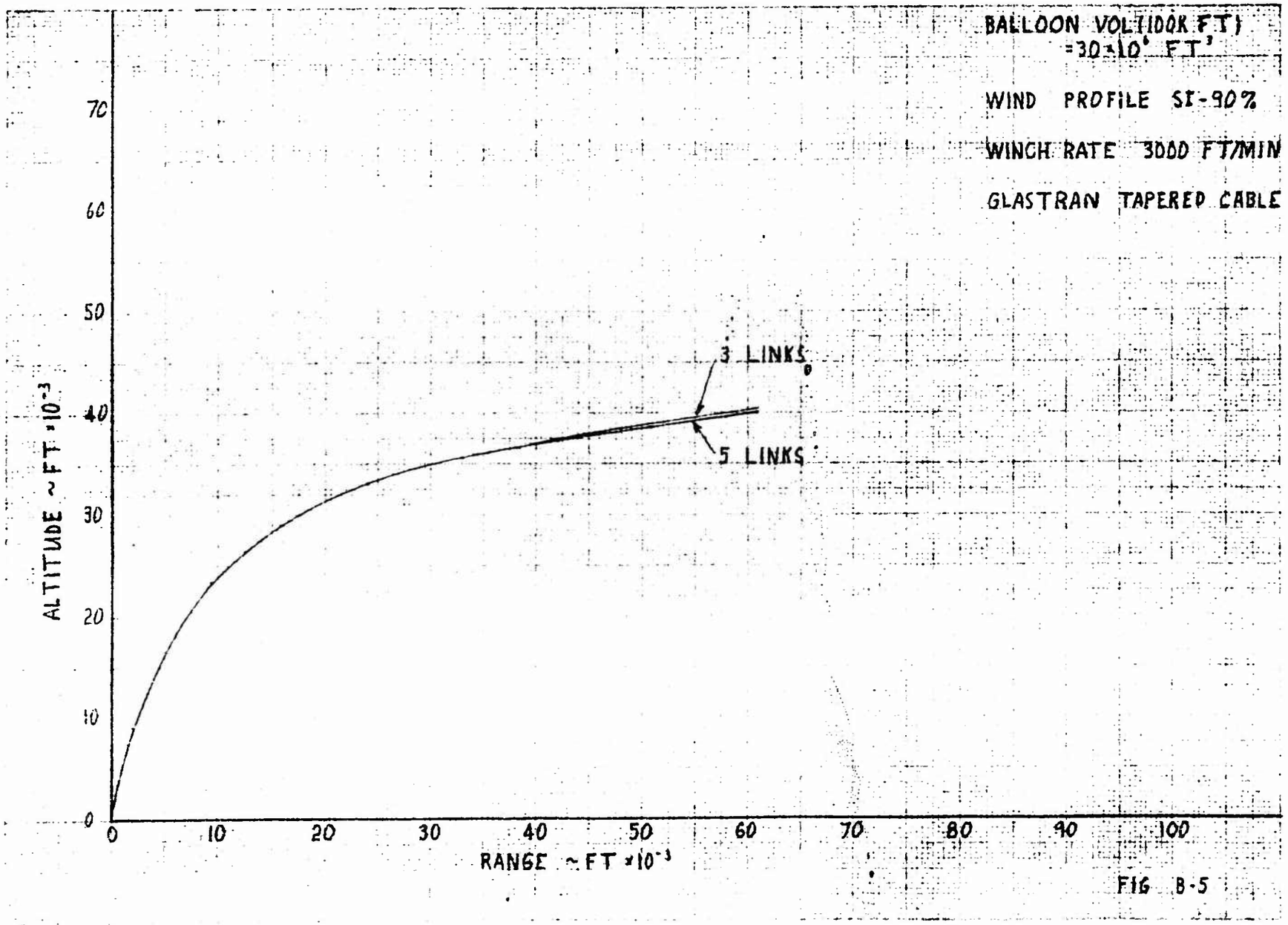

FIG B-5

DATE
REV DATE
REV DATE

GOODYEAR AEROSPACE CORPORATION
AKRON 15, OHIO

PAGE B-14
GER-13711
CODE IDENT NO. 25500

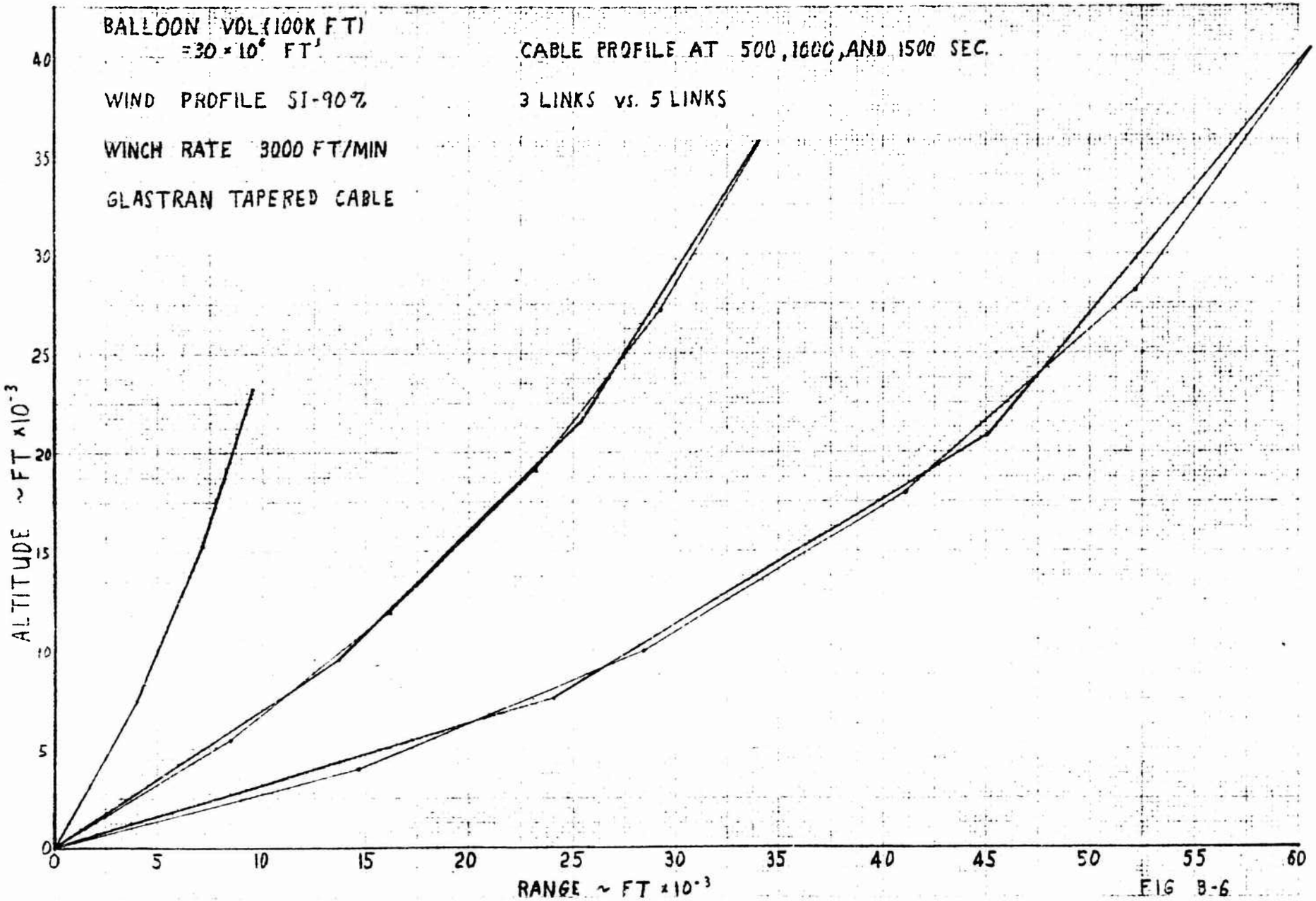

FIG B-6

DATE
REV DATE
REV DATE

GOODYEAR AEROSPACE CORPORATION
AKRON 15, OHIO

PAGE B-15
GER. 13714
CODE IDENT NO. 25500

9. Inputs

The format for all inputs is F10.0. The following is a list of all needed variables with appropriate units:

a. Stop Altitude - The program may be stopped when the balloon reaches any given altitude (ft) and a new simulation started. This variable is good only for ascent simulation.

b. Stop Time - The program may be stopped at any given time (sec) during the simulation and new simulation began.

c. Stop Tether Length - The program may be stopped when a certain length of cable (ft) has been winched out.

d. Acceleration of Gravity at Sea Level - Ft/sec^2

e. Radius of Earth - Ft

f. Integration Step Size - The program is started with a relatively small time increment (.5 sec) to allow for large acceleration to damp out.

g. Printout Time - In the majority of simulations, it is not necessary to printout after every integration. Since printing time wastes computer time, it is most desirable to make several integrations before printing out data. This input variable should be equal to the number of integrations made before each printout.

h. Number of Links

E-TD-15(7-64)(77-10)
REF: ENGINEERING PROCEDURE S 017

i. Weight of Payload Attached at Balloon - Tether Junction - lb

j. Time - For an ascent simulation, the time is arbitrarily set at 4 sec. The program then starts with a relatively small length of tether winched out. If the length of tether were zero initially, oscillations of a very high frequency would take place for a short period of time because the moment arm is very small. For descent simulations, the time (sec) must be equal to a value which, when multiplied by a positive winching rate, will equal the total length of tether payed-out at the start of the descent.

k. Initial Tether Length - Ft

l. Second Integration Step Size - After the first several seconds (sec f) the time increment is increased in order to speed up the calculations.

m. Second Time - This variable is set equal to the time (see j) plus several seconds (10-20). After the second time is reached, a second larger integration step size is used (see l) because accelerations are relatively low..

n. Initial Altitude - Ft

o. Drag Coefficient of Cable - A value of 1.2 (cylinder) was used for this simulation.

p. Drag coefficient of balloon - A value of .15 (sphere) was used for this simulation.

q. Reference Volume of Balloon - The program uses the volume (ft^3) of the balloon at sea level as a reference.

E-ID-15(7-64)(77-10)
REF: ENGINEERING PROCEDURE S-017

r. Harness Mass - Slugs (zero in these runs)

s. Balloon Structural Weight - Lb

t. Weight Density of Helium at Sea Level - Lb/ft^3

u. Initial Pitch Angle of Balloon - Rad (zero in these runs)

v. Initial Pitch Rate of Balloon - Rad/sec (zero in these runs)

aa. An array of N variables representing the initial time rates of change of the angles of the N links - positive counterclockwise - Rad/sec

bb. An array of N variables representing the angles of N links - positive counterclockwise from the right horizontal - Rad

cc. An array of eight variables representing times at which the winching rate is changed - sec

dd. An array of eight variables representing winching rates corresponding to (cc). The first value is the initial winching rate and corresponds to zero time. The second value is also the initial winching rate and corresponds to the time at which the winching rate is to be changed. The third value is the second winching rate and corresponds to the time at which the winching rate is to be changed again, and so forth. -Ft/sec.

ee. An array of twenty-four variables representing altitudes - Ft.

ff. An array of twenty-four variables representing wind velocities corresponding to the altitudes given in (ee) - Ft/sec.

gg. An array of thirty-two variables representing lengths of the tether starting at the balloon - ft.

E-1D-15(7-60)(77-10)
REF: ENGINEERING PROCEDURE S.017

hh. An array of thirty-two variables representing diameters of the tether corresponding to (gg).- Ft.

ii. An array of thirty-two variables representing weights per unit length of the tether corresponding to (gg) - Lb/ft.

10. Outputs

At predetermined time intervals (see input g.) the following data is outputted in format F9.2.

a. The angle formed by each link from the horizon - Deg

b. The angular velocity of each link - Deg/sec

c. The tension at the top of each link - Lb

d. Time - Sec

e. Altitude of Balloon - Ft

f. Range of Balloon - Ft

g. Horizontal and vertical velocities of balloon - Ft/sec

h. Pitch angle of balloon - Deg

i. Pitch rate of balloon - Deg/sec

j. Length of one link - Ft

k. Winching rate - ft/min

l. Wind velocity at balloon's altitude - Ft/sec

m. Harness length (balloon radius) - Ft

n. Tension at winch - Lb

B-ID-15(7-64)(77-10) REF: ENGINEERING PROCEDURE S.017

o. Total weight of cable winched out - Lb

p. Horizontal drag force on balloon - Lb

q. Vertical drag force on balloon - Lb

r. Total vertical force acting on balloon, including the buoyant lift, structural weight, weight of helium and vertical drag force. This force must be greater than the weight of the tether plus the payload in order to have an ascending balloon - Lb.

s. Dynamic pressure acting on the balloon relative to the free stream velocity - Lb/ft^2

11. Fortran IV Program

A listing of the program is contained in APPENDIX C. The functions of the main program and the subroutines are as follows:

a. Main Program

1) Define the two functions to be solved (equations (39) and (40)).

2) Read input variables

3) Initialize program

4) Check if end constraints (balloon altitude, time, and tether length) are met. If one condition is met, print output, and start new program; otherwise, continue.

5) Check if printout time is reached. If it is reached, calculate the tensions at the top of each link and at the winch, print output and continue; if not reached, continue..

E-ID-15(7-60)(77-10) REF: ENGINEERING PROCEDURE S 017

6) Advance the generalized coordinates and velocities through one time increment by Runge-Kutta integration.

7) Calculate altitude, range, horizontal and vertical velocities and accelerations of balloon.

8) Calculate time rate of change of mass of each link and time rate of change of moment of inertia of balloon.

b. Subroutine Head (N)

This subroutine writes out the headings $\phi_1, \ldots, \phi_{12}, \dot{\phi}_1 \ldots, \dot{\phi}_{12}$ and $TENS_1, \ldots, TENS_{12}$.

c. Subroutine Subrb

1) Find the atmospheric density surrounding the balloon by using an "in-house" subroutine based on 1962 US Standard Atmosphere.

2) Calculate volume, moment of inertia about c.g., radius and aerodynamic reference area of balloon.

3) Calculate horizontal wind velocity at balloon's altitude.

4) Calculate horizontal and vertical drags on balloon due to relative velocity between balloon and wind.

5) Calculate directional masses of balloon.

6) Calculate static lift of balloon.

7) Calculate generalized force acting on balloon.

B-ID-15(7-64)(77-10) REF: ENGINEERING PROCEDURE S.017

d. Subroutine Subrc

1) Identify several variables with the appropriate link.

2) Calculate the generalized force acting on the "r" link.

e. Subroutine Sumb

1) Evaluate all of the summations found in the $\ddot{\theta}$ equation (39).

f. Subroutine Sumc

1) Evaluate the remaining summations to be used in the $\ddot{\phi}_r$ equation (40).

g. Subroutine Tether

1) Calculate the length and time rate of change of the links.

2) Calculate the mass and aerodynamic reference area of each link.

3) Calculate altitude, horizontal and vertical velocities and accelerations of the geometric center of each link.

4) Find the atmospheric density at the geometric center of each link.

5) Calculate the wind velocity at the geometric center of each link.

6) Calculate the horizontal and vertical drag of each link.

12. Recommendations

Throughout APPENDICES A and B assumptions and approximations were made so that the complexity of the equations of motion and the computer program would be held to a minimum. Since the program called for a feasibility study of a balloon-tether system, the results obtained are considered meaningful and

E-ID-15(7-64)(77-10)
REF: ENGINEERING PROCEDURE S.017

fairly accurate. However, if a complete parametric study is attempted, several refinements could be made.

a. The location of the center of pressure and center of gravity of each link should be calculated and not assumed to be at the geometric center.

b. A better description of the physical and aerodynamic properties of the balloon and harness should be defined.

c. A variable wind profile over each link and a link that varies in diameter should be considered in the computer program.

d. The weight of each link should be found by integrating a polynomial which represents the weight per unit length rather than averaging end conditions.

B-ID-15(7-64)(77-10)
REF: ENGINEERING PROCEDURE S.017

APPENDIX C
Program Listing

DISK OPERATING SYSTEM/360 FORTRAN 360N-FO-451 22

```
      DOUBLE PRECISION T,DT
      DIMENSION AA(4,12),BB(4),PHIDEG(12),PHIDDE(12),MC1(12),DDD(12)
      DIMENSION ZC(12),SC(12),RHOC(12),VC(12),VGC(12),XCD(12),ZCD(12)
      DIMENSION VF(12),HF(12)
      REAL MC(12),MCD(12),LH,LC,M1,M2,MH,LCD,IB,LCLC,MCRD,MCR,LCLH,
     1LCLCD,LLCD(8),LL(32),MM1(8),MM2(8),LCSL,NCR,NC(12),IBD,IB1,MC1,LS
     2,NCV(12),NCVR
      COMMONT,S1,S2,S3,S4,S5,S6,S7,S8,S9,S10,S11,S12,S13,S14,S15,S16,S17
     1,S18,S19,S20,S21,S22,S23,S24,SS1,SS2,SS3,SS4,SS5,PHID(12),PHI(12),
     2THE,PHIDD(12),PHIR,SB,DYPRB,CDB,H,B,VOLB,RHO,G,WB,CM,CMQ,CMS,VG,
     3VB,THED,FTHE,FPHI,AN,AR,IR,X,Z,XD,ZD,N,TT(8),RREN(8),PHIRD,VOLC,
     4CCD(8),VVG(24),ZZ(24),WDHSL,WBS,DD(32),NC,SC,VGC,VC,NCV,NCVR,
     5MC,MCD,LH,LC,M1,M2,MH,LCD,IB,LCLC,MCRD,MCR,LCLH,LCLCD,WWPUL(32),
     6LLCD,LL,MM1,MM2,TETH,S25,S26,WH,WT(12),NCR,D(12),CDC,WTCT,TENS(12)
     7,TENSW,DVB,PL,ZCDD(12),DVC,XCDD(12)
C
C                    EQUATIONS OF MOTION
C
 1000 FTHEDD(THED)=(FTHE+(M2+MH/2.)*(S1+S2)*LCLH
     1+(2.*M2+MH)*LH*LCD*S3+(M2-M1)*(LC*S3*(LC*S4+LCD*S5)-LCD*S6*(LC*S4+
     2LCD*S5))-THED*IBD)/(IB+LH*LH*(MH/3.+M2))
 2000 FPHIDD(PHID)=(FPHI+LCLC*(-SS1+SS4 +(-S17-S19+S21-MCRD*S9-MCR*S10
     1+MCR*S12)/2.-S25*S10-SS5-MH*S16+MH*S22+M1*THED*SIN(THE+PHIR)*
     2S4-M1*COS(THE+PHIR)*(S23+S15-S7-THED*S3)-M2*COS(THE+PHIR)*THED*
     3S3-M2*SIN(THE+PHIR)*(S13+S14+S1+THED*S4)-MH*S10-MCRD*PHIRD/3.)+
     4LCLCD*(-2.*SS2-SS3-S18-S20/2.-MCR*S9-MCRD*S11/2.-2.*MCR*PHIRD/3.
     5-2.*MH*S8-2.*M1*COS(THE+PHIR)*S4+M1*SIN(THE+PHIR)*THED*S5-
     6M1*COS(THE+PHIR)*THED*S6-M2*SIN(THE+PHIR)*(2.*S3+THED*S5)+
     7M2*COS(THE+PHIR)*THED*S6)
     8+LCLH*THED*THED*COS(THE+PHIR)*(MH/2.+M2))/(LCLC*(S25+MCR/3.+
     9MH+M1*COS(THE+PHIR)*COS(THE+PHIR)+M2*SIN(THE+PHIR)*SIN(THE+PHIR)))
   50 FORMAT(14X,4HTIME,6X,3HALT,7X,5HRANGE,5X,6HHORVEL,4X,7HVERTVEL,3X,
     15HTHETA,5X,8HTHE-RATE,2X,4HLINK,6X,7HPO-RATE,3X,7HWINDVEL,3X,2HLH,
     28X,5HTENSW/14X,7HWTCABLE,3X,5HDRAGH,5X,5HDRAGV,5X,8HVERTFORC,2X,
     35HDYPRB//)
   51 FORMAT(11X,12(F9.2,1X)/11X,5(F9.2,1X)/)
   52 FORMAT(11X,12(F9.2,1X))
    1 FORMAT(8F10.0)
      CALL MASK(0)
C
C                    INPUT VARIABLES
C
   97 READ(1,1)HHH,TTT,TETHM,GR,R,DT,DT1,AN
      IF(HHH-1.)98,99,98
   99 CALL EXIT
   98 READ(1,1)PL,T,TETH,DTS,TS,Z
      READ(1,1)CDC,CDB,VOLC,MH,WBS,WDHSL,THE,THED
      N=AN
      READ(1,1) (PHID(I),I=1,N)
      READ(1,1)(PHI(I),I=1,N)
      READ(1,1)(TT(I),I=1,8)
      READ(1,1)(LLCD(I),I=1,8)
```

```
01/19/68                FORTMAIN
      READ(1,1)(ZZ(I),I=1,24)
      READ(1,1)(VVG(I),I=1,24)
      READ(1,1)(LL(I),I=1,32)
      READ(1,1)(DD(I),I=1,32)
      READ(1,1)(HWPUL(I),I=1,32)
C
C                    INITIALIZATION
C
      JJ=1
      JJJ=1
      C2=0.0
      XD=0.0
      ZD=0.0
      IBD=0.0
      THEDD=0.0
      DO 12 I=1,N
      MCD(I)=0.0
   12 PHIDD(I)=0.0
      IB1=(.6667*WBS+PL/GR)*(.75*VOL0/3.14159)**.6667
      DIST=(.75*VOL0/3.14159)**.3333
      LH=DIST
      LH1=LH
      LHD=0.0
C
C                    OUTPUT PROCEDURES
C
      CALL HEAD(N)
      WRITE(3,50)
  100 G=GR*R*R/((R+Z)*(R+Z))
      IF(Z-HHH)31,31,32
   31 IF(T-TTT)33,32,32
   33 IF(TETH-TETHM)34,34,32
   32 THEDEG=THE*57.2958
      THEDDE=THED*57.2958
      TENS(N)=SQRT((B-PL-M1*ZDD)*(B-PL-M1*ZDD)+(H-M1*XDD)*(H-M1*XDD))
      VF(N)=-B+M1*ZDD
      HF(N)=-H+M1*XDD
      IF(N-1)901,901,902
  902 NN=N-I
      DO 903 I=1,NN
      J=N-I
      VF(J)=-VF(J+1)-NCV(J+1)-WT(J+1)-MC(J+1)*ZCDD(J+1)
      VF(J)=-VF(J)
      HF(J)=-HF(J+1)+NC(J+1)-MC(J+1)*XCDD(J+1)
      HF(J)=-HF(J)
  903 TENS(J)=SQRT(VF(J)*VF(J)+HF(J)*HF(J))
  901 VFW=-VF(1)-NCV(1)-WT(1)-MC(1)*ZCDD(1)
      HFW=-HF(1)+NC(1)-MC(1)*XCDD(1)
      TENSW=SQRT(VFW*VFW+HFW*HFW)
      WR=LCD*AN*60.
      DO 35 I=1,N
      PHIDEG(I)=PHI(I)*57.2958
   35 PHIDDE(I)=PHID(I)*57.2958
```

```
01/19/68              FORTMAIN
      WRITE(3,36)
   36 FORMAT(/1X,24HRUN ENDED BY CONSTRAINT /)
      WRITE(3,52)(PHIDEG(I),I=1,N)
      WRITE(3,52)(PHIDDE(I),I=1,N)
      WRITE(3,52)(TENS(I),I=1,N)
      WRITE(3,51)T,Z,X,XD,ZD,THEDEG,THEDDE,LC,WR,VG,LH,TENSW,WTCT,H,DVB,
     1B,DYPRB
      GO TO 97
   34 IF(JJJ-1)38,25,38
   38 C2=C2+1.
      IF(C2-DT1)23,24,24
   24 JJ=JJ+1
      IF(JJ-8)25,25,26
   26 CALL HEAD(N)
      WRITE(3,50)
      JJ=1
   25 THEDEG=THE*57.2958
      THEDDE=THED*57.2958
C
C                    TENSION IN TETHER
C
      TENS(N)=SQRT((B-PL-M1*ZDD)*(B-PL-M1*ZDD)+(H-M1*XDD)*(H-M1*XDD))
      VF(N)=-B+M1*ZDD
      HF(N)=-H+M1*XDD
      IF(N-1)101,101,102
  102 NN=N-1
      DO 103 I=1,NN
      J=N-I
      VF(J)=-VF(J+1)-NCV(J+1)-WT(J+1)-MC(J+1)*ZCDD(J+1)
      VF(J)=-VF(J)
      HF(J)=-HF(J+1)+NC(J+1)-MC(J+1)*XCDD(J+1)
      HF(J)=-HF(J)
  103 TENS(J)=SQRT(VF(J)*VF(J)+HF(J)*HF(J))
  101 VFW=-VF(1)-NCV(1)-WT(1)-MC(1)*ZCDD(1)
      HFW=-HF(1)+NC(1)-MC(1)*XCDD(1)
      TENSW=SQRT(VFW*VFW+HFW*HFW)
      WR=LCD*AN*60.
      DO 37 I=1,N
      PHIDEG(I)=PHI(I)*57.2958
   37 PHIDDE(I)=PHID(I)*57.2958
      WRITE(3,52)(PHIDEG(I),I=1,N)
      WRITE(3,52)(PHIDDE(I),I=1,N)
      WRITE(3,52)(TENS(I),I=1,N)
      WRITE(3,51)T,Z,X,XD,ZD,THEDEG,THEDDE,LC,WR,VG,LH,TENSW,WTCT,H,DVB,
     1B,DYPRB
      C2=0.0
C
C                    RUNGE-KUTTA INTEGRATION
C
   23 DO 74 J=1,4
      CALL SUBRB
      BB(J)=FTHEDD(THED)*DT
      GO TO (71,72,73,74),J
```

```
01/19/68                FORTMAIN
      71 DO 91 I=1,N
         IR=I
         CALL SUBRC
      91 AA(1,I)=FPHIDD(PHID)*DT
         DO 81 I=1,N
         PHI(I)=PHI(I)+PHID(I)*DT/2.
      81 PHID(I)=PHID(I)+AA(1,I)/2.
         THE=THE+THED*DT/2.
         THED=THED+BB(1)/2.
         THED=0.0
         THE=0.0
         T=T+DT/2.
         DO 61 I=1,N
      61 PHIDD(I)=AA(1,I)/DT
         GO TO 74
      72 DO 92 I=1,N
         IR=I
         CALL SUBRC
      92 AA(2,I)=FPHIDD(PHID)*DT
         DO 82 I=1,N
         PHID(I)=PHID(I)-AA(1,I)/2.+AA(2,I)/2.
      82 PHI(I)=PHI(I)+AA(1,I)*DT/4.
         THED=THED-BB(1)/2.+BB(2)/2.
         THED=0.0
         THE=THE+BB(1)*DT/4.
         THE=0.0
         DO 62 I=1,N
      62 PHIDD(I)=AA(2,I)/DT
         GO TO 74
      73 DO 93 I=1,N
         IR=I
         CALL SUBRC
      93 AA(3,I)=FPHIDD(PHID)*DT
         DO 83 I=1,N
         PHI(I)=PHI(I)+DT*(PHID(I)/2.-AA(1,I)/4.+AA(2,I)/4.)
      83 PHID(I)=PHID(I)-AA(2,I)/2.+AA(3,I)
         THE=THE+DT*(THED/2.-BB(1)/4.+BB(2)/4.)
         THE=0.0
         THED=THED-BB(2)/2.+BB(3)
         THED=0.0
         T=T+DT/2.
         DO 63 I=1,N
      63 PHIDD(I)=AA(3,I)/DT
      74 CONTINUE
         DO 94 I=1,N
         IR=I
         CALL SUBRC
      94 AA(4,I)=FPHIDD(PHID)*DT
         DO 84 I=1,N
         PHID(I)=PHID(I)-AA(3,I)
         PHI(I)=PHI(I)-DT*(PHID(I)+AA(2,I)/2.)
         PHI(I)=PHI(I)+PHID(I)*DT+(AA(1,I)+AA(2,I)+AA(3,I))*DT/6.
      84 PHID(I)=PHID(I)+(AA(1,I)+2.*AA(2,I)+2.*AA(3,I)+AA(4,I))/6.
```

```
01/19/68                FORTMAIN
      THED=THED-BB(3)
      THE=THE-DT*(THED+BB(2)/2.)
      THE=THE+THED*DT+(BB(1)+BB(2)+BB(3))*DT/6.
      THE=0.0
      THED=THED+(BB(1)+2.*BB(2)+2.*BB(3)+BB(4))/6.
      THED=0.0
      DO 86 I=1,N
      PHIDD(I)=AA(4,I)/DT
      MCD(I)=(MC(I)-MC1(I))/DT
   86 MC1(I)=MC(I)
C
C                    LINEAR DIST.,VEL.,AND ACC. OF BALLOON
C
      X=0.0
      Z=0.0
      XD=0.0
      ZD=0.0
      XDD=0.0
      ZDD=0.0
      DO 85 I=1,N
      X=X+LC*COS(PHI(I))
      Z=Z+LC*SIN(PHI(I))
      XD=XD+LCD*COS(PHI(I))-LC*SIN(PHI(I))*PHID(I)
      XDD=XDD-2.*LCD*SIN(PHI(I))*PHID(I)-LC*COS(PHI(I))*PHID(I)*PHID(I)-
     1LC*SIN(PHI(I))*PHIDD(I)
      ZDD=ZDD+2.*LCD*COS(PHI(I))*PHID(I)-LC*SIN(PHI(I))*PHID(I)*PHID(I)+
     1LC*COS(PHI(I))*PHIDD(I)
   85 ZD=ZD+LCD*SIN(PHI(I))+LC*COS(PHI(I))*PHID(I)
      X=X+LH*SIN(THE)
      Z=Z+LH*COS(THE)
      XD=XD+LH*COS(THE)*THED
      ZD=ZD-LH*SIN(THE)*THED
      XDD=XDD-LH*SIN(THE)*THED*THED+LH*COS(THE)*THEDD
      ZDD=ZDD-LH*COS(THE)*THED*THED-LH*SIN(THE)*THEDD
      VB=SQRT(XD*XD+ZD*ZD)
      DIST=SQRT(X*X+Z*Z)
      IBD=(IB-IB1)/DT
      IB1=IB
      JJJ=2
      IF(TENSW+100.)97,97,104
  104 CONTINUE
      IF(T-TS)10,11,11
   11 DT=DTS
   10 GO TO 100
      END
```

```
C
C                    HEADINGS FOR OUTPUT
C
      SUBROUTINE HEAD(N)
   51 FORMAT(1H1,13X,6HPHI(1)/14X,7HPHID(I)/14X,7HTENS(1))
   52 FORMAT(1H1,13X,6HPHI(1),4X,6HPHI(2)/14X,7HPHID(1),3X,7HPHID(2)/14X
     1,7HTENS(1),3X,7HTENS(2))
   53 FORMAT(1H1,13X,6HPHI(1),4X,6HPHI(2),4X,6HPHI(3)/14X,7HPHID(1),3X,
     17HPHID(2),3X,7HPHID(3)/14X,7HTENS(1),3X,7HTENS(2),3X,7HTENS(3))
   54 FORMAT(1H1,13X,6HPHI(1),4X,6HPHI(2),4X,6HPHI(3),4X,6HPHI(4)/14X,
     17HPHID(1),3X,7HPHID(2),3X,7HPHID(3),3X,7HPHID(4)/14X,7HTENS(1),3X,
     27HTENS(2),3X,7HTENS(3),3X,7HTENS(4))
   55 FORMAT(1H1,13X,6HPHI(1),4X,6HPHI(2),4X,6HPHI(3),4X,6HPHI(4),4X,
     16HPHI(5)/14X,7HPHID(1),3X,7HPHID(2),3X,7HPHID(3),3X,7HPHID(4),3X,
     27HPHID(5)/14X,7HTENS(1),3X,7HTENS(2),3X,7HTENS(3),3X,7HTENS(4),3X,
     37HTENS(5))
   56 FORMAT(1H1,13X,6HPHI(1),4X,6HPHI(2),4X,6HPHI(3),4X,6HPHI(4),4X,
     16HPHI(5),4X,6HPHI(6)/14X,7HPHID(1),3X,7HPHID(2),3X,7HPHID(3),3X,
     27HPHID(4),3X,7HPHID(5),3X,7HPHID(6)/14X,7HTENS(1),3X,7HTENS(2),3X,
     37HTENS(3),3X,7HTENS(4),3X,7HTENS(5),3X,7HTENS(6))
   57 FORMAT(1H1,13X,6HPHI(1),4X,6HPHI(2),4X,6HPHI(3),4X,6HPHI(4),4X,
     16HPHI(5),4X,6HPHI(6),4X,6HPHI(7)/14X,7HPHID(1),3X,7HPHID(2),3X,
     27HPHID(3),3X,7HPHID(4),3X,7HPHID(5),3X,7HPHID(6),3X,7HPHID(7)/14X,
     37HTENS(1),3X,7HTENS(2),3X,7HTENS(3),3X,7HTENS(4),3X,7HTENS(5),3X,
     47HTENS(6),3X,7HTENS(7))
   58 FORMAT(1H1,13X,6HPHI(1),4X,6HPHI(2),4X,6HPHI(3),4X,6HPHI(4),4X,
     16HPHI(5),4X,6HPHI(6),4X,6HPHI(7),4X,6HPHI(8)/14X,7HPHID(1),3X,
     27HPHID(2),3X,7HPHID(3),3X,7HPHID(4),3X,7HPHID(5),3X,7HPHID(6),3X,
     37HPHID(7),3X,7HPHID(8)/14X,7HTENS(1),3X,7HTENS(2),3X,7HTENS(3),3X,
     47HTENS(4),3X,7HTENS(5),3X,7HTENS(6),3X,7HTENS(7),3X,7HTENS(8))
   59 FORMAT(1H1,13X,6HPHI(1),4X,6HPHI(2),4X,6HPHI(3),4X,6HPHI(4),4X,
     16HPHI(5),4X,6HPHI(6),4X,6HPHI(7),4X,6HPHI(8),4X,6HPHI(9)/14X,
     27HPHID(1),3X,7HPHID(2),3X,7HPHID(3),3X,7HPHID(4),3X,7HPHID(5),3X,
     37HPHID(6),3X,7HPHID(7),3X,7HPHID(8),3X,7HPHID(9)/14X,7HTENS(1),3X,
     47HTENS(2),3X,7HTENS(3),3X,7HTENS(4),3X,7HTENS(5),3X,7HTENS(6),3X,
     57HTENS(7),3X,7HTENS(8),3X,7HTENS(9))
   60 FORMAT(1H1,13X,6HPHI(1),4X,6HPHI(2),4X,6HPHI(3),4X,6HPHI(4),4X,
     16HPHI(5),4X,6HPHI(6),4X,6HPHI(7),4X,6HPHI(8),4X,6HPHI(9),4X,
     27HPHI(10)/14X,7HPHID(1),3X,7HPHID(2),3X,7HPHID(3),3X,7HPHID(4),3X,
     37HPHID(5),3X,7HPHID(6),3X,7HPHID(7),3X,7HPHID(8),3X,7HPHID(9),3X,
     48HPHID(10)/14X,7HTENS(1),3X,7HTENS(2),3X,7HTENS(3),3X,7HTENS(4),
     53X,7HTENS(5),3X,7HTENS(6),3X,7HTENS(7),3X,7HTENS(8),3X,7HTENS(9),
     63X,8HTENS(10))
   61 FORMAT(1H1,13X,6HPHI(1),4X,6HPHI(2),4X,6HPHI(3),4X,6HPHI(4),4X,
     16HPHI(5),4X,6HPHI(6),4X,6HPHI(7),4X,6HPHI(8),4X,6HPHI(9),4X,
     27HPHI(10),3X,7HPHI(11)/14X,7HPHID(1),3X,7HPHID(2),3X,7HPHID(3),3X,
     37HPHID(4),3X,7HPHID(5),3X,7HPHID(6),3X,7HPHID(7),3X,7HPHID(8),3X,
     47HPHID(9),3X,8HPHID(10),2X,8HPHID(11)/14X,7HTENS(1),3X,7HTENS(2),
     53X,7HTENS(3),3X,7HTENS(4),3X,7HTENS(5),3X,7HTENS(6),3X,7HTENS(7),
     63X,7HTENS(8),3X,7HTENS(9),3X,8HTENS(10),2X,8HTENS(11))
   62 FORMAT(1H1,13X,6HPHI(1),4X,6HPHI(2),4X,6HPHI(3),4X,6HPHI(4),4X,
     16HPHI(5),4X,6HPHI(6),4X,6HPHI(7),4X,6HPHI(8),4X,6HPHI(9),4X,
```

```
01/10/68              HEAD
      27HPHI(10),3X,7HPHI(11),3X,7HPHI(12)/14X,7HPHID(1),3X,7HPHID(2),3X,
      37HPHID(3),3X,7HPHID(4),3X,7HPHID(5),3X,7HPHID(6),3X,7HPHID(7),3X,
      47HPHID(8),3X,7HPHID(9),3X,8HPHID(10),2X,8HPHID(11),2X,8HPHID(12)/
      514X,7HTENS(1),3X,7HTENS(2),3X,7HTENS(3),3X,7HTENS(4),3X,7HTENS(5),
      63X,7HTENS(6),3X,7HTENS(7),3X,7HTENS(8),3X,7HTENS(9),3X,8HTENS(10),
      72X,8HTENS(11),2X,8HTENS(12))
       GO TO (1,2,3,4,5,6,7,8,9,10,11,12),N
     1 WRITE(3,51)
       RETURN
     2 WRITE(3,52)
       RETURN
     3 WRITE(3,53)
       RETURN
     4 WRITE(3,54)
       RETURN
     5 WRITE(3,55)
       RETURN
     6 WRITE(3,56)
       RETURN
     7 WRITE(3,57)
       RETURN
     8 WRITE(3,58)
       RETURN
     9 WRITE(3,59)
       RETURN
    10 WRITE(3,60)
       RETURN
    11 WRITE(3,61)
       RETURN
    12 WRITE(3,62)
       RETURN
       END
```

DISK OPERATING SYSTEM/360 FORTRAN 360N-FO-451 22

```
C
C                    GENERALIZED FORCES ACTING ON BALLOON
C
      SUBROUTINE SUBRB
      DOUBLE PRECISION T,DT
      DIMENSION AA(4,12),BB(4),PHIDEG(12),PHIDDE(12),MC1(12),DDD(12)
      DIMENSION ZC(12),SC(12),RHOC(12),VC(12),VGC(12),XCD(12),ZCD(12)
      REAL MC(12),MCD(12),LH,LC,M1,M2,MH,LCD,IB,LCLC,MCRD,MCR,LCLH,
     1LCLCD,LLCD(8),LL(32),MM1(8),MM2(8),LCSL,NCR,NC(12),IBD,IB1,MC1,LS
     2,NCV(12),NCVR
      COMMONT,S1,S2,S3,S4,S5,S6,S7,S8,S9,S10,S11,S12,S13,S14,S15,S16,S17
     1,S18,S19,S20,S21,S22,S23,S24,SS1,SS2,SS3,SS4,SS5,PHID(12),PHI(12),
     2THE,PHIDD(12),PHIR,SB,DYPRB,CDB,H,B,VOLB,RHO,G,WB,CM,CMQ,CMS,VG,
     3VB,THED,FTHE,FPHI,AN,AR,IR,X,Z,XD,ZD,N,TT(8),RREN(8),PHIRD,VOLO,
     4CCD(8),VVG(24),ZZ(24),WDHSL,WBS,DD(32),NC,SC,VGC,VC,NCV,NCVR,
     5MC,MCD,LH,LC,M1,M2,MH,LCD,IB,LCLC,MCRD,MCR,LCLH,LCLCD,WWPUL(32),
     6LLCD,LL,MM1,MM2,TETH,S25,S26,WH,WT(12),NCR,D(12),CDC,WTCT,TENS(12)
     7,TENSW,DVB,PL,ZCDD(12),DVC
      RHOC=.002377
      CALL DENS(Z,PR,RHO,VS)
      VOLB=VOLO*RHOO/RHO
      IB=(.6667*WBS+PL)*LH*LH/G
      LH=(.75*VOLB/3.14159)**.3333
      I=1
  512 IF(Z-ZZ(I))510,511,511
  511 I=I+1
      GO TO 512
  510 ZSL=(Z-ZZ(I-1))/(ZZ(I)-ZZ(I-1))
      VG=VVG(I-1)+(VVG(I)-VVG(I-1))*ZSL
      SB=3.14159*(3.*VOLB/(4.*3.14159))**.6667
      XDB=XD-VG
      ZDB=ZD
      ALP=ARGD(ZDB,XDB)/57.2958
      DYPRB=.5*RHO*(XDB*XDB+ZDB*ZDB)
      H=-DYPRB*SB*CDB*COS(ALP)
      WH=WDHSL*VOLO
      WB=WH+WBS+PL
      M1=WB/32.174+.5*RHOO*VOLO
      M2=M1
      LS=VOLO*RHOO*32.174
      CALL TETHER
      DVB=DYPRB*SB*CDB*SIN(ALP)
      B=LS-WH-WBS-DVB
      FTHE=LH*(H*COS(THE)-B*SIN(THE))
      CALL SUMB
      RETURN
      END
```

DISK OPERATING SYSTEM/360 FORTRAN 360N-FO-451 22

```
C
C                    GENERALIZED FORCES ACTING ON LINKS
C
      SUBROUTINE SUBRC
      DOUBLE PRECISION T,DT
      DIMENSION AA(4,12),BB(4),PHIDEG(12),PHIDDE(12),MC1(12),DDD(12)
      DIMENSION ZC(12),SC(12),RHOC(12),VC(12),VGC(12),XCD(12),ZCD(12)
      DIMENSION VF(12),HF(12)
      REAL MC(12),MCD(12),LH,LC,M1,M2,MH,LCD,IB,LCLC,MCRD,MCR,LCLH,
     1LCLCD,LLCD(8),LL(32),MM1(8),MM2(8),LCSL,NCR,NC(12),IBD,IB1,MC1,LS
     2,NCV(12),NCVR
      COMMONT,S1,S2,S3,S4,S5,S6,S7,S8,S9,S10,S11,S12,S13,S14,S15,S16,S17
     1,S18,S19,S20,S21,S22,S23,S24,SS1,SS2,SS3,SS4,SS5,PHID(12),PHI(12),
     2THE,PHIDD(12),PHIR,S8,DYPRB,CDB,H,B,VCLB,RHO,G,WB,CM,CMQ,CMS,VG,
     3VB,THED,FTHE,FPHI,AN,AR,IR,X,Z,XD,ZD,N,TT(8),RREN(8),PHIRD,VOLO,
     4CCD(8),VVG(24),ZZ(24),WDHSL,WBS,DD(32),NC,SC,VGC,VC,NCV,NCVR,
     5MC,MCD,LH,LC,M1,M2,MH,LCD,IB,LCLC,MCRD,MCR,LCLH,LCLCD,WWPUL(32),
     6LLCD,LL,MM1,MM2,TETH,S25,S26,WH,WT(12),NCR,D(12),CDC,WTCT,TENS(12)
     7,TENSW,DVB,PL,ZCDD(12),DVC,XCDD(12)
      PHIR=PHI(IR)
      PHIRD=PHID(IR)
      NCR=NC(IR)
      NCVR=NCV(IR)
      MCR=MC(IR)
      MCRD=MCD(IR)
      CALL SUMC
      CALL SUMB
      FPHI=LC*COS(PHIR)*(-.5*MCR*G+B-PL-G*S25)+LC*SIN(PHIR)*(-.5*NCR*
     1SIN(PHIR)-H)-LC*S26-LC*COS(PHIR)*COS(PHIR)*.5*NCVR
      RETURN
      END
```

DISK OPERATING SYSTEM/360 FORTRAN 360N-FO-451 22

```
C
C                    SUMMATIONS NEEDED FOR THETA EQUATION
C
      SUBROUTINE SUMB
      DOUBLE PRECISION T,DT
      DIMENSION AA(4,12),BB(4),PHIDEG(12),PHIDDE(12),MC1(12),DDD(12)
      DIMENSION ZC(12),SC(12),RHOC(12),VC(12),VGC(12),XCD(12),ZCD(12)
      DIMENSION VF(12),HF(12)
      REAL MC(12),MCD(12),LH,LC,M1,M2,MH,LCD,IB,LCLC,MCRD,MCR,LCLH,
     1LCLCD,LLCD(8),LL(32),MM1(8),MM2(8),LCSL,NCR,NC(12),IBD,IB1,MC1,LS
     2,NCV(12),NCVR
      COMMONT,S1,S2,S3,S4,S5,S6,S7,S8,S9,S10,S11,S12,S13,S14,S15,S16,S17
     1,S18,S19,S20,S21,S22,S23,S24,SS1,SS2,SS3,SS4,SS5,PHID(12),PHI(12),
     2THE,PHIDD(12),PHIR,SB,DYPRB,CDB,H,B,VOLB,RHO,G,WB,CM,CMQ,CMS,VG,
     3VB,THED,FTHE,FPHI,AN,AR,IR,X,Z,XD,ZD,N,TT(8),RREN(8),PHIRD,VOLC,
     4CCD(8),VVG(24),ZZ(24),WDHSL,WBS,DD(32),NC,SC,VGC,VC,NCV,NCVR,
     5MC,MCD,LH,LC,M1,M2,MH,LCD,IB,LCLC,MCRD,MCR,LCLH,LCLCD,WWPUL(32),
     6LLCD,LL,MM1,MM2,TETH,S25,S26,WH,WT(12),NCR,D(12),CDC,WTCT,TENS(12)
     7,TENSW,DVB,PL,ZCDD(12),DVC,XCDD(12)
      S1=0.0
      S2=0.0
      S3=0.0
      S4=0.0
      S5=0.0
      S6=0.0
      DO 1 I=1,N
      S1=S1+PHID(I)*PHID(I)*COS(PHI(I)+THE)
      S3=S3+PHID(I)*SIN(PHI(I)+THE)
      S4=S4+PHID(I)*COS(PHI(I)+THE)
      S5=S5+SIN(PHI(I)+THE)
    1 S6=S6+COS(PHI(I)+THE)
      RETURN
      END
```

DISK OPERATING SYSTEM/360 FORTRAN 360N-FO-451 22

```
C
C                    SUMMATIONS NEEDED FOR PHI EQUATION
C
      SUBROUTINE SUMC
      DOUBLE PRECISION T,DT
      DIMENSION AA(4,12),BB(4),PHIDEG(12),PHIDDE(12),MC1(12),DDD(12)
      DIMENSION ZC(12),SC(12),RHOC(12),VC(12),VGC(12),XCD(12),ZCD(12)
      DIMENSION VF(12),HF(12)
      REAL MC(12),MCD(12),LH,LC,M1,M2,MH,LCD,IB,LCLC,MCRD,MCR,LCLH,
     1LCLCD,LLCD(8),LL(32),MM1(8),MM2(8),LCSL,NCR,NC(12),IBD,IB1,MC1,LS
     2,NCV(12),NCVR
      COMMONT,S1,S2,S3,S4,S5,S6,S7,S8,S9,S10,S11,S12,S13,S14,S15,S16,S17
     1,S18,S19,S20,S21,S22,S23,S24,SS1,SS2,SS3,SS4,SS5,PHID(12),PHI(12),
     2THE,PHIDD(12),PHIR,SB,DYPRB,CDB,H,B,VOLB,RHO,G,WB,CM,CMQ,CMS,VG,
     3VB,THED,FTHE,FPHI,AN,AR,IR,X,Z,XD,ZD,N,TT(8),RREN(8),PHIRD,VOLC,
     4CCD(8),VVG(24),ZZ(24),WDHSL,WBS,DD(32),NC,SC,VGC,VC,NCV,NCVR,
     5MC,MCD,LH,LC,M1,M2,MH,LCD,IB,LCLC,MCRD,MCR,LCLH,LCLCD,WWPUL(32),
     6LLCD,LL,MM1,MM2,TETH,S25,S26,WH,WT(12),NCR,D(12),CDC,WTCT,TENS(12)
     7,TENSW,DVB,PL,ZCDD(12),DVC,XCDD(12)
      S7=0.0
      S8=0.0
      S9=0.0
      S10=0.0
      S11=0.0
      S12=0.0
      S13=0.0
      S14=0.0
      S15=0.0
      S16=0.0
      S17=0.0
      S18=0.0
      S19=0.0
      S20=0.0
      S21=0.0
      S22=0.0
      S23=0.0
      S25=0.0
      S26=0.0
      SS1=0.0
      SS2=0.0
      SS3=0.0
      SS4=0.0
      SS5=0.0
      DO 1 I=1,N
      S7=S7+PHID(I)*PHID(I)*SIN(PHI(I)+THE)
      S8=S8+PHID(I)*COS(PHI(I)-PHIR)
      S22=S22+PHID(I)*PHID(I)*SIN(PHI(I)-PHIR)
    1 CONTINUE
      IF(1-IR+1)9,9,11
    9 J=IR-1
      DO 2 I=1,J
      S9=S9+PHID(I)*COS(PHI(I)-PHIR)
```

```
01/12/68                SUMC
      S11=S11+SIN(PHI(I)-PHIR)
      S12=S12+PHID(I)*PHID(I)*SIN(PHI(I)-PHIR)
    2 CONTINUE
   11 CONTINUE
      IF(IR+1-N)8,8,6
    8 J=IR+1
      DO 3 I=J,N
      IN=I-1
      DO 7 II=1,IN
      SS1=SS1+MCD(J)*PHID(II)*COS(PHI(II)-PHIR)
      SS2=SS2+MC(J)*PHID(II)*COS(PHI(II)-PHIR)
      SS3=SS3+MCD(J)*SIN(PHI(II)-PHIR)
    7 SS4=SS4+MC(J)*PHID(II)*PHID(II)*SIN(PHI(II)-PHIR)
    3 CONTINUE
      J=IR+1
      DO 4 IN=J,N
      S17=S17+MCD(IN)*PHID(IN)*COS(PHI(IN)-PHIR)
      S18=S18+MC(IN)*PHID(IN)*COS(PHI(IN)-PHIR)
      S20=S20+MCD(IN)*SIN(PHI(IN)-PHIR)
      S21=S21+MC(IN)*PHID(IN)*PHID(IN)*SIN(PHI(IN)-PHIR)
      S25=S25+MC(IN)
      S26=S26+(NC(IN)*SIN(PHI(IN))*SIN(PHI(IN))+NCV(IN)*COS(PHI(IN))*
     1COS(PHI(IN)))*COS(PHIR-PHI(IN))
    4 CONTINUE
    6 CONTINUE
      RETURN
      END
```

```
                        DISK OPERATING SYSTEM/360 FORTRAN   36CN-FO-451 22

C
C                              FORCES ACTING ON TETHER
C
      SUBROUTINE TETHER
      DOUBLE PRECISION T,DT
      DIMENSION AA(4,12),BB(4),PHIDEG(12),PHIDDE(12),MC1(12),DDD(12)
      DIMENSION ZC(12),SC(12),RHOC(12),VC(12),VGC(12),XCD(12),ZCD(12)
      DIMENSION VF(12),HF(12)
      REAL MC(12),MCD(12),LH,LC,M1,M2,MH,LCD,IB,LCLC,MCRD,MCR,LCLH,
     1LCLCD,LLCD(8),LL(32),MM1(8),MM2(8),LCSL,NCR,NC(12),IBD,IB1,MC1,LS
     2,NCV(12),NCVR
      COMMONT,S1,S2,S3,S4,S5,S6,S7,S8,S9,S10,S11,S12,S13,S14,S15,S16,S17
     1,S18,S19,S20,S21,S22,S23,S24,SS1,SS2,SS3,SS4,SS5,PHID(12),PHI(12),
     2THE,PHIDD(12),PHIR,SB,DYPRB,CDB,H,B,VOLB,RHO,G,WB,CM,CMQ,CMS,VG,
     3VB,THED,FTHE,FPHI,AN,AR,IR,X,Z,XD,ZD,N,TT(8),RREN(8),PHIRD,VOLC,
     4CCD(8),VVG(24),ZZ(24),WDHSL,WBS,DD(32),NC,SC,VGC,VC,NCV,NCVR,
     5MC,MCD,LH,LC,M1,M2,MH,LCD,IB,LCLC,MCRD,MCR,LCLH,LCLCD,WWPUL(32),
     6LLCD,LL,MM1,MM2,TETH,S25,S26,WH,WT(12),NCR,D(12),CDC,WTCT,TENS(12)
     7,TENSW,DVB,PL,ZCDD(12),DVC,XCDD(12)
C
C                        LINK LENGTH,RATE OF CHANGE,MASS,AND REF. AREA
C
      I=1
  512 IF(T-TT(I))510,511,511
  511 I=I+1
      GO TO 512
  510 III=I-1
      TETH=0.0
      IF(III-2)515,514,514
  514 DO 513 II=2,III
  513 TETH=TETH+LLCD(II)*(TT(II)-TT(II-1))
  515 TETH=TETH+LLCD(I)*(T-TT(I-1))
      LC=TETH/AN
      LCD=LLCD(I)/AN
      D2=DD(1)
      WPUL=WWPUL(1)
      WTCT=0.0
      DO 599 J=1,N
      AJ=J
      I=1
  612 IF(AJ*LC-LL(I))610,611,611
  611 I=I+1
      GO TO 612
  610 LCSL=(LC*AJ-LL(I-1))/(LL(I)-LL(I-1))
      D1=D2
      WPUL1=WPUL
      WPUL=WWPUL(I-1)+(WWPUL(I)-WWPUL(I-1))*LCSL
      D2=DD(I-1)+(DD(I)-DD(I-1))*LCSL
      DDD(J)=(D1+D2)/2.
      WT(J)=(WPUL+WPUL1)*LC/2.
  599 WTCT=WTCT+WT(J)
      DO 598 I=1,N
```

```
01/12/68                    TETHER
                ZC(I)=0.0
                XCD(I)=0.0
                ZCD(I)=0.0
                ZCDD(I)=0.0
                XCDD(I)=0.0
                LLL=N+1-I
                D(LLL)=DDD(I)
            598 MC(LLL)=WT(I)/32.174
                DO 100 I=1,N
                WT(I)=MC(I)*32.174
                SC(I)=LC*D(I)
          C
          C                     LINEAR DYNAMICS OF LINKS
          C
                IF(I-1)103,103,101
            101 I1=I-1
                DO 102 J=1,I1
                XCD(I)=XCD(I)+LCD*COS(PHI(J))-LC*SIN(PHI(J))*PHID(J)
                ZCD(I)=ZCD(I)+LCD*SIN(PHI(J))+LC*COS(PHI(J))*PHID(J)
                ZCDD(I)=ZCDD(I)+LCD*COS(PHI(J))*PHID(J)*2.+LC*COS(PHI(J))*PHIDD(J)
               1-LC*SIN(PHI(J))*PHID(J)*PHID(J)
                XCDD(I)=XCDD(I)-2.*LCD*SIN(PHI(J))*PHID(J)-LC*COS(PHI(J))*PHID(J)*
               1PHID(J)-LC*SIN(PHI(J))*PHIDD(J)
            102 ZC(I)=ZC(I)+LC*SIN(PHI(J))
            103 ZC(I)=ZC(I)+.5*LC*SIN(PHI(I))
                XCD(I)=XCD(I)+.5*LCD*COS(PHI(I))-.5*LC*SIN(PHI(I))*PHID(I)
                ZCD(I)=ZCD(I)+.5*LCD*SIN(PHI(I))+.5*LC*COS(PHI(I))*PHID(I)
                ZCDD(I)=ZCDD(I)+LCD*COS(PHI(I))*PHID(I)+.5*LC*COS(PHI(I))*PHIDD(I)
               1-.5*LC*SIN(PHI(I))*PHID(I)*PHID(I)
                XCDD(I)=XCDD(I)-LCD*SIN(PHI(I))*PHID(I)-.5*LC*COS(PHI(I))*PHID(I)*
               1PHID(I)-.5*LC*SIN(PHI(I))*PHIDD(I)
          C
          C                     DRAG FORCES ON LINKS
          C
                CALL DENS(ZC(I),PR,RHOC(I),VSC)
            100 VC(I)=SQRT(XCD(I)*XCD(I)+ZCD(I)*ZCD(I))
                DO 713 J=1,N
                I=1
            712 IF(ZC(J)-ZZ(I))710,711,711
            711 I=I+1
                GO TO 712
            710 ZCSL=(ZC(J)-ZZ(I-1))/(ZZ(I)-ZZ(I-1))
                VGC(J)=VVG(I-1)+(VVG(I)-VVG(I-1))*ZCSL
                NCV(J)=CDC*.5*RHOC(J)*SC(J)*ZCD(J)*ZCD(J)
            713 NC(J)=CDC*.5*RHOC(J)*SC(J)*((VGC(J)-XCD(J))*(VGC(J)-XCD(J)))
                DO 200 J=1,N
                IF(ZCD(J))202,202,203
            202 NCV(J)=-NCV(J)
            203 CONTINUE
                DVC=0.0
                DO 204 I=1,N
            204 DVC=DVC+NCV(I)
                IF(VGC(J)-XCD(J))201,200,200
```

```
01/12/68                    TETHER
   201 NC(J)=-NC(J)
   200 CONTINUE
       LCLC=LC*LC
       LCLH=LC*LH
       LCLCD=LC*LCD
       RETURN
       END
```